ENERGY*SOLUTIONS*
CLASS A WEST
DISPOSAL CELL
INFILTRATION AND TRANSPORT
MODELING REPORT

Prepared for

EnergySolutions, LLC
423 West 300 South, Suite 200
Salt Lake City, UT 84101

Prepared by

Whetstone Associates, Inc.
104 W Ruby Avenue
Gunnison, Colorado 81230
970-641-7471

Document 4104K.110419

April 19, 2011

TABLE OF CONTENTS

LIST OF TABLES

LIST OF FIGURES

LIST OF ATTACHMENTS

1. INTRODUCTION

Energy*Solutions* operates a radioactive waste and mixed waste disposal facility in Tooele County, Utah. Waste disposal cells at the site (Figure 1) are permanent, clay-lined cells with composite clay and rock cap designed to perform for a minimum of 500 years. The existing Class A and Class A North disposal cells occupy the western portion of Section 32 of T1S, R11W and are partially filled. Energy*Solutions* proposes to combine the existing Class A disposal cell with the Class A North disposal cell, and to increase the maximum waste height to approximately 76 ft. The combined facility would be called the Class A West (CAW) cell, and would occupy 133 acres at completion.

Although the modeling builds upon previous modeling reports and technical memoranda submitted for the Energy*Solutions* site, this report is intended as a standalone document that describes the model methods, assumptions, input parameters, and results.

1.1 Purpose and Objective

The Groundwater Quality Discharge Permit for the Energy*Solutions* site (UGW450005) requires that environmental impacts to groundwater are kept within tolerable risk levels. To assess these risks, groundwater models are used to evaluate the potential flow of water and transport of constituents from the disposal cell to a compliance well located 90 feet from the edge of the waste. The models predict groundwater concentrations at the compliance well for a period of 200 and 500 years after closure, for hazardous and radioactive constituents, respectively. The purpose of this document is to describe the assumptions, input parameters, and results of the infiltration and fate and transport modeling.

1.2 Previous Modeling

Fate and transport modeling of a similar nature has been performed previously for the Class A cell, LARW cell, 11e.(2) cell, and Mixed Waste cell at the Energy*Solutions* Clive facility. This modeling has been based on site-specific parameters, where available, or conservative assumptions where no site-specific data existed. Over time, as more data have been collected for the site, these models have been refined and updated to provide more accurate yet extremely environmentally conservative estimates of the leaching, transport, and arrival of constituents at compliance monitoring wells for decades and centuries into the future.

Previous groundwater flow and contaminant transport models of the Envirocare facility have been generated by Rogers and Associates Engineering (1990), Bingham Environmental (1991, 1993a. 1993b, 1994a, 1995a, 1995c), Adrian Brown Consultants (1996a, 1996b, 1997a, 1997b, 1997d, 1998), the Utah Department of Environmental Quality (DEQ) Division of Water Quality (1993, 1994), and Whetstone Associates (2000a, 2000d, 2000e, 2000f, 2001a, 2001b, 2003, 2005, 2006a, 2006b). The methodology used in the modeling was initially described in detail in a two-volume comprehensive modeling report for the LARW cell, prepared by Adrian Brown Consultants in 1997.

The refinements in radionuclide inventory, half lives, and K_d values for the Class A radionuclides that developed over time in the course of modeling (and in response to Utah Division of Radiation Control [DRC] comments) have been incorporated into the current modeling of the CAW cell. The model uses the most up-to-date Class A nuclide inventory approved by DRC. Aquifer hydraulic conductivity and meteorological data have also been updated.

The engineering design for the proposed CAW cell is very similar to that of the existing Class A cell. Although the CAW cell is larger, the approach and methodology for the modeling are similar.

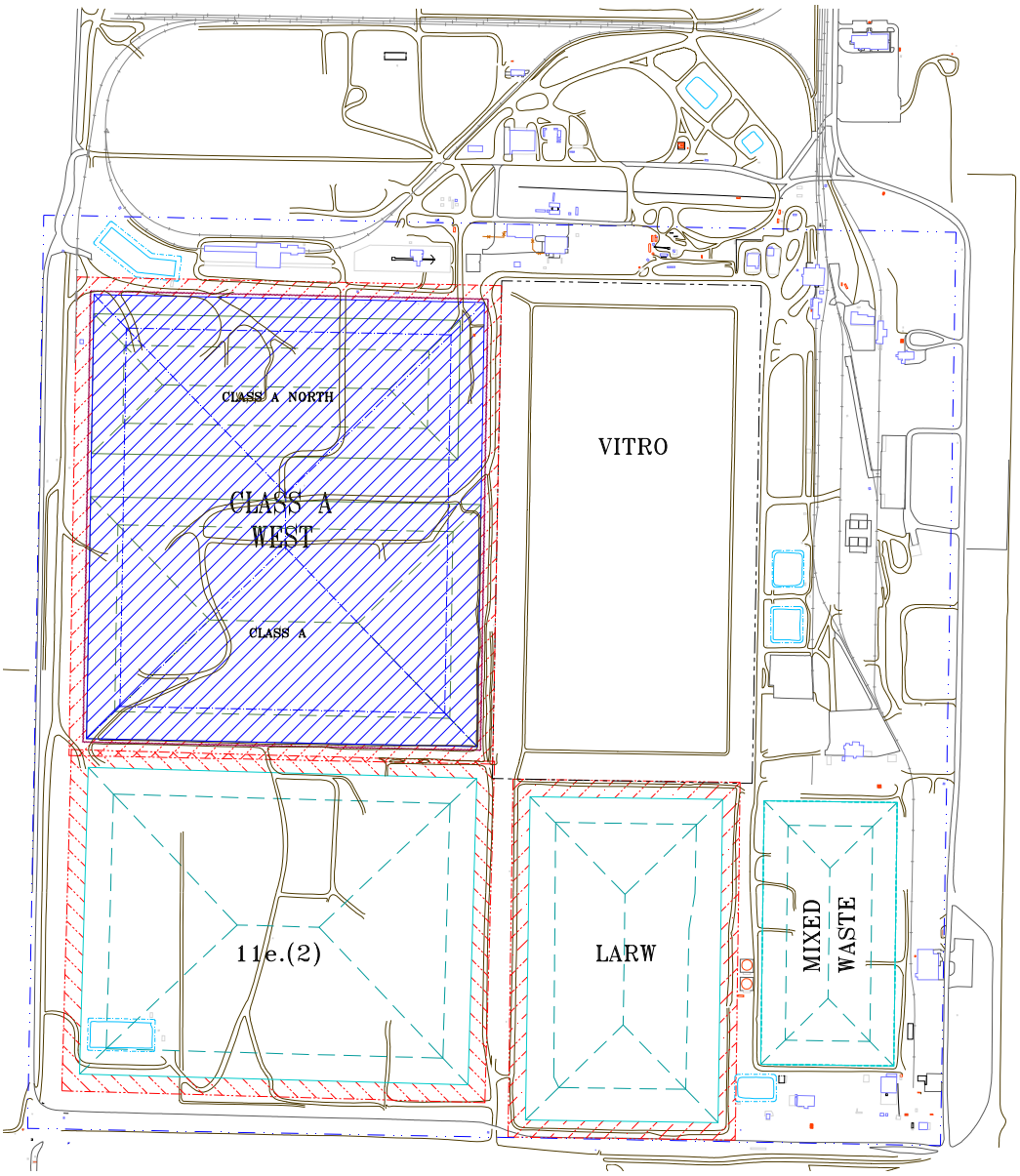

Figure 1. Plan View Map of Section 32 Showing Embankments, Buffer Zones, and Proposed Class A West Cell

1.3 Modeling Method

The potential migration of hazardous and radioactive constituents from the CAW cell were investigated using the EPA HELP model (Schroeder and Peyton, 1995), the Pacific Northwest Laboratories UNSAT-H model (Fayer and Jones, 1990), and the PATHRAE-RAD model (Merrell, et al, 1995).

The modeling project was divided into the following four phases:

1. The infiltration through the closed CAW cell was predicted using the EPA HELP model;
2. Percolation rates predicted by the HELP model were input into the UNSAT-H model to predict the moisture content and time of travel from the bottom of the waste to the top of the aquifer;

3. A dispersive solution for contaminant transport from the base of the cell to the top of the water table (vertical solution) was determined using the PATHRAE model; and
4. The horizontal migration of constituents through the saturated zone to a compliance well was modeled, again using PATHRAE.

The infiltration (HELP) and moisture content (UNSAT-H) models are described in Sections 2 and 3 of this report. The contaminant transport (PATHRAE) modeling is described in Sections 4 through 6.

2. INFILTRATION (HELP) MODELING

The infiltration modeling code and input are briefly described below. More detailed information on the infiltration modeling approach, code, and design in relation to the Energy*Solutions* site is contained in the 1997 document prepared for the LARW cell entitled "Volume I. Final Report on Infiltration Modeling" (ABC, 1997).

2.1 Code

Infiltration through the CAW cell was modeled using the EPA Hydrologic Evaluation of Landfill Performance (HELP) model (version 3.06). The HELP program (Schroeder and Peyton, 1995) is a quasi-two-dimensional code developed by Paul Schroeder (U.S. Army Corps of Engineers) and R. Lee Peyton (University of Missouri, Columbia). The model was adapted from the EPA HSSWDS model (Perrier and Gibson, 1980) and various codes from the US Agricultural Research Service, and National Weather Service, and it uses weather, soil, and landfill design data to perform water balance analysis of the designed cell. Surface storage, snowmelt, runoff, infiltration, evapotranspiration, soil moisture storage, lateral subsurface drainage, and unsaturated surface drainage can all be modeled.

The HELP code is distributed by EPA and has widespread acceptance as a tool for the evaluation of the hydrologic performance of landfills. The HELP code was used previously in the prediction of infiltration at the Energy*Solutions* site, and was accepted by DRC as part of license renewal.

2.2 Weather Data Input

The HELP weather data input to the CAW cell model was based on 17 years of meteorological data available for the Clive site, as reported by Meteorological Solutions, Inc (MSI, 2010). The average annual precipitation measured at the Energy*Solutions* Clive facility from 1993-2009 was 8.53 inches per year (in/yr). Based on site-specific data, input files for evapotranspiration, precipitation, temperature, and solar radiation data were generated using a synthetic weather generator. The weather generator routine, developed by the USDA Agricultural Research Service (Richardson and Wright, 1984), generated 100 years of daily climate data based on site-specific monthly average precipitation and temperature coupled with the climate distribution parameters for a selected analog city.

The climatological input values are summarized in Table 1 and described briefly in the following sections.

Table 1. Summary of HELP Model Weather and Climate Input

```
                          EVAPOTRANSPIRATION AND WEATHER DATA
-------------------------------------------------------------------------------------------------
          NOTE: EVAPOTRANSPIRATION DATA WAS OBTAINED FROM SALT LAKE CITY UTAH
            STATION LATITUDE                        =  40.69 DEGREES
            MAXIMUM LEAF AREA INDEX                 =   0.00
            START OF GROWING SEASON (JULIAN DATE)   =    117
            END OF GROWING SEASON (JULIAN DATE)     =    289
            EVAPORATIVE ZONE DEPTH                  =  18.0  INCHES
            AVERAGE ANNUAL WIND SPEED               =   7.20 MPH
            AVERAGE 1ST QUARTER RELATIVE HUMIDITY   =  50.50 %
            AVERAGE 2ND QUARTER RELATIVE HUMIDITY   =  28.60 %
            AVERAGE 3RD QUARTER RELATIVE HUMIDITY   =  22.70 %
            AVERAGE 4TH QUARTER RELATIVE HUMIDITY   =  47.90 %

          NOTE:  PRECIPITATION DATA WAS SYNTHETICALLY GENERATED USING
                    COEFFICIENTS FOR    SALT LAKE CITY      UTAH

                    NORMAL MEAN MONTHLY PRECIPITATION (INCHES)
       JAN/JUL     FEB/AUG     MAR/SEP     APR/OCT     MAY/NOV     JUN/DEC
       -------     -------     -------     -------     -------     -------
         0.79        0.86        0.85        1.18        0.95        0.89
         0.30        0.33        0.40        0.74        0.50        0.51

          NOTE:  TEMPERATURE DATA WAS SYNTHETICALLY GENERATED USING
                    COEFFICIENTS FOR    SALT LAKE CITY      UTAH

              NORMAL MEAN MONTHLY TEMPERATURE (DEGREES FAHRENHEIT)
       JAN/JUL     FEB/AUG     MAR/SEP     APR/OCT     MAY/NOV     JUN/DEC
       -------     -------     -------     -------     -------     -------
        29.10       32.40       41.40       49.10       60.30       69.60
        79.50       76.80       64.90       50.20       37.00       27.70

          NOTE:  SOLAR RADIATION DATA WAS SYNTHETICALLY GENERATED USING
                    COEFFICIENTS FOR    SALT LAKE CITY      UTAH
                       AND STATION LATITUDE  =  40.69 DEGREES
```

2.2.1 Evapotranspiration

Evapotranspiration was calculated by HELP using the location, maximum leaf area, and evaporative zone depth (EZD) specified for the site.

Location. Salt Lake City appears to be the most appropriate analog city for the Clive site (DRC, 1997). Therefore, Salt Lake City was used in the model as the analog city, from which HELP generated synthetic evapotranspiration data. The default latitude (40.76°) was adjusted to 40.6858°(40°41'15") for the Clive site.

Evaporative Zone Depth (EZD). The EZD is defined as the depth to which evaporation and transpiration from the soil or rock can occur. Because the CAW cell will not be vegetated, the EZD represents the maximum depth of evaporation. In the HELP model, any water that percolates below the EZD can only be routed laterally, via a filter (or lateral drainage) layer, or vertically downward as percolation. The model determined the amount of evaporation that occurred in the evaporative zone based on the available energy in the system, according to the temperature, solar radiation, and wind speed for each given day.

The modeling was conducted using an 18-inch EZD, which only allows water to evaporate from the 18-inch thick rip rap layer. Water that percolates down to the upper filter layer or to the sacrificial soil cannot be removed from the HELP model by evaporation. This input value is considered to be extremely environmentally conservative, because extensive monitoring of drainage from the site's Test Cell indicates that the actual site-specific EZD is at least 30 inches (Whetstone, 2005).

Maximum Leaf Area Index. The maximum leaf area was set to zero, which is appropriate for bare ground. The CAW cell will not be vegetated.

Growing Season. The model is insensitive to the input values for the start and end of growing season, because the CAW cell will not be vegetated. The growing season for Salt Lake City (start day 117, end day 289) was left as the default input.

Wind Speed. The site-specific 17-year average wind speed (July 1, 1992 through December 31, 2009) of 3.2 meters per second (7.2 miles per hour) was used in the base case model. This value is 25% higher than the long-term average wind speed from Dugway, Utah (5.75 mph) used in previous modeling.

Previous sensitivity analyses using wind speeds of 5.75, 7.27, and 8.8 mph (ABC, 1997) indicated that the HELP model is insensitive to slight variations in wind speed. As stated in the 1997 report:

> "Long-term climatic data from Dugway … indicates that the average annual wind speed is 5 knots (5.75 mph). The long term average wind speed measured at the site from April through September 1994 was 3.5 meters per second … or 7.27 mph. The default wind speed for Salt Lake City is 8.8 mph. The long-term Dugway value of 5 knots (5.75 mph) was used in the modeling. A sensitivity analysis … indicates that the model was insensitive to these slight variations in wind speed."

The site-specific average wind speed (3.2 meters per second, 7.2 mph) used in the CAW cell modeling is within the range of previous sensitivity analyses.

Relative Humidity. The long-term relative humidity data from Dugway was used in the HELP model simulations. The data are based on a 20-year period of record of monthly mean relative humidity values, from 13:00 hours local standard time from NWS, NOAA. The quarterly values were derived as a simple average of the monthly values.

Table 2. Quarterly Relative Humidity at Dugway Proving Ground

Quarter	Month 1	Month 2	Month 3	Quarterly Average
1st (Jan., Feb., Mar.)	57.9	52.8	40.9	50.5
2nd (Apr., May, June)	33.4	27.5	25	28.6
3rd (July, Aug., Sept.)	19.8	21.8	26.7	22.7
4th (Oct., Nov., Dec.)	34.3	47.2	62.4	47.9

Note: Dugway average monthly relative humidity data from 13:00 hours local standard time from NWS, NOAA (summarized from NOAA internet site data)

2.2.2 Precipitation

Precipitation data were generated using the HELP synthetic precipitation generator to stochastically generate 100 years of daily precipitation data. The mean monthly precipitation values, from which the 100 years of daily precipitation data were generated, include 17 years of recorded precipitation available for the Clive site (MSI, 2010). The precipitation measured from 1992 – 2009 at the Clive meteorological station is summarized in Table 3. The annual average precipitation, based on valid data from the 17-year record, is 8.53 in/yr. The monthly values were input to the HELP synthetic weather generator, which generated a 100-year data set with an average annual precipitation of 8.44 in/yr[1].

[1] The synthetic weather generator created a 100-year synthetic precipitation data set having a mean annual precipitation of 8.44 inches per year, which was 99% of the sum of the monthly values (8.53 inches) input to the weather generator. The difference of 1% (0.09 inches) in the mean is within the expected range of variability in data sets produced by the synthetic weather generator.

A statistical analysis of the 100-year synthetic precipitation data set indicates that the synthetic weather generator produced daily data having a mean annual precipitation of 8.44 in/yr, with a minimum of 4.87 in/yr and a maximum of 12.65 in/yr. The 100-year data set contains 232 days having precipitation greater than 0.4 inches, 53 days having precipitation greater than 0.6 inches, and 19 days having precipitation greater than 0.8 inches. The complete data set is presented in Attachment 4, file U100.d4.

Table 3. Summary of Precipitation at Clive, Utah July 1992 through December 2009

Year	Jan	Feb	Mar	Apr	May	Jun	Jul	Aug	Sep	Oct	Nov	Dec	Annual
1992							0.51	0.24	0.07	0.89	0.33	1.03	n/a
1993	1.17	0.39	0.67	0.17	0.99	0.7	0.03	0.1	0.27	0.78	0.33	0.18	5.78
1994	0.13	0.63	1.14	1.66	0.79	0.02	0.06	0.39	0.51	0.89	1.91	0.22	8.35
1995	0.95	0.78	1.74	0.44	2.58	1.88	0.17	0.04	0.15	0.06	0.24	0.78	9.81
1996	1.31	0.78	0.88	0.91	1.9	0.29	1.1	0.01	0.41	0.69	0.6	0.77	9.65
1997	1.56	0.87	0.17	1.42	0.98	2.36	1.19	0.32	0.9	0.47	0.72	0.6	11.56
1998	0.71	2.21	1.67	1.63	1.04	2.69	0.43	0.28	0.52	1.94	0.1	0.32	13.54
1999	0.81	0.64	0.46	2.65	0.41	1.84	0.06	0.68	0.12	0.04	0.13	0.18	8.02
2000	1.31	1.87	0.23	0.38	0.53	0.10	0.07	1.05	0.15	1.92	0.15	0.44	8.2
2001	0.21	0.55	1.48	1.17	0.0	0.52	0.13	0.25	0.22	0.2	1.25	0.81	6.79
2002	0.50	0.07	0.44	1.36	0.57	0.08	0.24	0.01	0.52	0.95	0.50[a]	0.51[a]	5.75[b]
2003	0.79[a]	0.86[a]	0.85[a]	1.18[a]	0.91	0.12	0.03	0.45	0.21	0.17	0.62	1.27	7.46[b]
2004	0.06	1.3	0.43	1.98	0.6	0.19	0.35	0.57	0.99	1.5	0.91	0.18	9.06
2005	1.15	1.09	0.93	1.29	2.94	0.92	0.01	0.60	0.09	0.4	0.36	0.38	10.16
2006	0.82	0.25	1.58	1.24	0.51	0.33	0.32	0.58	0.35	0.94	0.25	0.22	7.39
2007	0.35	1.15	1.27	0.55	0.45	1.32	0.78	0.07	0.89	0.49	0.04	0.93	8.29
2008	0.5	0.26	0.24	0.13	0.33	0.42	0.01	0.19	0.08	0.46	0.36	0.22	3.2
2009	1.04	0.86	0.31	1.97	0.64	1.32	0.05	0.06	0.48	0.76	0.05	0.58	8.12
17-yr avg	**0.79[c]**	**0.86[c]**	**0.85[c]**	**1.18[c]**	**0.95**	**0.89**	**0.3**	**0.33**	**0.4**	**0.74**	**0.50[c]**	**0.51[c]**	**8.53**

Source: MSI (2010)
a) Monthly totals based on 16-year climatological average
b) Annual total based on valid data and 15-year climatological averages
c) Mean is based on 16 years of data (excludes 2002 and 2003 climatological averages)

The 100-year synthetic data set had a mean precipitation of 8.44 inches. For comparison, the 8.44 inches of precipitation used in the HELP model is 11% higher than the long-term average annual precipitation measured at Dugway from September 1950 – December 2009. The monthly precipitation received at Clive has been similar to that received at Dugway over a 17-year period (Figure 2). The monthly average during this period has been similar (Figure 3), although the precipitation received at the Energy*Solutions* Clive site has exceeded Dugway's by 3.5% (Table 4).

Precipitation in recent years has exceeded the long-term average. During the 17-year period from July 1992 to December 2009, the average precipitation at Dugway exceeded the long-term average by 8% (Table 4). Assuming that the Clive precipitation has also exceeded the long-term average by 8%, the calculated long-term precipitation at Clive is 7.88 inches per year (Table 4) and the 8.44 inches used in the model is conservatively high.

The synthetic precipitation data set (with a long-term mean of 8.44 in/yr) used in the HELP model is considered environmentally conservative because 1) the precipitation data set is based on a 17-year period of above-average precipitation in the region and 2) the data set captures extreme precipitation events.

Figure 2. Monthly Precipitation at Clive and Dugway, July 1992 – December 2009

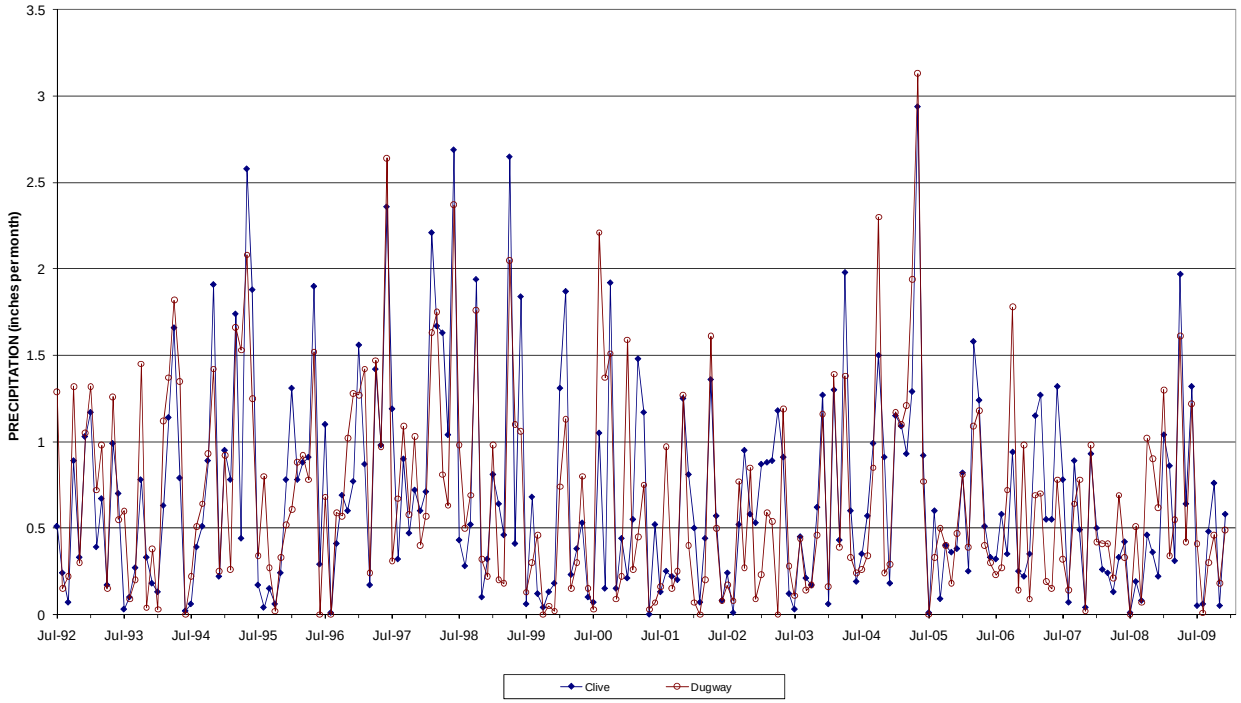

Figure 3. 17-Year Mean Monthly Precipitation at Clive and Dugway, July 1992 – December 2009

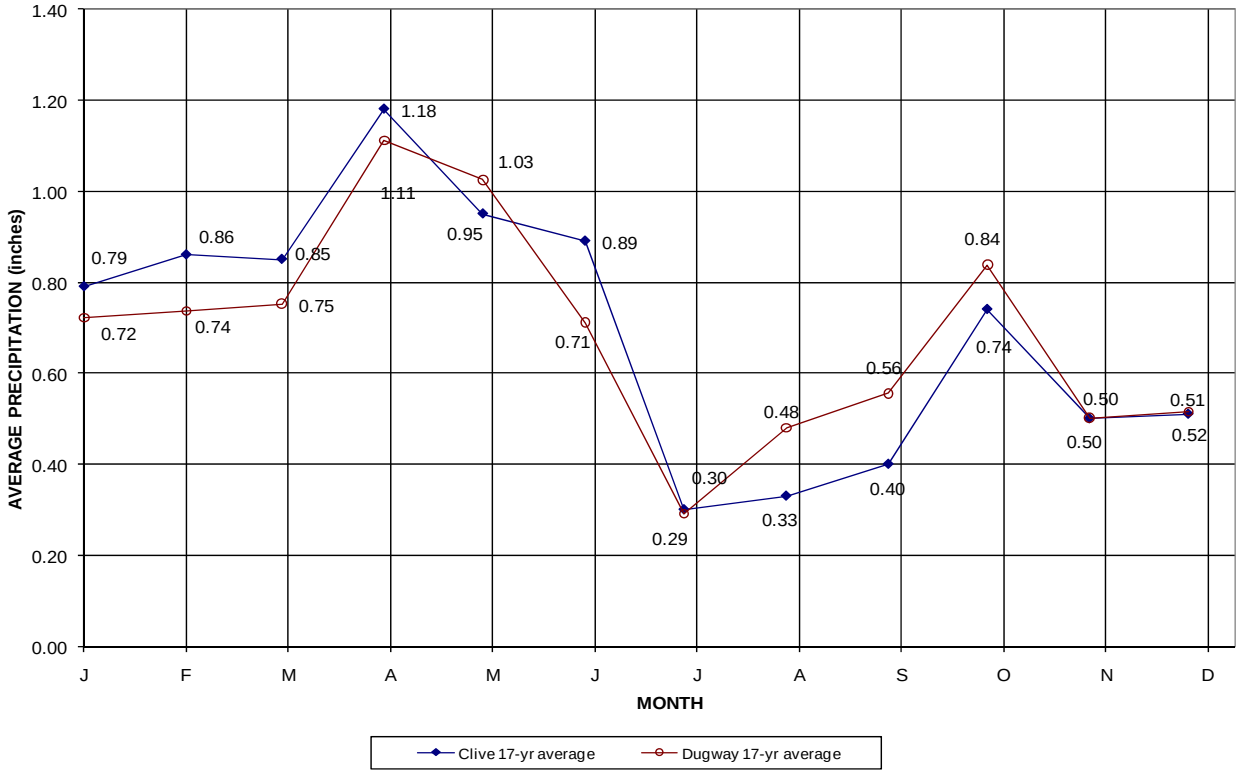

Table 4. Monthly Precipitation (in inches) at Clive and Dugway Stations July 1992-Dec 2009 with Comparison to Long-Term Mean

DATA	J	F	M	A	M	J	J	A	S	O	N	D	ANNUAL
17-yr Average Clive	0.79	0.86	0.85	1.18	0.95	0.89	0.30	0.33	0.40	0.74	0.50	0.51	8.53
17-yr Average Dugway	0.72	0.74	0.75	1.11	1.03	0.71	0.29	0.48	0.56	0.84	0.50	0.52	8.24
1950-2009 Avg. Dugway	0.56	0.61	0.73	0.84	0.98	0.55	0.46	0.55	0.58	0.73	0.53	0.56	7.61
Dugway 17-yr avg./Long-term	1.29	1.21	1.03	1.32	1.05	1.29	0.63	0.87	0.96	1.15	0.95	0.92	1.083
Clive fraction of Dugway	1.09	1.17	1.13	1.06	0.93	1.25	1.03	0.69	0.72	0.88	1.00	0.99	1.035
Clive long-term	0.58	0.63	0.76	0.87	1.01	0.57	0.48	0.57	0.60	0.76	0.55	0.58	7.88
Clive long-term (sum of monthly means)													7.95

NOTES:
Precipitation data reported in inches.
17-year average: Monthly averages for Dugway are based on mean monthly values for July 1992 – December 2009. Annual average is calculated as the sum of the mean monthly values.
% of long-term: Calculated by dividing seventeen-year average at Dugway by the long term average at Dugway; determined that Dugway precipitation from July 1992 - December 2009 has been 8.3% higher than the long-term average.
Clive fraction: Calculated by dividing seventeen-year average at Clive by the seventeen-year average at Dugway; Determined that on an annualized basis, the precipitation at Clive is 103.5% of that at Dugway
Clive long-term: Calculated by multiplying the long-term average at Dugway by the annualized conversion factor (103.5%).
DATA SOURCES:
Dugway data for 1950-December 2009 from Western Regional Climate Center (WRCC, 2010)
Clive data from Meteorological Solutions, Inc. (MSI, 2010)
Long-term statistics for Dugway calculated by WRCC
17-year statistics for Clive calculated by MSI
17-year statistics for Dugway calculated by MSI and include 7 monthly values from Sep 2006 – Mar 2007 substituted from Mesowest Station DPG01

3.2.3 Temperature

One hundred years of temperature data were created using the HELP synthetic temperature generator based on coefficients for Salt Lake City and the monthly average temperature at the Clive site. A statistical analysis of the 100 years of synthetic daily precipitation data indicates that the mean daily temperature is 51.74 °F, with a minimum of 2.5 °F and a maximum of 95.1 °F (Table 5). The 100-year data set contains 22,677 days having temperatures lower than 60 °F, 12,062 days having temperatures lower than 40 °F, and 1,218 days having temperatures lower than 20 °F (Table 6).

Table 5. Summary and Evaluation of Daily Temperature Data in HELP Model 100-Year Synthetic Weather Data Set

(See large tables at end of report document)

Table 6. Event Distribution of Mean Daily Temperature in 100-year Synthetic Data Set

Temperature (°F)	Number of Events
<95	36,524
<90	36,485
<80	33,970
<70	28,114
<60	22,677
<50	17,512
<40	12,062
<30	5,746
<20	1,218
<10	61
<5	6

The 17-year average monthly temperatures from the Energy*Solutions* meteorological station (MSI, 2010) compare favorably with the long-term (Sept. 1950 – May 2010) average monthly temperatures at Dugway, Utah (Table 7, Figure 4) indicating that the temperature values from Dugway used in previous modeling were representative of the site. Long-term temperatures for Dugway tend to be slightly higher in the winter and lower in the summer than the 17-year average temperatures for the Clive site.

Table 7. Mean Monthly Temperature for the EnergySolutions Site

Month	17 -Year Average Temperature (°C) at Energy*Solutions* Site	17 -Year Average Temperature (°F) at Energy*Solutions* Site	Long-Term Average Temperature (°F) at Dugway Sept 1950 – May 2010
January	-1.6	29.1	27.2
February	0.2	32.4	33.9
March	5.2	41.4	41.3
April	9.5	49.1	49.3
May	15.7	60.3	58.9
June	20.9	69.6	69.1
July	26.4	79.5	78.1
August	24.9	76.8	75.6
September	18.3	64.9	64.6
October	10.1	50.2	51.4
November	2.8	37.0	38.1
December	-2.4	27.7	28.4

Data Sources: Energy*Solutions* 17-year data: MSI (2010)
Dugway 1950-2010 data: Western Regional Climate Center (WRCC, 2010)

Figure 4. Comparison of 12-Year Mean Monthly Temperature at Clive (July 1992 – Dec 2009) with Long-term at Dugway (Sept 1950 – May 2010)

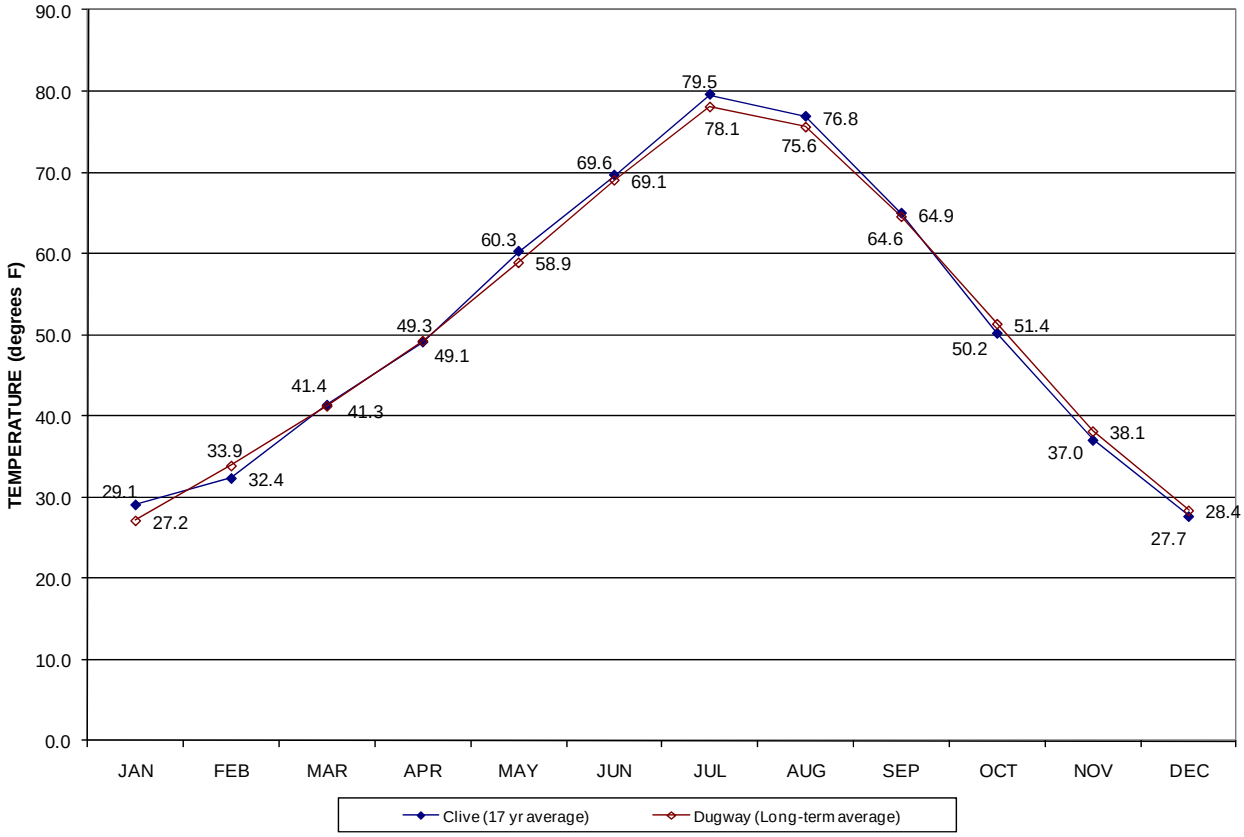

2.2.4 Solar Radiation Data

The synthetic generation of solar radiation data is a strong function of precipitation, therefore the precipitation data sets were generated first, followed by temperature, followed by solar radiation. The solar radiation data set was generated by first generating precipitation data (based the long-term average of 8.53 in/yr), then generating synthetic temperature data (based on long-term mean monthly temperatures at the Energy*Solutions* Clive meteorological station), then generating the solar radiation data using the location coefficients for Salt Lake City and the latitude (40°41'15", 40.6858°) for the Clive site.

Solar radiation data collected at the site over a 17-year period indicates that the maximum solar radiation occurs in June and averages 674 Langleys per day (MSI, 2010).

2.3 Landfill Soil and Design Data

The design of the CAW cell is similar to the design of the existing Class A cell, with a larger footprint. At completion, the CAW disposal cell will occupy 2,569 x 2,259 feet (approximately 133 acres). The cell will be excavated into the native Unit 4 silty clay soil. Waste will be placed above a layer of compacted Unit 4 clayey soils, and covered with a layered engineered cover constructed of natural (no man-made) materials. The top slopes of the cell will be finished at a 4.0% grade, with side slopes no steeper than 5:1 (20%).

The cover design is engineered to reduce infiltration, prevent erosion, and protect from radionuclide exposure. As shown in Figure 5, the landfill design includes both a low-angled top slope and steeper side slope section of the cover. The layers to be used in the CAW top slope cover are listed in Table 8, and consist of the following, from bottom to top:

- Lower liner. The cell will be lined with a 2-foot thick layer of compacted clayey native soil (Unit 4). This bottom clay liner will be constructed with a field hydraulic conductivity of $1.0x10^{-6}$ centimeters per second (cm/sec) or less.
- Waste. The waste layer will not exceed a final thickness of 75.3 feet above the top of the clay bottom liner. The height of waste at the shoulder of the top slope (the contact between the top slope and side slope) will be approximately 37.6 feet. Therefore the average waste height in the top slope area is 56.5 feet ((75.3+37.6)/2). Since the moisture contents of the waste in the model are initialized to steady state (no moisture goes into or out of storage in the waste), the model is completely insensitive to waste thickness. A unit thickness of 100 inches was used for the waste in all model runs.
- Radon Barrier. The top slope cover design contains an upper radon barrier consisting of 12 inches of compacted clay with a maximum hydraulic conductivity of $5x10^{-8}$ cm/sec and a lower radon barrier consisting of 12 inches of compacted clay with a hydraulic conductivity of $1x10^{-6}$ cm/sec or less.
- Filter Zone (Lower). Six inches of Type-B filter material will be placed above the radon barrier in the top slope cover. This filter material ranges in size from <0.187 to 1.5 inches, with 100% passing a 1 1/2-inch sieve, 24.5% passing a 3/4-inch sieve, and 0.4% passing a no. 4 sieve (0.187 inch). The Type-B size gradation corresponds to a coarse sand and fine gravel mix, according to the Universal Soil Classification System.
- Sacrificial Soil (Frost Protection Layer). A 12-inch layer consisting of a mixture of silty sand and gravel will be placed above the lower filter zone to protect the lower layers of the cover from freeze/thaw effects. The sacrificial soil material ranges in size from <0.003 to 0.75 inches, with 100% passing a 3/4-inch sieve, 50.2% passing a no. 8 sieve (0.093 inch), and 7.6% passing a no. 200 sieve (0.003 inch).
- Filter Zone (Upper). Six inches of Type-A filter material, will be placed above the sacrificial soil in the top slope cover. The Type-A filter material ranges in size from <0.003 to 6.0 inches, with 100% passing a 6-inch sieve, 70% passing a 3-inch sieve, and not more than 10% passing a no. 10 sieve (0.079 inch). The Type-A size gradation corresponds to a poorly sorted mixture of coarse sand to coarse gravel and cobble, according to the Universal Soil Classification System.
- Rip Rap cobbles. Approximately 18-inches of Type-B rip rap will be placed on the top slopes, above the upper (Type-A) filter zone. The Type-B rip rap used on the top slopes ranges in size from <0.003 to 4.5 inches with a nominal diameter of approximately 1.25 to 2 inches. Engineering specifications indicate that not more than 50% of the Type B rip rap would pass a 1 1/4-inch sieve.

The design for the side slope is similar to the top slope (Figure 5), except for the thickness of the waste layer and the material used in the rip rap layer. The layers used in the CAW side slope cover are listed in Table 8 and consist of the following, from bottom to top:

- Lower liner. (Same design as top slope.)
- Waste. The thickness of waste will range from zero at the edge of the cell to 37.6 feet at the shoulder, for an average waste height of 18.8 feet ((0+37.6)/2). The side-slope infiltration modeling used a unit waste thickness of 100 inches, as discussed above for the top-slope simulations.
- Radon Barrier. (Same design as top slope.)
- Filter Zone (Lower). (Same design as top slope.)
- Frost Protection Layer (Sacrificial Soil). (Same design as top slope.)
- Filter Zone (Upper). (Same design as top slope.)

- Rip Rap cobbles. Approximately 18-inches of Type-A rip rap will be placed on the side slopes above the Type-A filter zone. The Type-A rip rap ranges in size from <0.003 to 16 inches (equivalent to coarse gravel to boulders) with a nominal diameter of 12 inches. Engineering specifications indicate that 100% of the Type-A rip rap would pass a 16-inch screen, not more than 50% would pass a 4 1/2-inch screen, and not more than 5% would pass a no. 200 sieve (0.003-inch).

Figure 5. Insert 11x17 CAW Cover Detail

Table 8. Class A West Cell HELP Model Layers and Material Properties

TOP SLOPE DESIGN - CLASS A WEST CELL										
Layer	Material	Thickness (inches)	n (v/v)	θ_{fc} (v/v)	θ_{wp} (v/v)	θ_i (v/v)	K_s (cm/sec)	Layer Type n/a	Size (inches)	Material Description
Layer 1	Type-B Rip Rap	18	0.190	0.024	0.007	initialized to ss	42	vertical percolation	0.75-4.5	1.25 inches
Layer 2	Type-A Filter (upper)	6	0.190	0.024	0.007	initialized to ss	42	vertical percolation	0.08-6.0	Coarse Sand - Fine Cobble
Layer 3	Sacrificial Soil	12	0.31	0.2	0.025	initialized to ss	4.00E-03	vertical percolation	<0.75	Silty Sand and Gravel
Layer 4	Type-B Filter (lower)	6	0.28	0.032	0.013	initialized to ss	3.5	lateral drainage	0.2-1.5	Coarse Sand -Fine Gravel
Layer 5	Upper Radon Barrier	12	0.430	0.390	0.28	0.43	5.00E-08	barrier soil	n/a	Clay
Layer 6	Lower Radon Barrier	12	0.430	0.390	0.28	initialized to ss	1.00E-06	vertical percolation	n/a	Clay
Layer 7	Waste	100	0.437	0.062	0.024	initialized to ss	5.00E-04	vertical percolation	n/a	Sand
Layer 8	Clay Liner	24	0.430	0.390	0.28	0.43	1.00E-06	barrier soil	n/a	Clay

SIDE SLOPE DESIGN - CLASS A WEST CELL										
Layer	Material	Thickness (inches)	n (v/v)	θ_{fc} (v/v)	θ_{wp} (v/v)	θ_i (v/v)	K_s (cm/sec)	Layer Type n/a	Size (inches)	Material Description
Layer 1	Type-A Rip Rap	18	0.170	0.007	0.003	initialized to ss	80	vertical percolation	2.0-16.0	12 inches
Layer 2	Type-A Filter (upper)	6	0.190	0.024	0.007	initialized to ss	42	vertical percolation	0.08-6.0	Coarse Sand - Fine Cobble
Layer 3	Sacrificial Soil	12	0.31	0.2	0.025	initialized to ss	4.0E-03	vertical percolation	<0.75	Silty Sand and Gravel
Layer 4	Type-B Filter (lower)	6	0.28	0.032	0.013	initialized to ss	3.5	lateral drainage	0.2-1.5	Coarse Sand -Fine Gravel
Layer 5	Upper Radon Barrier	12	0.430	0.390	0.28	0.43	5.0E-08	barrier soil	n/a	Clay
Layer 6	Lower Radon Barrier	12	0.430	0.390	0.28	initialized to ss	1.0E-06	vertical percolation	n/a	Clay
Layer 7	Waste (Side Slopes)	100	0.437	0.062	0.024	initialized to ss	5.0E-04	vertical percolation	n/a	Sand
Layer 8	Clay Liner (Side Slope)	24	0.430	0.390	0.28	0.43	1.0E-06	barrier soil	n/a	Clay

Notes:
n = porosity
θ_{fc} = field capacity
θ_{wp} = wilting point
θ_i = initial moisture content
K_s = saturated hydraulic conductivity
n/a = not applicable
ss = steady state

2.3.1 Side Slope Run-On

The side-slope modeling includes the effects of run-on from the filter layers in the Top Slope. As described in previous reports, run-on or drainage from up-slope can be simulated by adjusting the slope length to an effective length (L'). The procedure is summarized as follows:

1. Run the HELP3 simulation on the up-slope panel (which is the Top Slope, in this case.) Note the initial volume estimate of drainage (D_u).
2. Run the simulation on the receiving (down-slope) panel using the actual slope length (L) for that section. Note the initial volume estimate of drainage (D_{d1}).
3. Determine an incremental increase in slope length (ΔL):

$$\Delta L = L \cdot \left(\frac{D_u}{D_d} \right)$$

4. Add the incremental increase in slope length to the initial slope length to determine the effective slope length:

$$L' = \Delta L + L$$

5. If the new estimate of drainage (D_{d2}) is significantly different from the previous estimate (D_{d1}), repeat the process to calculate a new effective length (L') and run the simulation again to compute a final estimate of drainage (D_d), runoff, evapotranspiration, and percolation.

The effective slope length calculations are shown in Table 9.

Table 9. CAW Cell HELP Infiltration Modeling – Effective Slope Length For Lateral Drainage Run-On To Side Slopes

RUN	DESCRIPTION	SLOPE LENGTH ft.	WIDTH ft.	AREA acres	PERC. in.	LATERAL DRAINAGE			ΔL	L'
							in.	ft^3/yr		
MT6	Upslope Drainage	942	100	2.163	0.094	D_u	3.191	25051		
MS6	Downslope Drainage, Without Run-on	188	100	0.432	0.080	D_{d1}	3.153	4940	953	1141
MS6-R1	Downslope Drainage, 1st Iteration	1141	100	0.432	0.146	D_{d2}	3.075	4818	978	1166
MS6-R2	Downslope Drainage, 2nd Iteration	1166	100	0.432	0.132	D_{d3}	3.077	4821	977	1165
MS6-R3	Downslope Drainage, 3rd Iteration	1165	100	0.432	0.132	D_{d4}	3.077	4821	977	1165

Note: PERC. = percolation
ΔL = change in slope length
L' = effective slope length

2.4 HELP Infiltration Modeling Results

The results of the HELP modeling runs are summarized in Table 10 and Table 11 and discussed in the following sections. The output files are provided in Attachment 1.

Table 10. CAW Cell HELP Infiltration Model Results

RUN:	CASE:	INFILTRATION (inches)	(cm)
MT6	Top-slope, 942 ft length, 6" Type-B filter	0.094	0.238
MS6	Side-slope, 188 ft length, 6" thick Type-B filter, no run-on	0.080	0.203
MS6-R1	Side-slope, 1141 ft length, 6" thick Type-B filter, with run-on, 1st iteration	0.146	0.371
MS6-R2	Side-slope, 1166 ft length, 6" thick Type-B filter, with run-on, 2nd iteration	0.132	0.335
MS6-R3	Side-slope, 1165 ft length, 6" thick Type-B filter, with run-on, 3rd iteration	0.132	0.335

Table 11. CAW Cell HELP Infiltration Model Water Balance Summary (in/yr)

HELP Results (inches of water)	Top Slope MT6	Side Slope MS6-R3
Precipitation	8.44	8.44
Runoff	0.035	0.041
Evapotranspiration	5.121	5.191
Drainage Collected from Type B Filter	3.191	3.077
Percolation/leakage through Upper Radon Barrier	0.094	0.132
Average Head on Top of Upper Radon Barrier	0.010	0.003
Percolation/Leakage through Clay Liner	0.094	0.132
Average Head on Top of Clay Liner	0.000	0.000
Change in Water Storage	0.000	0.000

2.4.1 Top Slope Infiltration Results

The top slope infiltration modeling indicates that an average of 0.094 in/yr (0.238 cm/yr) will infiltrate through the CAW cell top slope under long-term quasi-steady state. The infiltration rate is affected by the relatively long slope length, low precipitation, and lateral drainage layers. Because the moisture contents of the lower radon barrier in the model are initialized to steady state (no moisture goes into or out of storage in the lower radon barrier), the model is completely insensitive to lower radon barrier thickness.

2.4.2 Side Slope Infiltration Results

The side slope infiltration modeling indicates that an average of 0.132 in/yr (0.335 cm/yr) would infiltrate through the side slope cover. The infiltration rate is affected by the relatively long slope length, low precipitation, and lateral drainage layers. Because the moisture contents of the lower radon barrier in the model are initialized to steady state (no moisture goes into or out of storage in the lower radon barrier), the model is completely insensitive to lower radon barrier thickness.

3. MOISTURE CONTENT (UNSAT-H) MODELING

The UNSAT-H model was used to predict the moisture content in the radon barrier, waste, clay liner, and Unit 3 sand to the top of the aquifer. The final moisture content from UNSAT-H is used as input to the contaminant transport modeling (PATHRAE). Although the HELP model does report the final moisture content in each model layer for each simulation, the UNSAT-H model is considered to be more accurate with regard to predicting moisture content.

3.1 UNSAT-H Code

The UNSAT-H code was developed at Pacific Northwest Laboratory for assessing the water dynamics of arid sites which are used or proposed for near-surface waste disposal. The code can be used to estimate recharge/percolation rates and to assist in optimizing barrier design. Groundwater flow in the vadose zone is modeled using a one-dimensional finite-difference analysis.

The UNSAT-H code models groundwater flow in the unsaturated zone using a modified form of the Richards Equation (Richards, 1931), which describes the change in water storage and redistribution at every point within the soil profile. The flows across the boundaries of the profile are represented by specified fluxes (precipitation, evaporation, and drainage). The Richards Equation is given by:

$$C(h)\frac{\partial h}{\partial t} = \frac{\partial}{\partial z}\left(K_l(h)\frac{\partial H}{\partial z} \right)$$

where C(h) represents the negative of the specific moisture capacity (L^3/L^3T)
h is the negative of ψ, the matric (or suction) head potential (L/T)
$K_l(h)$ is the unsaturated hydraulic conductivity function
H is the total hydraulic head (L)

To solve the flow equation, UNSAT-H was supplied with van Genuchten parameters, which define the soil water retention curve, and saturated hydraulic conductivity values. Given the relationships for both hydraulic conductivity and water content as functions of suction head (h), UNSAT-H calculates the capacity term (C). Simply stated, where the volumetric water content in a soil exceeds the soil capacity, water flows downward in response to gravity.

UNSAT-H also has the ability to model heat flow and vapor diffusion. These features were not invoked in the CAW cell model, because the vadose zone modeled below the CAW cell is considered to be below the influence of surface heat flux and above any significant geothermal gradient.

UNSAT-H calculates the unsaturated hydraulic conductivity at each node, at each time step, based on user specifications for the hydraulic conductivity model. The Mualem hydraulic conductivity model (the Mualem [m = 1-(1/n)] restriction) was imposed during this modeling exercise, in part because it is recommended for all data sets except for those having a very well-defined soil water retention data set. Also, it is necessary to invoke one of the restrictions ([m = 1-(1/n)], [m = 1-(2/n)] or $n\rightarrow\infty$) for structured (clay) or coarse-textured (filter zone) soils, and the Mualem [m = 1-(1/n)] restriction is consistent with previous modeling.

3.1.1 UNSAT-H Model Limitations

The UNSAT-H code is strictly one-dimensional. As such, it is not suited to the analysis of facility designs that route water laterally (Meyer, et al., 1996). Because the UNSAT-H model was used only to determine the moisture contents and unsaturated hydraulic conductivities (HELP performed the water balance, including lateral water routing), this limitation is not of concern in the current application of the model. Also, the version of UNSAT-H code used (ver. 2.05) allows a maximum of 5 layers per model.

Another consideration is that careful user oversight is required to avoid potentially large mass balance errors, especially when modeling arid environments (Meyer, et al, 1996). The model calculation variables were adjusted in this modeling exercise to prevent overly large mass balance errors.

3.2 UNSAT-H Node Geometry

The UNSAT-H model node geometry started at the top of the radon barrier and included the waste, clay liner, and the Unit 3 sand. The waste was modeled using the approximate average[2] thickness of 1,737 cm (57 feet) in the top slope area and 579 cm (19 feet) in the side slope area.

The vertical distance was discretized into nodes, with a finer nodal spacing near layer boundaries and a coarser nodal spacing toward the center of each material layer. In the top slope model, a total of 129 nodes were used to represent the 30.5 cm (12 inches) of upper radon barrier, 30.5 cm (12 inches) of lower radon barrier, 1,737 cm of waste (57 feet), 61 cm (24 inches) of clay liner, and 409 cm (13.4 feet) of Unit 3 sand, with a maximum nodal spacing of 337 cm and a minimum of 0.1 cm. In the side slope model, a total of 125 nodes were used to represent the 30.5 cm (12 inches) of upper radon barrier, 30.5 cm (12 inches) of lower radon barrier, 579 cm of waste (19 feet), 61 cm (24 inches) of clay liner, and 409 cm (13.4 feet) of Unit 3 sand, with a maximum nodal spacing of 128 cm and a minimum of 0.1 cm. The node geometry used for each UNSAT-H model is shown in Table 12.

Table 12. Layer Thicknesses Used in UNSAT-H Model Runs

Model	# of Nodes	Upper Radon Barrier (cm)	Lower Radon Barrier (cm)	Waste (cm)	Clay Liner (cm)	Unit 3 Sand (cm)
Top Slope	129	30.5	30.5	1,737	61	409
Side Slope	125	30.5	30.5	579	61	409

The Unit 3 sand underlying the CAW cell was modeled with a thickness of 13.4 feet (Table 14), which is the distance from the base of the clay liner to the top of the aquifer. The top and base of the clay liner occur at design elevations of 4,265.0 and 4,263.0 ft, respectively. The top of the aquifer occurs at an average elevation of 4,249.6 ft, based on fresh water heads calculated from saline heads measured in 39 wells near the CAW cell in August 2010 (Table 13). The use of the average water level from these 39 wells is conservative, because the length of the capillary zone calculated by UNSAT-H was subtracted from the vertical transport distance in the PATHRAE model, thus decreasing the vertical transport distance even further. The standard deviation of freshwater heads in the 39 wells is 0.49 ft (Table 13), indicating relatively little spatial variation in freshwater equivalent heads beneath the disposal cell in August 2010.

[2] The UNSAT-H model runs use an approximate average waste thickness of 57 feet for the top slope and 19 feet for the side slope, compared to the design average waste thicknesses of 56.5 feet and 18.8 feet. The model is insensitive to slight differences in waste thickness, with respect to the final stabilized moisture content in the waste profile.

Table 13. Groundwater Elevation Below the CAW Cell

Well ID	STATE PLANE COORDINATES		Top of Casing	Depth to Water	Fresh Water Correction	Fresh Water Groundwater Elevation
	(feet)	(feet)	(feet)	(feet)	(feet)	(feet)
GW-25	1191653.78	7423063.07	4276.24	26.03	5.04	4250.40
GW-26	1190914.85	7423076.13	4274.67	24.37	3.86	4250.46
GW-27	1190080.14	7423096.01	4272.43	22.50	4.77	4250.10
GW-81	1190443.90	7424663.46	4276.78	27.14	4.90	4249.81
GW-82	1190775.09	7424656.41	4276.81	27.12	4.82	4249.84
GW-83	1191104.52	7424649.76	4276.90	27.25	4.70	4249.78
GW-84	1191437.33	7424643.60	4277.29	27.70	4.55	4249.73
GW-85	1191760.63	7424637.19	4277.88	28.49	4.40	4249.53
GW-86	1192156.78	7424629.75	4278.15	29.07	6.31	4249.26
GW-88	1192544.56	7424621.61	4279.58	30.38	3.28	4249.31
GW-89	1192538.62	7424228.21	4279.35	30.02	3.36	4249.45
GW-90	1192532.94	7423836.73	4278.76	29.28	3.82	4249.58
GW-91	1192526.75	7423442.09	4278.48	29.00	3.82	4249.61
GW-92	1192519.86	7423043.16	4279.05	28.80	4.02	4250.32
GW-93	1192132.23	7423053.12	4277.86	27.81	4.70	4250.23
GW-94	1191333.27	7423069.20	4276.55	26.30	5.32	4250.43
GW-95	1190503.49	7423084.58	4274.63	24.71	3.82	4250.07
GW-99	1190086.62	7423490.09	4273.71	23.70	4.19	4250.14
GW-100	1190095.32	7423883.07	4274.37	24.51	3.91	4249.97
GW-101	1190103.65	7424276.48	4275.03	25.50	5.77	4249.70
GW-102	1190112.50	7424670.52	4275.47	25.88	5.39	4249.77
GW-106	1190128.01	7424985.74	4276.18	26.80	7.71	4249.62
GW-107	1190138.43	7425378.55	4276.26	26.50	7.87	4249.99
GW-108	1190148.09	7425724.70	4275.96	26.26	7.95	4249.95
GW-109	1190431.34	7425719.12	4276.46	26.99	7.49	4249.67
GW-110	1190759.58	7425712.95	4276.72	27.38	7.31	4249.53
GW-111	1191086.37	7425706.84	4277.07	27.72	7.18	4249.56
GW-112	1191421.81	7425701.46	4277.40	28.40	6.87	4249.25
GW-113	1191832.38	7425665.32	4278.80	29.77	6.22	4249.26
GW-114	1191980.82	7425661.87	4279.19	30.36	5.74	4249.00
GW-115	1192131.65	7425659.50	4279.87	30.82	5.72	4249.26
GW-116	1192281.72	7425655.99	4280.68	31.83	5.07	4249.03
GW-117	1192491.00	7425331.85	4279.84	31.16	5.48	4248.88
GW-125	1192483.38	7424975.36	4280.27	31.19	5.59	4249.24
GW-137	1191789.80	7425698.91	4278.43	29.52	4.87	4249.05
GW-138	1192096.34	7425695.21	4279.42	30.65	5.69	4248.94
GW-139	1192429.66	□ÿ25689.53	4282.92	34.27	3.71	4248.72
GW-140	1192424.28	7425362.15	4280.88	32.20	5.17	4248.81
GW-141	1192420.84	7425032.89	4280.19	31.32	-4.22	4248.78
Mean Elevation						**4249.59**
Standard Deviation						**0.49**

Note: Depth to water measured August 2010

Table 14. Thickness of Unsaturated Unit 3 Sand Below the CAW Cell

Top of Clay Elevation	4265.0	ft amsl
Clay thickness	2.0	ft
Base of clay elevation	4263.0	ft amsl
Water table elevation (Aug 2010)	4249.6	ft amsl
Thickness of unsaturated Unit 3 Sand	**13.4**	**ft**

3.3 Boundary Conditions

The lower boundary of the model was set at a constant head of zero cm, to represent the top of the water table. The layers modeled in UNSAT-H are located below the zone of evaporation and drainage. Therefore, evaporation at the upper boundary was set to zero and "precipitation" was set to the percolation rate predicted by the HELP model.

The upper boundary of the model received moisture as a constant, steady-state application to the top of the radon barrier. The average annual infiltration predicted by HELP was distributed over 24 hours per day, 365 days per year. For the top slope simulation, the infiltration was applied at a rate of 0.00065 cm/day, which equals the 0.238238 cm/yr of total infiltration calculated by HELP model run MT6 (Table 15). For the side slope simulation, the infiltration was applied at a rate of 0.00092 cm/day, which equals the 0.335 cm/yr of total infiltration calculated by HELP model run MS6-R3 (Table 15).

Table 15. Steady-State Seepage Applied to UNSAT-H Model

Cell Area	Top Slope	Side Slope
HELP Model Run	MT6	MS6-R3
Infiltration (inches/yr)	0.094	0.132
Infiltration (cm/yr)	0.238238	0.335
Infiltration (cm/day)	0.00065	0.00092
UNSAT-H Model Run	T6E_21	S6E_8

According to Meyer, et al. (1996), the UNSAT-H program predicts a higher infiltration rate when the precipitation is distributed as a 24-hour total. Therefore, this approach is conservative, and all of the applied water had the greatest opportunity to infiltrate into the radon barrier.

3.4 Initial Head Conditions

The suction head (Ψ) was iterated to quasi-steady state, in order to predict the long-term moisture content and velocity in the cover, waste, liner, and underlying soil. The suction head from each run was used as input to the next simulation. Each series was run for an adequate time (80 - 210 years), until quasi-steady state head conditions were achieved.

3.5 Material Properties

The UNSAT-H model with the van Genuchten option, required the input of θ_r, θ_s, K_s, α, n, and m for each material modeled. These included the radon barrier, waste, clay liner, and underlying Unit 3 Sand. The material properties used in the UNSAT-H modeling of the CAW waste disposal cell (Table 17) are similar to those used in previous modeling. The hydraulic conductivity of the Unit 3 sand is 7.53×10^{-4} cm/sec, which is the 90% UCL for the Unit 3 sand, based on 118 slug test results (Table 16). The geometric mean hydraulic conductivity of the 188 slug tests is 6.16×10^{-4} cm/sec (Table 16).

Table 16. Site-Wide Hydraulic Conductivity Values

(See large tables at end of report document)

Table 17. UNSAT-H Model Material Properties Input Parameters

Model	Van Genuchten Parameter	Upper Radon Barrier	Lower Radon Barrier	Waste	Clay Liner	Unit 3 Sand
Moisture Retention	θ_s	0.432	0.432	0.35	0.432	0.34
	θ_r	0.1	0.1	0.02	0.100	0.02
	α	0.003	0.003	0.115	0.003	0.055
	n	1.172	1.172	2.013	1.172	2.518
	m	Mualem	Mualem	Mualem	Mualem	Mualem
Conductivity	K_s (cm/sec)	5.00E-08	1.00E-06	5.00E-04	1.00E-06	7.53E-04
	α	0.003	0.003	0.115	0.003	0.055
	n	1.172	1.172	2.013	1.172	2.518
	m	Mualem	Mualem	Mualem	Mualem	Mualem
	l	4.5	4.5	0.5	4.5	0.5

NOTES:
θ_s = saturated moisture content (v/v)
θ_r = residual moisture content (v/v)
α = air entry pressure (bubbling pressure)
n = van Genuchten's n, fitting parameter
K_s = saturated hydraulic conductivity (cm/sec)
m = Mualem's m
l = pore connectivity parameter

3.6 UNSAT-H Modeling Results

The UNSAT-H model was run in ten year increments, using output heads from each model run as input into the successive run. Quasi-steady-state is achieved by running the model for sufficient time that moisture contents stabilize, and water is not taken into or released from storage. The model was run 21 times (210 years) for the top slope, 8 times (80 years) for the side slope design case, to approach quasi-steady-state conditions. The resulting moisture contents represent the long-term modeled moisture contents in the CAW cell materials and the underlying subsurface.

3.6.1 Moisture Content

The final average moisture content for each model material is summarized in Table 18. Moisture content versus depth for the CAW cell top slope and side slope design are listed in Table 19 and Table 20 and the results are shown graphically in Figure 6 and Figure 7.

The clay layers in the cover and liner of the CAW cell retain high volumetric moisture contents (approximately 0.42 v/v) while the waste and native soil layers have relatively low moisture contents (Table 18). For the top slope model with 0.238 cm/yr infiltration, the average moisture content stabilized at 0.0573 v/v in the waste and 0.0434 v/v in the native soil below the cell (Table 19). The predicted volumetric moisture contents for the CAW cell side slope model is slightly higher than for the top slope model, due to a higher infiltration rate. For the side slope model with 0.335 cm/yr infiltration, the average moisture content stabilized at 0.0599 v/v in the waste and 0.0451 v/v in the native soil below the cell (Table 20). The soil suction head versus depth for the CAW top slope and side slope design are shown in Figure 6 and Figure 7.

Table 18. UNSAT-H Model Results – Average Moisture Content in Waste, Clay Liner, and Unit 3 Sand

UNSAT-H Model Run			Average Moisture Content (v/v)				
Run Name	Description	Infiltration (cm/yr)	Radon Barrier (Upper)	Radon Barrier (Lower)	Waste	Clay Liner	Unit 3 Sand
T6E_21	Top Slope, 0.238 cm/yr	0.238	0.4245	0.4232	0.0573	0.4182	0.0434
S6E_8	Side Slope, 0.335 cm/yr	0.335	0.4260	0.4238	0.0599	0.4191	0.0451

3.6.2 Capillary Fringe

The moisture content of the Unit 3 sand was determined for the zone from the bottom of the clay liner to the top of the capillary fringe. This approach is conservative because 1) a higher vadose zone velocity is calculated using the lower moisture content ($v_v=q/n_e$) and 2) the length of the vertical path was decreased in the PATHRAE model to exclude the capillary fringe.

The UNSAT-H results for the top slope and side slope models (Figure 6 and Figure 7) indicate that the capillary fringe may extend as far as 62.3 cm above the water table. To account for this phenomenon, the distance from the bottom of the waste to the water table was decreased by 2.04 feet in PATHRAE runs, and the moisture contents from the vadose zone (omitting the capillary fringe) were used in determining vertical transport velocities.

Table 19. Moisture Content vs. Depth - UNSAT-H Results for CAW Cell Top Slope

TOP SLOPE, 0.238 cm/yr				
NODE NUMBER	DEPTH	θ	Average θ	Unit / Material
1	0.0	0.4271		Upper Radon Barrier
2	0.1	0.4271		Upper Radon Barrier
3	0.3	0.4271		Upper Radon Barrier
4	0.6	0.4270		Upper Radon Barrier
5	1.1	0.4270		Upper Radon Barrier
6	2.0	0.4269		Upper Radon Barrier
7	3.5	0.4267		Upper Radon Barrier
8	6.5	0.4264		Upper Radon Barrier
9	11.5	0.4257		Upper Radon Barrier
10	19.0	0.4244		Upper Radon Barrier
11	24.0	0.4233		Upper Radon Barrier
12	27.0	0.4226		Upper Radon Barrier
13	28.5	0.4222		Upper Radon Barrier
14	29.4	0.4219		Upper Radon Barrier
15	29.9	0.4218		Upper Radon Barrier
16	30.2	0.4217		Upper Radon Barrier
17	30.4	0.4216		Upper Radon Barrier
18	30.5	0.4216	0.4245	Upper Radon Barrier
19	30.6	0.4216		Lower Radon Barrier
20	30.8	0.4216		Lower Radon Barrier
21	31.1	0.4216		Lower Radon Barrier
22	31.6	0.4217		Lower Radon Barrier
23	32.5	0.4218		Lower Radon Barrier
24	34.0	0.4219		Lower Radon Barrier
25	37.0	0.4222		Lower Radon Barrier
26	42.0	0.4226		Lower Radon Barrier
27	49.5	0.4233		Lower Radon Barrier
28	54.5	0.4238		Lower Radon Barrier
29	57.5	0.4240		Lower Radon Barrier
30	59.0	0.4242		Lower Radon Barrier
31	59.9	0.4243		Lower Radon Barrier
32	60.4	0.4243		Lower Radon Barrier
33	60.7	0.4243		Lower Radon Barrier
34	60.9	0.4244		Lower Radon Barrier
35	61.0	0.4244	0.4232	Lower Radon Barrier
36	61.1	0.0574		Waste
37	61.3	0.0574		Waste
38	61.6	0.0574		Waste
39	62.1	0.0574		Waste
40	63.0	0.0574		Waste
41	64.5	0.0574		Waste
42	67.5	0.0574		Waste
43	72.5	0.0574		Waste
44	82.5	0.0574		Waste
45	102.5	0.0574		Waste
46	142.5	0.0574		Waste
47	222.5	0.0574		Waste
48	372.5	0.0575		Waste
49	592.5	0.0574		Waste
50	929.5	0.0575		Waste
51	1266.5	0.0574		Waste
52	1486.5	0.0575		Waste
53	1636.5	0.0574		Waste
54	1716.5	0.0575		Waste
55	1756.5	0.0567		Waste
56	1776.5	0.0542		Waste
57	1786.5	0.0508		Waste
58	1791.5	0.0476		Waste
59	1794.5	0.0446		Waste
60	1796.0	0.0425		Waste
61	1796.9	0.0408		Waste
62	1797.4	0.0397		Waste
63	1797.7	0.0390		Waste
64	1797.9	0.0384		Waste
65	1798.0	0.0381		Waste
66	1798.1	0.0378	0.0573	Waste

TOP SLOPE, 0.238 cm/yr				
NODE NUMBER	DEPTH	θ	Average θ	Unit / Material
67	1798.2	0.4158		Clay Liner
67	1798.2	0.4158		Clay Liner
68	1798.4	0.4158		Clay Liner
69	1798.7	0.4158		Clay Liner
70	1799.2	0.4158		Clay Liner
71	1799.9	0.4159		Clay Liner
72	1800.9	0.4159		Clay Liner
73	1802.4	0.4160		Clay Liner
74	1804.1	0.4162		Clay Liner
75	1808.1	0.4164		Clay Liner
76	1814.1	0.4169		Clay Liner
77	1824.1	0.4176		Clay Liner
78	1833.1	0.4183		Clay Liner
79	1843.1	0.4190		Clay Liner
80	1849.1	0.4195		Clay Liner
81	1853.1	0.4198		Clay Liner
82	1854.8	0.4200		Clay Liner
83	1856.3	0.4201		Clay Liner
84	1857.3	0.4202		Clay Liner
85	1858.0	0.4203		Clay Liner
86	1858.5	0.4203		Clay Liner
87	1858.8	0.4203		Clay Liner
88	1859.0	0.4203		Clay Liner
89	1859.1	0.4203	0.4182	Clay Liner
90	1859.2	0.0404		Unit 3 Sand
91	1859.4	0.0404		Unit 3 Sand
92	1859.7	0.0404		Unit 3 Sand
93	1860.2	0.0404		Unit 3 Sand
94	1860.9	0.0404		Unit 3 Sand
95	1861.9	0.0404		Unit 3 Sand
96	1863.4	0.0404		Unit 3 Sand
97	1865.4	0.0404		Unit 3 Sand
98	1868.4	0.0404		Unit 3 Sand
99	1872.4	0.0404		Unit 3 Sand
100	1878.4	0.0404		Unit 3 Sand
101	1888.4	0.0404		Unit 3 Sand
102	1903.4	0.0404		Unit 3 Sand
103	1921.4	0.0404		Unit 3 Sand
104	1942.4	0.0404		Unit 3 Sand
105	1966.4	0.0404		Unit 3 Sand
106	1990.4	0.0404		Unit 3 Sand
107	2014.4	0.0404		Unit 3 Sand
108	2038.4	0.0404		Unit 3 Sand
109	2064.5	0.0404		Unit 3 Sand
110	2088.5	0.0405		Unit 3 Sand
111	2112.5	0.0407		Unit 3 Sand
112	2136.5	0.0415		Unit 3 Sand
113	2160.5	0.0445		Unit 3 Sand
114	2184.5	0.0525		Unit 3 Sand
115	2205.5	0.0684	0.0434	Unit 3 Sand
116	2223.5	0.0980		Unit 3 Sand – Capillary Fringe
117	2238.5	0.1524		Unit 3 Sand – Capillary Fringe
118	2248.5	0.2210		Unit 3 Sand – Capillary Fringe
119	2254.5	0.2752		Unit 3 Sand – Capillary Fringe
120	2258.5	0.3089		Unit 3 Sand – Capillary Fringe
121	2261.5	0.3273		Unit 3 Sand – Capillary Fringe
122	2263.5	0.3350		Unit 3 Sand – Capillary Fringe
123	2265.0	0.3383		Unit 3 Sand – Capillary Fringe
124	2266.0	0.3394		Unit 3 Sand – Capillary Fringe
125	2266.7	0.3398		Unit 3 Sand – Capillary Fringe
126	2267.2	0.3400		Unit 3 Sand – Capillary Fringe
127	2267.5	0.3400		Unit 3 Sand – Capillary Fringe
128	2267.7	0.3400		Unit 3 Sand – Capillary Fringe

Table 20. Moisture Content vs. Depth - UNSAT-H Results for CAW Cell Side Slope

SIDE SLOPE, 0.335 cm/yr				
NODE NUMBER	DEPTH	θ	Average θ	Unit / Material
1	0.0	0.4290		Upper Radon Barrier
2	0.1	0.4290		Upper Radon Barrier
3	0.3	0.4290		Upper Radon Barrier
4	0.6	0.4290		Upper Radon Barrier
5	1.1	0.4289		Upper Radon Barrier
6	2.0	0.4288		Upper Radon Barrier
7	3.5	0.4287		Upper Radon Barrier
8	6.5	0.4283		Upper Radon Barrier
9	11.5	0.4276		Upper Radon Barrier
10	19.0	0.4261		Upper Radon Barrier
11	24.0	0.4247		Upper Radon Barrier
12	27.0	0.4237		Upper Radon Barrier
13	28.5	0.4232		Upper Radon Barrier
14	29.4	0.4228		Upper Radon Barrier
15	29.9	0.4226		Upper Radon Barrier
16	30.2	0.4225		Upper Radon Barrier
17	30.4	0.4224		Upper Radon Barrier
18	30.5	0.4224	.4260	Upper Radon Barrier
19	30.6	0.4224		Lower Radon Barrier
20	30.8	0.4224		Lower Radon Barrier
21	31.1	0.4224		Lower Radon Barrier
22	31.6	0.4224		Lower Radon Barrier
23	32.5	0.4225		Lower Radon Barrier
24	34.0	0.4226		Lower Radon Barrier
25	37.0	0.4229		Lower Radon Barrier
26	42.0	0.4233		Lower Radon Barrier
27	49.5	0.4240		Lower Radon Barrier
28	54.5	0.4244		Lower Radon Barrier
29	57.5	0.4247		Lower Radon Barrier
30	59.0	0.4248		Lower Radon Barrier
31	59.9	0.4249		Lower Radon Barrier
32	60.4	0.4249		Lower Radon Barrier
33	60.7	0.4250		Lower Radon Barrier
34	60.9	0.4250		Lower Radon Barrier
35	61.0	0.4250	.4238	Lower Radon Barrier
36	61.1	0.0605		Waste
37	61.3	0.0605		Waste
38	61.6	0.0605		Waste
39	62.1	0.0605		Waste
40	63.0	0.0605		Waste
41	64.5	0.0605		Waste
42	67.5	0.0605		Waste
43	72.5	0.0605		Waste
44	82.5	0.0605		Waste
45	102.5	0.0605		Waste
46	142.5	0.0605		Waste
47	222.5	0.0604		Waste
48	350.5	0.0605		Waste
49	478.5	0.0604		Waste
50	558.5	0.0605		Waste
51	598.5	0.0599		Waste
52	618.5	0.0574		Waste
53	628.5	0.0538		Waste
54	633.5	0.0503		Waste
55	636.5	0.0470		Waste
56	638.0	0.0446		Waste
57	638.9	0.0427		Waste
58	639.4	0.0415		Waste
59	639.7	0.0406		Waste
60	639.9	0.0400		Waste
61	640.0	0.0396		Waste
62	640.1	0.0393	.0599	Waste
63	640.2	0.4169		Clay Liner

SIDE SLOPE, 0.335 cm/yr				
NODE NUMBER	DEPTH	θ	Average θ	Unit / Material
64	640.4	0.4169		Clay Liner
65	640.7	0.4170		Clay Liner
66	641.2	0.4170		Clay Liner
67	641.9	0.4170		Clay Liner
68	642.9	0.4171		Clay Liner
69	644.4	0.4172		Clay Liner
70	646.1	0.4173		Clay Liner
71	650.1	0.4175		Clay Liner
72	656.1	0.4179		Clay Liner
73	666.1	0.4185		Clay Liner
74	675.1	0.4191		Clay Liner
75	685.1	0.4199		Clay Liner
76	691.1	0.4203		Clay Liner
77	695.1	0.4206		Clay Liner
78	696.8	0.4207		Clay Liner
79	698.3	0.4208		Clay Liner
80	699.3	0.4209		Clay Liner
81	700.0	0.4210		Clay Liner
82	700.5	0.4210		Clay Liner
83	700.8	0.4210		Clay Liner
84	701.0	0.4210		Clay Liner
85	701.1	0.4210	.4191	Clay Liner
86	701.2	0.0424		Unit 3 Sand
87	701.4	0.0424		Unit 3 Sand
88	701.7	0.0424		Unit 3 Sand
89	702.2	0.0424		Unit 3 Sand
90	702.9	0.0424		Unit 3 Sand
91	703.9	0.0424		Unit 3 Sand
92	705.4	0.0424		Unit 3 Sand
93	707.4	0.0424		Unit 3 Sand
94	710.4	0.0424		Unit 3 Sand
95	714.4	0.0424		Unit 3 Sand
96	720.4	0.0424		Unit 3 Sand
97	730.4	0.0424		Unit 3 Sand
98	745.4	0.0424		Unit 3 Sand
99	763.4	0.0424		Unit 3 Sand
100	784.4	0.0424		Unit 3 Sand
101	808.4	0.0424		Unit 3 Sand
102	832.4	0.0424		Unit 3 Sand
103	856.4	0.0424		Unit 3 Sand
104	880.4	0.0424		Unit 3 Sand
105	906.5	0.0424		Unit 3 Sand
106	930.5	0.0424		Unit 3 Sand
107	954.5	0.0425		Unit 3 Sand
108	978.5	0.0431		Unit 3 Sand
109	1002.5	0.0455		Unit 3 Sand
110	1026.5	0.0529		Unit 3 Sand
111	1047.5	0.0685	.0451	Unit 3 Sand
112	1065.5	0.0980		Unit 3 Sand – Capillary Fringe
113	1080.5	0.1524		Unit 3 Sand – Capillary Fringe
114	1090.5	0.2210		Unit 3 Sand – Capillary Fringe
115	1096.5	0.2752		Unit 3 Sand – Capillary Fringe
116	1100.5	0.3089		Unit 3 Sand – Capillary Fringe
117	1103.5	0.3273		Unit 3 Sand – Capillary Fringe
118	1105.5	0.3350		Unit 3 Sand – Capillary Fringe
119	1107.0	0.3383		Unit 3 Sand – Capillary Fringe
120	1108.0	0.3394		Unit 3 Sand – Capillary Fringe
121	1108.7	0.3398		Unit 3 Sand – Capillary Fringe
122	1109.2	0.3400		Unit 3 Sand – Capillary Fringe
123	1109.5	0.3400		Unit 3 Sand – Capillary Fringe
124	1109.7	0.3400		Unit 3 Sand – Capillary Fringe
125	1109.8	0.3400		Unit 3 Sand – Capillary Fringe

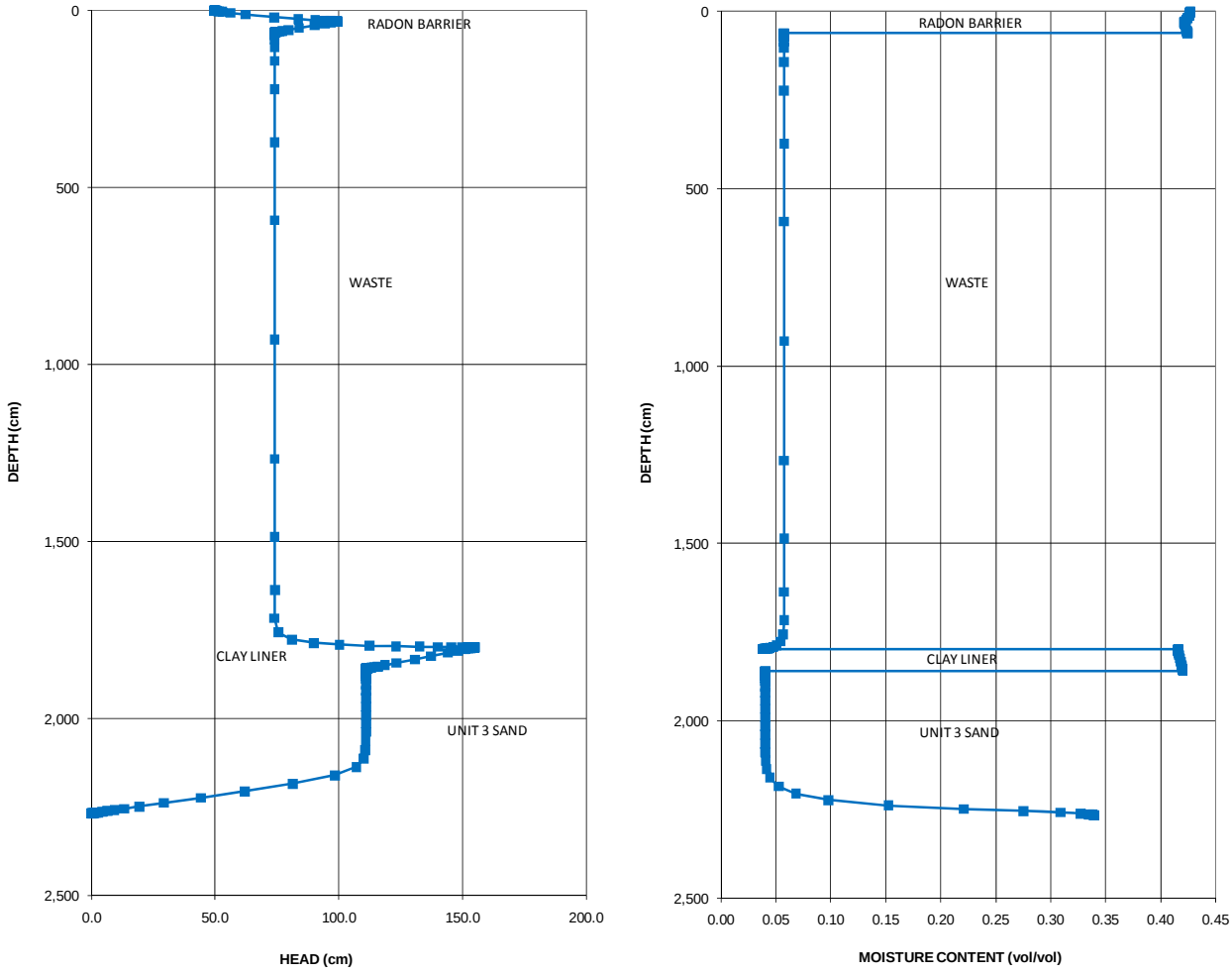

Figure 6. Suction Head and Moisture Content vs. Depth Below Top of Radon Barrier – UNSAT-H Top Slope Model Results

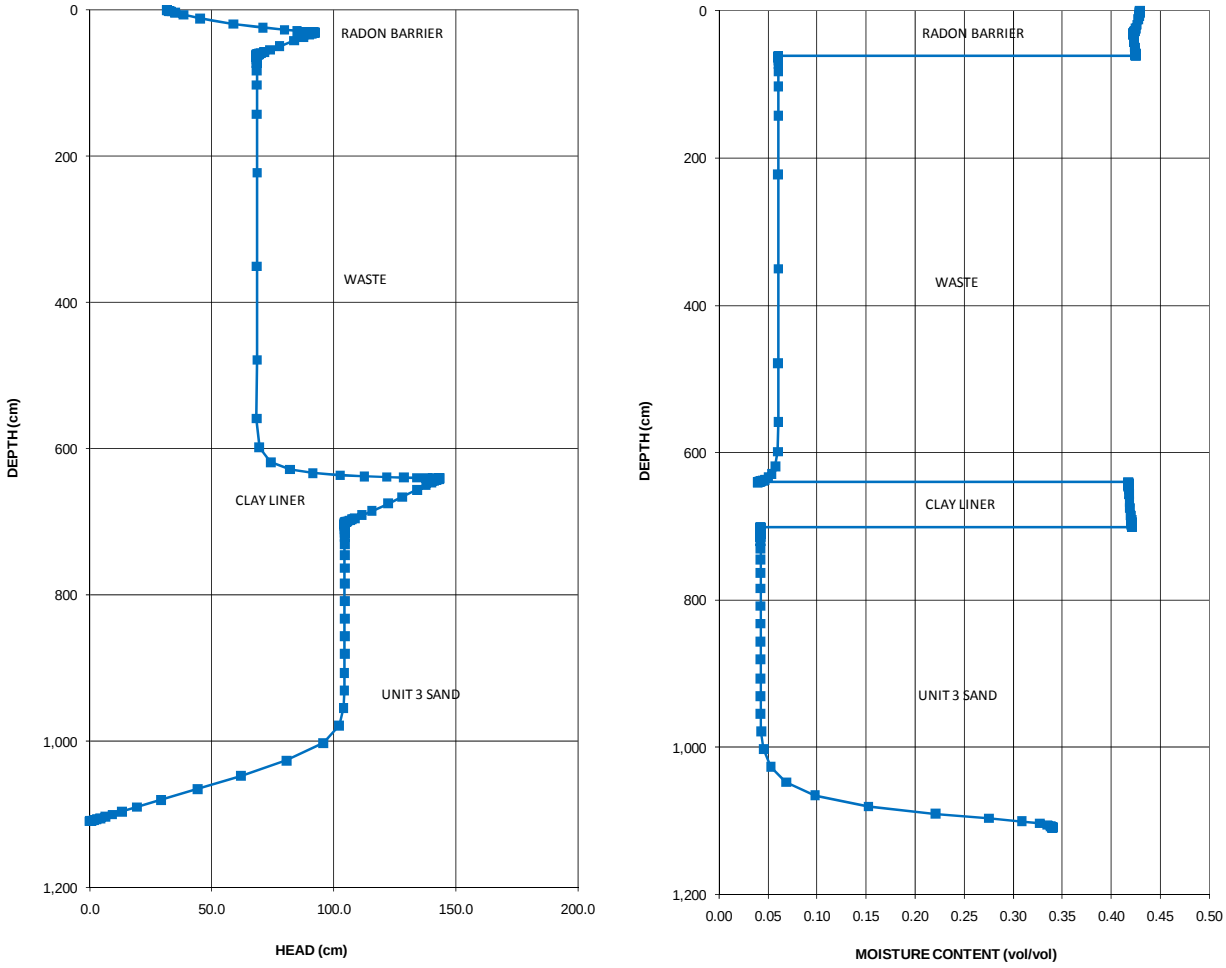

Figure 7. Suction Head and Moisture Content vs. Depth Below Top of Radon Barrier – UNSAT-H Side Slope Model Results

4. FATE AND TRANSPORT MODELING APPROACH

4.1 PATHRAE Code

Transport modeling was performed using the PATHRAE-RAD Performance Assessment Code for the Land Disposal of Radioactive Wastes (Merrell, et. al, 1995). The PATHRAE code was first developed for the US EPA in the 1980s, for use in assessing the maximum annual dose to a critical population group resulting from the disposal of "below regulatory concern" (BRC) wastes. The CAW cell modeling used the PATHRAE-RAD version of the code, which was released on February 9, 1995 (code) and March 1995 (documentation). A modification to the code to allow for more than 10 output times was made by Adrian Brown Consultants in 1997, was verified in the 1998 modeling report (ABC, 1998).

The PATHRAE code is generally made up of three components: release, transport, and uptake solutions. The model calculates a closed form solution for dose (or concentration) at a point in each pathway at a user-specified set of times. The code can be used to simulate multiple transport/receptor pathways. In the CAW cell model, the groundwater to a river pathway was applied, in order to determine the concentration at a compliance point located 90 feet from the edge of the disposal cell. The three PATHRAE components are described below:

- *Release.* PATHRAE uses a constant rate for predicting the release of contaminants from the waste, in the current modeling exercise. That is, the model assumes that the quantity of contaminant released each year is a constant fraction of the amount of waste initially present[3].
- *Transport.* The transport component of PATHRAE is similar to that in many other groundwater contaminant transport models. PATHRAE solves the advection/dispersion equation, includes aquifer diffusion, assumes that diffusion is Fickian, allows for retardation of contaminants using a blanket K_d (retardation coefficient), and includes radioactive decay.
- *Uptake.* PATHRAE also calculates the maximum annual doses to a receptor consuming river or well water and crops grown using that water. However, the groundwater protection levels for the Energy*Solutions* site are given as concentrations derived from dose/uptake conversions. Therefore, PATHRAE was used to determine concentrations, rather than dose.

If modeled constituents fail to meet applicable groundwater standards at the water table, then both a vertical transport path and a horizontal transport path are modeled. The vertical model is run first, to determine the arrival time and concentrations of constituents at the water table. The output from the vertical model is then input into the horizontal model, using the discrete dispersed source method which is described in previous reports.

4.2 Groundwater Protection Levels

Ground Water Protection Levels (GWPLs) are numerical standards that are set by UDEQ in the groundwater quality discharge permit. Groundwater in the vicinity of the site is defined as Class IV, saline ground water (UDEQ, 2009), and GWPLs for existing wells surrounding the Class A and Class A North cells (the site of the proposed CAW cell) were determined by UDEQ according to administrative rules for Class IV saline aquifers. GWPLs were set at the greater of either the Ground Water Quality Standard (GWQS) or the upper boundary of the Background Concentration[4]. Table 1A of the Permit lists

[3] The assumption that the release rate (leach rate) is constant over time is conservative. The release rate would actually decrease over time as the source term concentration decreases.

[4] The upper boundary of the Background Concentration was calculated as the mean concentration plus two standard deviations for each constituent in each individual well, based on Clive facility groundwater quality samples.

"universal" GWPLs that apply to all LARW, Class A, Class A North, and Evaporation Pond wells while Table 1B of the Permit lists GWPL exceptions that apply to specific LARW, Class A, Class A North, and Evaporation Pond wells.

The GWPLs listed in the Permit include only a portion of the 260 Class A radionuclides evaluated in the current modeling. Groundwater standards for the remaining nuclides (not specifically listed in the Permit) were developed from several sources, and all of the compiled standards are referred to as "GWPLs" for convenience. Table 21 lists the numeric GWPLs for all constituents modeled, along with the source of each GWPL. These sources include the following:

- Maximum contaminant levels (MCLs) and secondary MCLs (SMCLs) in drinking water established by UDEQ and the US EPA.
- Proposed drinking water standards for alpha emitters, as published in the EPA 1991 Proposed Rules, Federal Register, Vol. 56, No. 138, 40 CFR Parts 141 and 142, Appendix C - Alpha Emitters. The EPA's proposed standards for beta, gamma, and alpha emitters were also published in the Federal Register on April 21, 2000.
- Proposed drinking water standards for beta emitters, as published in the - EPA 1991 Proposed Rules, Federal Register, Vol. 56, No. 138, 40 CFR Parts 141 and 142, Appendix B - Beta Particle and Photon Emitters.
- Site specific GWPL exceptions established by UDEQ for the existing Class A and Class A North monitoring wells. These standards are listed in Table 1B of Energy*Solutions*' groundwater quality discharge permit.
- GWPLs used in previous modeling performed by UDEQ DRC.
- Calculated values using Federal Guidance Report (FGR) 11 or FGR 13. The most conservative (lowest) value calculated by Loren Morton (UDEQ DRC) were selected for nuclides which were not included in EPA's proposed rules or for which background GWPLs had not been established. GWPLs for two nuclides that were not provided in the spreadsheet from Loren Morton were calculated by Wayne Johns using FGR 11. Both Loren Morton and Wayne Johns calculated the GWPL using the following equation:

$$GWPL = \frac{4mrem(CEDE)}{Year} \times \frac{1ALI(\mu Ci)}{5000mrem} \times \frac{10^6\, pCi}{\mu Ci} \times \frac{1year}{365days} \times \frac{1day}{2Liters} = \frac{pCi}{Liter}$$

  Where: CEDE = committed effective dose equivalent
  ALI = annual limits of intake

- The GWPL for Nb-94 was also used for Nb-91 and Nb-92, because no values for these two nuclides are listed in MCLs, FGR 11, or FGR 13. The Nb-94 GWPL would be lower than those of Nb-91, Nb-92 based on radioactive half-life, decay products, and decay energies.
- GWPLs estimated using International Commission on Radiological Protection (ICRP) 30 (for Po-208, Po-209).

The final output from the PATHRAE model was compared to the GWPLs in Table 21 to determine the year in which the GWPL is first exceeded. The year to exceed is conservatively reported as the next *lowest* model output time.

Table 21. Ground Water Protection Levels (GWPLs) for CAW Cell Monitoring Wells

Radiological Constituents:

PARAMETER		GWPL (pCi/L)	GWPL (Ci/m^3)	Ref.
Actinium	Ac-227	1.27E+00	1.27E-09	2
Silver-108m	Ag-108m	7.23E+02	7.23E-07	2
Silver-110m	Ag-110m	5.12E+02	5.12E-07	2
Aluminum-26	Al-26	4.38E+02	4.38E-07	5
Americium-241	Am-241	6.45E+00	6.45E-09	1
Americium-242m	Am-242m	1.27E+00	1.27E-09	2
Americium-243	Am-243	6.49E+00	6.49E-09	1
Barium-133	Ba-133	1.52E+03	1.52E-06	2
Beryllium-7	Be-7	4.35E+04	4.35E-05	2
Beryllium-10	Be-10	1.10E+03	1.10E-06	5
Bismuth-207	Bi-207	1.01E+03	1.01E-06	2
Bismuth-210m	Bi-210m	3.46E+01	3.46E-08	4
Berkelium-247	Bk-247	5.48E-01	5.48E-10	4
Carbon-14	C-14	3.20E+03	3.20E-06	2
Calcium-41	Ca-41	3.29E+03	3.29E-06	5
Calcium-45	Ca-45	1.73E+03	1.73E-06	2
Cadmium-109	Cd-109	2.27E+02	2.27E-07	2
Cadmium-113	Cd-113	2.19E+01	2.19E-08	5
Cadmium-113m	Cd-113m	2.19E+01	2.19E-08	4
Californium-249	Cf-249	5.48E-01	5.48E-10	4
Californium-250	Cf-250	1.10E+00	1.10E-09	4
Californium-251	Cf-251	5.48E-01	5.48E-10	4
Californium-252	Cf-252	1.70E+01	1.70E-08	1
Chlorine-36	Cl-36	1.85E+03	1.85E-06	2
Curium-242	Cm-242	1.45E+02	1.45E-07	1
Curium-243	Cm-243	8.47E+00	8.47E-09	1
Curium-244	Cm-244	1.00E+01	1.00E-08	1
Curium-245	Cm-245	6.35E+00	6.35E-09	1
Curium-246	Cm-246	6.38E+00	6.38E-09	1
Curium-247	Cm-247	6.93E+00	6.93E-09	1
Curium-248	Cm-248	1.71E+00	1.71E-09	1
Cobalt-57	Co-57	4.87E+03	4.87E-06	2
Cobalt-60	Co-60	2.18E+02	2.18E-07	2
Cesium-134	Cs-134	8.13E+01	8.13E-08	2
Cesium-135	Cs-135	7.94E+02	7.94E-07	2
Cesium-137	Cs-137	1.19E+02	1.19E-07	2
Europium-152	Eu-152	8.41E+02	8.41E-07	2
Europium-154	Eu-154	5.73E+02	5.73E-07	2
Europium-155	Eu-155	3.59E+03	3.59E-06	2
Iron-55	Fe-55	9.25E+03	9.25E-06	2
Iron-60	Fe-60	7.96E+00	7.96E-09	4
Gadolinium-148	Gd-148	1.10E+01	1.10E-08	4
Tritium H-3	H-3	6.09E+04	6.09E-05	2
Mercury-194	Hg-194	2.19E+01	2.19E-08	4
Holmium-166m	Ho-166m	6.58E+02	6.58E-07	5
Iodine-129	I-129	2.10E+01	2.10E-08	2
Manganese-53	Mn-53	5.48E+04	5.48E-05	5
Sodium-22	Na-22	4.66E+02	4.66E-07	2
Niobium-91	Nb-91	7.07E+02	7.07E-07	6
Niobium-92	Nb-92	7.07E+02	7.07E-07	6
Niobium-93m	Nb-93m	1.05E+04	1.05E-05	2
Niobium-94	Nb-94	7.07E+02	7.07E-07	2
Nickel-59	Ni-59	2.70E+04	2.70E-05	2
Nickel-63	Ni-63	9.91E+03	9.91E-06	2
Neptunium-237	Np-237	7.19E+00	7.19E-09	1
Osmium-194	Os-194	1.28E+02	1.28E-07	4
Protactinium-231	Pa-231	1.02E+01	1.02E-08	1
Pb-202	Pb-202	5.48E+00	5.48E-09	5
Pb-203	Pb-203	5.05E+03	5.05E-06	2
Pb-210	Pb-210	1.01E+00	1.01E-09	2
Palladium-107	Pd-107	3.66E+04	3.66E-05	2
Promethium-145	Pm-145	1.10E+04	1.10E-05	5
Promethium-147	Pm-147	5.24E+03	5.24E-06	2
Polonium-208	Po-208	1.64E+00	1.64E-09	8
Polonium-209	Po-209	1.48E+00	1.48E-09	4
Platinum-193	Pt-193	4.61E+04	4.61E-05	2
Plutonium-236	Pu-236	3.33E+01	3.33E-08	1
Plutonium-238	Pu-238	7.15E+00	7.15E-09	1
Plutonium-239	Pu-239	6.49E+01	6.49E-08	1

Non-radiological Constituents:

PARAMETER	GWPL (mg/l)	GWPL (kg/m^3)
Arsenic	0.05	5.00E-05
Barium	2	2.00E-03
Beryllium	0.004	4.00E-06
Cadmium	0.005	5.00E-06
Chromium	0.1	1.00E-04
Copper	1.3	1.30E-03
Lead	0.015	1.50E-05
Mercury	0.002	2.00E-06
Molybdenum	0.04	4.00E-05
Nickel	0.1	1.00E-04
Selenium	0.05	5.00E-05
Silver	0.1	1.00E-04
Zinc	5	5.00E-03

Table 21. Ground Water Protection Levels (GWPLs) for CAW Cell Monitoring Wells (Continued)

PARAMETER		GWPL (pCi/L)	GWPL (Ci/m^3)	Ref.
Plutonium-240	Pu-240	6.49E+01	6.49E-08	1
Plutonium-241	Pu-241	1.60E+03	1.60E-06	7
Plutonium-242	Pu-242	6.83E+01	6.83E-08	1
Plutonium-244	Pu-244	7.02E+00	7.02E-09	1
Radium-226 + Radium-228	Ra-226	5.00E+00	5.00E-09	3
Rhenium-187	Re-187	5.82E+05	5.82E-04	2
Rubidium-83	Rb-83	6.58E+02	6.58E-07	5
Ruthenium-106	Ru-106	2.03E+02	2.03E-07	2
Selenium-79	Se-79	2.16E+02	2.16E-07	4
Silicon-32	Si-32	5.65E+02	5.65E-07	4
Samarium-151	Sm-151	1.41E+04	1.41E-05	2
Tin-121m	Sn-121m	2.26E+03	2.26E-06	2
Tin-126	Sn-126	2.29E+02	2.29E-07	2
Strontium-90	Sr-90	4.20E+01	4.20E-08	2
Tantalum-182	Ta-182	8.42E+02	8.42E-07	2
Terbium-157	Tb-157	2.19E+03	2.19E-06	5
Terbium-158	Tb-158	1.25E+03	1.25E-06	2
Technicium-99	Tc-99	3.79E+03	3.79E-06	2
Tellurium-123	Te-123	5.48E+02	5.48E-07	5
Thorium-229	Th-229	6.58E-01	6.58E-10	4
Thorium-230	Th-230	8.27E+01	8.27E-08	1
Thorium-232	Th-232	9.18E+01	9.18E-08	1
Titanium-44	Ti-44	7.26E+01	7.26E-08	4
Thallium-204	Tl-204	1.68E+03	1.68E-06	2
Thulium-170	Tm-170	1.03E+03	1.03E-06	2
Uranium-232	U-232	1.02E+01	1.02E-08	1
Uranium-233	U-233	2.56E+01	2.56E-08	1
Uranium-234	U-234	2.60E+01	2.60E-08	3
Uranium-235	U-235	2.65E+01	2.65E-08	1
Uranium-236	U-236	2.74E+01	2.74E-08	1
Uranium-238	U-238	2.60E+01	2.60E-08	3
Vanadium-50	V-50	2.19E+03	2.19E-06	5
Yttrium-88	Y-88	1.60E+02	1.60E-07	7
Zirconium-93	Zr-93	5.09E+03	5.09E-06	2
Zirconium-95	Zr-95	1.46E+03	1.32E-06	5

References:
1- EPA 1991 Proposed Rules, Federal Register, Vol. 56, No. 138, 40 CFR Parts 141 and 142, Appendix C - Alpha Emitters.
2- EPA 1991 Proposed Rules, Federal Register, Vol. 56, No. 138, 40 CFR Parts 141 and 142, Appendix B - Beta Particle and Photon Emitters.
3- Universal GWPL listed in Table 1A, Permit No. UGW450005.
4- Most conservative (lowest) value provided in spreadsheet from Loren Morton (UDEQ DRC).
5- Calculated based on FGR-11
6- Not listed in MCLs, FGR 11, or FGR 13. The Ni-94 GWPL was used, and would be lower than Ni-91, -92 based on radioactive half-life, decay products, and decay energies.
7- Used in previous modeling by UDEQ DRC.
8- Calculated using ICRP 30.

5. VERTICAL PATHRAE FATE AND TRANSPORT MODELING

The transport of constituents from the waste to the water table was modeled using PATHRAE. The input parameters for the vertical model are shown in the model output files (Attachment 3) and are described in detail below. The vertical model results (Section 5.3) serve as input to the horizontal PATHRAE model (Section 6.3.) Electronic files for both vertical and horizontal PATHRAE modeling are provided in Attachment 4.

5.1 Vertical Input Parameters for Contaminant Release

PATHRAE requires five input files, which define the waste release, transport conditions, and uptake.

5.1.1 Waste Source Term Concentrations

The Class A West cell will contain low-level radioactive waste and metals for permanent disposal. The current modeling evaluates a total of 260 isotopes and 13 metals. Radionuclide and metals waste concentrations are input to the PATHRAE model as Ci/m^3 and mg/m^3, respectively. Table 22 provides

source concentrations, half lives, and K_d values for each nuclide modeled. The derivation of source term concentrations is described in detail in the following sections.

5.1.1.1 Radionuclide Concentrations

The current modeling evaluates the 260 isotopes[5] listed in Table 22. The waste concentrations for each isotope were initially developed in 2000 from data supplied by the Manifest Information Management System (MIMS), a database managed by the Department of Energy (DOE) that summarizes national low-level radioactive waste disposal information. The list of radioisotopes established from the MIMS database was then classified by R313-15-1009 and their respective maximum Class A concentrations determined. If a radioisotope was not listed on Table I or Table II, it is Class A in accordance with R313-15-1009(2)(f). In these cases, the waste source term in the model was set at the specific activity. The specific activity, in picocuries per gram (pCi/g), was calculated using the following formula:

$$SA = \frac{\ln(2)}{t_{1/2}}\left(6.02x10^{23}\ \frac{molecules}{Mole}\right)\left(\frac{1}{GMW_{g/m}}\right) \div \left(3.7x10^{-2}\right)$$

where SA = Specific activity in pCi/g
$t_{1/2}$ = Half life in seconds
GMW= Gram molecular weight in grams per mole

The waste source term concentrations for the current version of the CAW cell modeling are identical to those used in previous modeling of the Class A cell (Whetstone, 2000e) with the following exceptions:

- K-40 is not a Class A nuclide and has been omitted from the current modeling;
- Bk-247 concentrations were increased to 10,000 pCi/g based on Class A limits;
- Ca-41 concentrations were increased from 440,000,000 pCi/g to 86,654,863,732 pCi/g based on specific activity;
- Cf-250 concentrations were increased from 500 pCi/g to 10,000 pCi/g based on Class A limits;
- Cl-36 concentrations were increased from 24.334 pCi/g to 33,522,654,030 pCi/g based on specific activity; and
- U-235 concentrations were increased from 1,900 pCi/g to 15,500 pCi/g based on the site license.
- Th-230 concentrations were increased from 150,000 pCi/g to 20,628,000,000 pCi/g.
- U-234 concentrations were increased from 370,000 pCi/g to 6,210,000,000 pCi/g.
- U-238 concentrations were increased from 330,000 pCi/g to 336,260 pCi/g.

The initial starting concentrations of Bk-47 and Cl-36 were based on License concentrations for the Class A facility (Bk-247) or specific activity (Cl-36), and were set at 10,000 pCi/g and 33,522,654,030 pCi/g, respectively. The initial model results based on these starting concentrations indicated exceedences of GWPLs at the water table and at the compliance well. The PATHRAE model was then used to back-calculate starting concentrations of Bk-247 and Cl-36 that would meet GWPLs at the water table and at a compliance well located 90 feet from the edge of the waste. The calculated starting concentrations are shown in Table 23.

The 92 nuclides selected for modeling are indicated with a check-mark listed in Table 22. Nuclides that were not modeled directly were represented by a synthetic (dummy) surrogate nuclide. The surrogates are not real nuclides, but have the K_d, half life, and concentration properties appropriate for a conservative surrogate for the real nuclide.

[5] Although 260 isotopes are evaluated, only 92 isotopes and 7 surrogates are explicitly modeled. Isotopes having very short half-lives and/or very high sorption coefficients (K_ds) are modeled using one of the 7 surrogate isotopes.

Table 22. List of Class A Radionuclides and Model Surrogates

ELEMENT	NUCLIDE	Maximum Concent. (pCi/gm)	Maximum Concentration (Ci/m3)	Concentration Data Source	Distribution Coefficient (K_d) (L/Kg)	1/2 life		1/2 life (Years)	Isotope to be Modeled	Model Surrogate
Actinium	Ac-225	440000000	488.4	Class A	4.5	10	d	2.74E-02		Ks-23
Actinium	Ac-227	72300000000000	80253000	SA	4.5	21.77	y	2.18E+01	✓	
Silver	Ag-105	440000000	488.4	Class A	2.7	41.3	d	1.13E-01		Ks-23
Silver	Ag-108	440000000	488.4	Class A	2.7	2.37	m	4.51E-06		Ks-23
Silver	Ag-108m	26081000000000	28949910	SA	2.7	418	y	4.18E+02	✓	
Silver	Ag-110m	440000000	488.4	Class A	2.7	249.8	d	6.84E-01		Ks-23
Silver	Ag-111	440000000	488.4	Class A	2.7	7.45	d	2.04E-02		Ks-23
Aluminum	Al-26	18600000000	20646	SA	15	740000	y	7.40E+05	✓	
Americium	Am-241	10000	0.0111	Class A	1	432.2	y	4.32E+02	✓	
Americium	Am-242	440000000	488.4	Class A	1	0.67	d	1.83E-03		Ks-23
Americium	Am-242m	10000	0.0111	Class A	1	141	y	1.41E+02	✓	
Americium	Am-243	10000	0.0111	Class A	1	7370	y	7.37E+03	✓	
Americium	Am-244	440000000	488.4	Class A	1	10.1	h	1.15E-03		Ks-23
Americium	Am-245	440000000	488.4	Class A	1	2.05	h	2.34E-04		Ks-23
Arsenic	As-73	440000000	488.4	Class A	1	80.3	d	2.20E-01		Ks-23
Arsenic	As-74	440000000	488.4	Class A	1	17.77	d	4.87E-02		Ks-23
Gold	Au-195	440000000	488.4	Class A	0.25	186.1	d	5.10E-01		Ks-22
Gold	Au-198	440000000	488.4	Class A	0.25	2.695	d	7.38E-03		Ks-22
Gold	Au-199	440000000	488.4	Class A	0.25	3.14	d	8.60E-03		Ks-22
Barium	Ba-133	2561600000000000	284337600	SA	10	10.51	y	1.05E+01	✓	
Barium	Ba-140	440000000	488.4	Class A	10	12.75	d	3.49E-02		Ks-22
Beryllium	Be-10	22000000000	24420	SA	2.5	1510000	y	1.51E+06	✓	
Beryllium	Be-7	440000000	488.4	Class A	2.5	53.29	d	1.46E-01		Ks-23
Bismuth	Bi-205	440000000	488.4	Class A	1	15.31	d	4.19E-02		Ks-23
Bismuth	Bi-206	440000000	488.4	Class A	1	6.243	d	1.71E-02		Ks-23
Bismuth	Bi-207	53670000000000	59573700	SA	1	31.55	y	3.16E+01	✓	
Bismuth	Bi-210m	567820000	630.2802	SA	1	3040000	y	3.04E+06	✓	
Bismuth	Bi-214	440000000	488.4	Class A	1	19.9	m	3.79E-05		Ks-23
Berkelium	Bk-247	10000	0.018	Class A	0.001	1400	y	1.40E+03	✓	
Berkelium	Bk-249	440000000	488.4	Class A	0.001	320	d	8.77E-01		Ks-20
Berkelium	Bk-250	440000000	488.4	Class A	0.001	0.134	d	3.68E-04		Ks-20
Carbon	C-14	7207207.21	8.000	Class A	8.52	5730	y	5.73E+03	✓	
Calcium	Ca-41	440000000	488.4	Class A	0.05	103000	y	1.03E+05	✓	
Calcium	Ca-45	440000000	488.4	Class A	0.05	162.61	d	4.46E-01		Ks-21
Calcium	Ca-47	440000000	488.4	Class A	0.05	4.536	d	1.24E-02		Ks-21
Cadmium	Cd-105	440000000	488.4	Class A	1	55.5	m	1.06E-04		Ks-23
Cadmium	Cd-107	440000000	488.4	Class A	1	6.5	h	7.42E-04		Ks-23
Cadmium	Cd-109	440000000	488.4	Class A	1	462.6	d	1.27E+00		Ks-26
Cadmium	Cd-113	0.4303	4.78E-07	SA	1	9.3E+15	y	9.30E+15	✓	
Cadmium	Cd-113m	224520000000000	249217200	SA	1	14.1	y	1.41E+01	✓	
Cerium	Ce-129	440000000	488.4	Class A	1	3.5	m	6.66E-06	✓	Ks-23
Cerium	Ce-133	440000000	488.4	Class A	1	1.6167	h	1.85E-04		Ks-23
Cerium	Ce-137	440000000	488.4	Class A	1	9	h	1.03E-03		Ks-23
Cerium	Ce-139	440000000	488.4	Class A	1	137.6	d	3.77E-01		Ks-23
Cerium	Ce-141	440000000	488.4	Class A	1	32.5	d	8.90E-02		Ks-23
Cerium	Ce-143	440000000	488.4	Class A	1	1.377	d	3.77E-03		Ks-23
Cerium	Ce-144	440000000	488.4	Class A	1	284.9	d	7.81E-01		Ks-23
Cerium	Ce-147	440000000	488.4	Class A	1	56.44944	s	1.79E-06		Ks-23
Californium	Cf-248	440000000	488.4	Class A	2	333.5	d	9.14E-01		Ks-20
Californium	Cf-249	10000	0.011	Class A	2	351	y	3.51E+02	✓	
Californium	Cf-250	10000	0.018	Class A	2	13.08	y	1.31E+01	✓	
Californium	Cf-251	10000	0.018	Class A	2	898	d	2.46E+00	✓	
Californium	Cf-252	440000000	792	Class A	2	2.65	y	2.65E+00	✓	
Chlorine	Cl-36	33522654030	6.03E+04	Class A	0.0025	301000	y	3.01E+05	✓	
Curium	Cm-241	440000000	792	Class A	93.3	32.8	d	8.99E-02		Ks-24
Curium	Cm-242	2000000	3.6	Class A	93.3	162.8	d	4.46E-01		Ks-24
Curium	Cm-243	10000	0.018	Class A	93.3	29.1	y	2.91E+01	✓	
Curium	Cm-244	10000	0.0111	Class A	93.3	18.1	y	1.81E+01	✓	
Curium	Cm-245	10000	0.0111	Class A	93.3	8500	y	8.50E+03	✓	
Curium	Cm-246	10000	0.0111	Class A	93.3	4730	y	4.73E+03	✓	
Curium	Cm-247	10000	0.0111	Class A	93.3	1.56E+07	y	1.56E+07	✓	
Curium	Cm-248	10000	0.0111	Class A	93.3	340000	y	3.40E+05	✓	
Curium	Cm-249	440000000	488.4	Class A	93.3	1.07	h	1.22E-04		Ks-23
Cobalt	Co-56	440000000	488.4	Class A	370	77.3	d	2.12E-01		Ks-25
Cobalt	Co-57	440000000	488.4	Class A	370	271.8	d	7.45E-01		Ks-25
Cobalt	Co-58	440000000	488.4	Class A	370	70.86	d	1.94E-01		Ks-25
Cobalt	Co-60	440000000	488.4	Class A	370	5.27	y	5.27E+00	✓	
Cobalt	Co-63	440000000	488.4	Class A	370	27.4	s	8.69E-07		Ks-25
Chromium	Cr-51	440000000	488.4	Class A	1	27.7	d	7.59E-02		Ks-23
Cesium	Cs-134	440000000	488.4	Class A	133	2.065	y	2.07E+00		Ks-25
Cesium	Cs-135	1152100000	1278.831	SA	133	2300000	y	2.30E+06	✓	
Cesium	Cs-136	440000000	488.4	Class A	133	13.16	d	3.61E-02		Ks-25
Cesium	Cs-137	630000	0.6993	Class A	133	30.07	y	3.01E+01	✓	
Copper	Cu-67	440000000	488.4	Class A	1	61.83	d	1.69E-01		Ks-23
Dysprosium	Dy-166	440000000	488.4	Class A	6.5	3.4	d	9.32E-03		Ks-23
Einsteinium	Es-253	440000000	488.4	Class A	0.001	20.47	d	5.61E-02		Ks-20
Einsteinium	Es-254	440000000	488.4	Class A	0.001	275.7	d	7.55E-01		Ks-20
Europium	Eu-152	173050000000000	192085500	SA	6.5	13.54	y	1.35E+01	✓	
Europium	Eu-154	270420000000000	300166200	SA	6.5	8.59	y	8.59E+00	✓	
Europium	Eu-155	440000000	488.4	Class A	6.5	4.76	y	4.76E+00	✓	

Table 22. List of Class A Radionuclides and Model Surrogates (Part 2)

ELEMENT	NUCLIDE	Maximum Concent. (pCi/gm)	Maximum Concentration (Ci/m3)	Concentration Data Source	Distribution Coefficient (K_d) (L/Kg)	1/2 life		1/2 life (Years)	Isotope to be Modeled	Model Surrogate
Europium	Eu-156	440000000	488.4	Class A	6.5	15.2	d	4.16E-02		Ks-23
Iron	Fe-52	440000000	488.4	Class A	1.4	0.345	d	9.45E-04		Ks-23
Iron	Fe-53	440000000	488.4	Class A	1.4	8.51	m	1.62E-05		Ks-23
Iron	Fe-55	440000000	488.4	Class A	1.4	2.73	y	2.73E+00	✓	
Iron	Fe-59	440000000	488.4	Class A	1.4	44.5	d	1.22E-01		Ks-23
Iron	Fe-60	3974800000	4412.028	SA	1.4	1500000	y	1.50E+06	✓	
Fermium	Fm-252	440000000	488.4	Class A	0.001	1.058	d	2.90E-03		Ks-20
Gallium	Ga-67	440000000	488.4	Class A	15	3.26	d	8.93E-03		Ks-23
Gadolinium	Gd-148	32228000000000	35773080	SA	6.5	74.6	y	7.46E+01	✓	
Gadolinium	Gd-151	440000000	488.4	Class A	6.5	124	d	3.40E-01		Ks-23
Gadolinium	Gd-153	440000000	488.4	Class A	6.5	241.6	d	6.62E-01		Ks-23
Germanium	Ge-68	440000000	488.4	Class A	0.25	270.8	d	7.42E-01		Ks-20
Hydrogen	H-3	25000000	27.75	Class A	0.04	12.33	y	1.23E+01	✓	
Hafnium	Hf-172	440000000	488.4	Class A	4.5	1.87	y	1.87E+00		Ks-26
Hafnium	Hf-175	440000000	488.4	Class A	4.5	70	d	1.92E-01		Ks-23
Hafnium	Hf-181	440000000	488.4	Class A	4.5	42.4	d	1.16E-01		Ks-23
Mercury	Hg-194	3546100000000	3936171	SA	10	444	y	4.44E+02	✓	
Mercury	Hg-203	440000000	488.4	Class A	10	46.6	d	1.28E-01		Ks-23
Holmium	Ho-166	440000000	488.4	Class A	2.5	1.115	d	3.05E-03		Ks-23
Holmium	Ho-166m	1800000000000	1998000	SA	2.5	1200	y	1.20E+03	✓	
Iodine	I-123	440000000	488.4	Class A	0.12	13.3	h	1.52E-03		Ks-22
Iodine	I-125	440000000	488.4	Class A	0.12	59.4	d	1.63E-01		Ks-22
Iodine	I-126	440000000	488.4	Class A	0.12	13.11	d	3.59E-02		Ks-22
Iodine	I-129	5000	0.00555	Class A	0.12	15700000	y	1.57E+07	✓	
Iodine	I-131	440000000	488.4	Class A	0.12	8.02	d	2.20E-02		Ks-22
Iodine	I-133	440000000	488.4	Class A	0.12	0.867	d	2.37E-03		Ks-22
Iodine	I-135	440000000	488.4	Class A	0.12	6.57	h	7.50E-04		Ks-22
Iodine	I-137	440000000	488.4	Class A	0.12	24.5	s	7.77E-07		Ks-22
Indium	In-111	440000000	488.4	Class A	15	2.8047	d	7.68E-03		Ks-23
Indium	In-113m	440000000	488.4	Class A	15	0.069	d	1.89E-04		Ks-23
Indium	In-114	440000000	488.4	Class A	15	0.00083	d	2.28E-06		Ks-23
Indium	In-114m	440000000	488.4	Class A	15	49.51	d	1.36E-01		Ks-23
Iridium	Ir-192	440000000	488.4	Class A	1.5	73.8	d	2.02E-01		Ks-23
Lanthanum	La-140	440000000	488.4	Class A	6.5	1.678	d	4.60E-03		Ks-23
Manganese	Mn-52	440000000	488.4	Class A	6.4	5.591	d	1.53E-02		Ks-23
Manganese	Mn-52m	440000000	488.4	Class A	6.4	0.0147	d	4.01E-05		Ks-23
Manganese	Mn-53	1800000000	1998	SA	6.4	3740000	y	3.74E+06	✓	
Manganese	Mn-54	440000000	488.4	Class A	6.4	312.3	d	8.56E-01		Ks-23
Molybdenum	Mo-99	440000000	488.4	Class A	1	2.748	d	7.53E-03		Ks-23
Sodium	Na-22	440000000	488.4	Class A	1	2.602	y	2.60E+00	✓	
Niobium	Nb-91	5780000000000	6415800	SA	1.6	680	y	6.80E+02	✓	
Niobium	Nb-92	112000000	124.32	SA	1.6	34700000	y	3.47E+07	✓	
Niobium	Nb-93m	263460000000000	292440600	SA	1.6	16.13	y	1.61E+01	✓	
Niobium	Nb-94	13000	0.01443	Class A	1.6	20300	y	2.03E+04	✓	
Neodymium	Nd-144	4.27	4.74322E-06	SA	6.5	2.29E+15	y	2.29E+15		stable
Neodymium	Nd-147	440000000	488.4	Class A	6.5	10.98	d	3.01E-02		Ks-23
Nickel	Ni-59	14000000	15.54	Class A	10	76000	y	7.60E+04	✓	
Nickel	Ni-63	2200000	2.442	Class A	10	100.1	y	1.00E+02	✓	
Neptunium	Np-235	440000000	488.4	Class A	3	1.085	y	1.09E+00		Ks-26
Neptunium	Np-237	10000	0.0111	Class A	3	2144000	y	2.14E+06	✓	
Osmium	Os-191	440000000	488.4	Class A	4.5	15.4	d	4.22E-02		Ks-23
Osmium	Os-191m	440000000	488.4	Class A	4.5	0.546	d	1.50E-03		Ks-23
Osmium	Os-194	307330000000000	341136300	SA	4.5	6	y	6.00E+00	✓	
Phosphorous	P-32	440000000	488.4	Class A	0.035	14.26	d	3.91E-02		Ks-21
Phosphorous	P-33	440000000	488.4	Class A	0.035	25.3	d	6.93E-02		Ks-21
Protactinium	Pa-231	47000000000	52170	SA	5.5	32760	y	3.28E+04	✓	
Protactinium	Pa-233	440000000	488.4	Class A	5.5	26.967	d	7.39E-02		Ks-23
Protactinium	Pa-234	440000000	488.4	Class A	5.5	6.7014	h	7.65E-04		Ks-23
Protactinium	Pa-234m	440000000	488.4	Class A	5.5	1.172088	m	2.23E-06		Ks-23
Lead	Pb-202	3400000000	3774	SA	19	52500	y	5.25E+04	✓	
Lead	Pb-203	440000000	488.4	Class A	19	2.1614	d	5.92E-03		Ks-23
Lead	Pb-210	76000000000000	84360000	SA	19	22.3	y	2.23E+01	✓	
Lead	Pb-214	440000000	488.4	Class A	19	26.8	m	5.10E-05		Ks-23
Palladium	Pd-103	440000000	488.4	Class A	0.55	16.991	d	4.66E-02		Ks-22
Palladium	Pd-107	510000000	566.1	SA	0.55	6500000	y	6.50E+06	✓	
Promethium	Pm-143	440000000	488.4	Class A	6.5	265	d	7.26E-01		Ks-23
Promethium	Pm-145	1400000000000	155400000	SA	6.5	17.7	y	1.77E+01	✓	
Promethium	Pm-147	440000000	488.4	Class A	6.5	2.6234	y	2.62E+00	✓	
Polonium	Po-208	440000000	488.4	Class A	9	2.9	y	2.90E+00	✓	
Polonium	Po-209	167810000000000	18626910	SA	9	102	y	1.02E+02	✓	
Polonium	Po-210	440000000	488.4	Class A	9	138.4	d	3.79E-01		Ks-23
Polonium	Po-214	440000000	488.4	Class A	9	164.3	us	5.21E-12		Ks-23
Platinum	Pt-193	370000000000000	41070000	SA	0.9	50	y	5.00E+01	✓	
Plutonium	Pu-236	500	0.000555	Class A	10	2.86	y	2.86E+00	✓	
Plutonium	Pu-238	10000	0.0111	Class A	10	87.7	y	8.77E+01	✓	
Plutonium	Pu-239	10000	0.0111	Class A	10	24110	y	2.41E+04	✓	
Plutonium	Pu-240	10000	0.0111	Class A	10	6564	y	6.56E+03	✓	
Plutonium	Pu-241	350000	0.3885	Class A	10	14.35	y	1.44E+01	✓	
Plutonium	Pu-242	10000	0.0111	Class A	10	373300	y	3.73E+05	✓	
Plutonium	Pu-243	500	0.000555	Class A	10	4.956	h	5.66E-04		Ks-23

Table 22. List of Class A Radionuclides and Model Surrogates (Part 3)

ELEMENT	NUCLIDE	Maximum Concent. (pCi/gm)	Maximum Concentration (Ci/m3)	Concentration Data Source	Distribution Coefficient (K_d) (L/Kg)	1/2 life		1/2 life (Years)	Isotope to be Modeled	Model Surrogate
Plutonium	Pu-244	500	0.000555	Class A	10	8.08E+07	y	8.08E+07	✓	
Radium	Ra-225	440000000	488.4	Class A	10	14.9	d	4.08E-02		Ks-23
Radium	Ra-226	10000	0.0111	Class A	10	1600	y	1.60E+03	✓	
Radium	Ra-228	272396000000000	302359560	SA	10	5.75	y	5.75E+00	✓	
Rubidium	Rb-82	440000000	488.4	Class A	0.55	0.0009	d	2.38E-06		Ks-22
Rubidium	Rb-83	440000000	488.4	Class A	0.55	86.2	d	2.36E-01		Ks-22
Rubidium	Rb-84	440000000	488.4	Class A	0.55	32.8	d	8.99E-02		Ks-22
Rubidium	Rb-86	440000000	488.4	Class A	0.55	18.63	d	5.10E-02		Ks-22
Rhenium	Re-183	440000000	488.4	Class A	0.075	70	d	1.92E-01		Ks-21
Rhenium	Re-184	440000000	488.4	Class A	0.075	38	d	1.04E-01		Ks-21
Rhenium	Re-184m	440000000	488.4	Class A	0.075	169	d	4.63E-01		Ks-21
Rhenium	Re-186	440000000	488.4	Class A	0.075	3.719	d	1.02E-02		Ks-21
Rhenium	Re-187	38000	0.04218	Class A	0.075	43500000000	y	4.35E+10	✓	
Rhenium	Re-188	440000000	488.4	Class A	0.075	0.709	d	1.94E-03		Ks-21
Rhodium	Rh-103m	440000000	488.4	Class A	0.001	0.039	d	1.07E-04		Ks-20
Ruthenium	Ru-103	440000000	488.4	Class A	5	39.26	d	1.08E-01		Ks-23
Ruthenium	Ru-106	440000000	488.4	Class A	5	1.02	y	1.02E+00		Ks-26
Sulfur	S-35	440000000	488.4	Class A	0.075	87.5	d	2.40E-01		Ks-21
Antimony	Sb-122	440000000	488.4	Class A	100	2.7	d	7.40E-03		Ks-25
Antimony	Sb-124	440000000	488.4	Class A	100	60.2	d	1.65E-01		Ks-25
Antimony	Sb-125	440000000	488.4	Class A	100	2.76	y	2.76E+00		Ks-25
Antimony	Sb-126	440000000	488.4	Class A	100	12.5	d	3.42E-02		Ks-25
Antimony	Sb-126m	440000000	488.4	Class A	100	0.013	d	3.61E-05		Ks-25
Antimony	Sb-129	440000000	488.4	Class A	100	4.4	h	5.02E-04		Ks-25
Scandium	Sc-41	440000000	488.4	Class A	10	0.596	s	1.89E-08		Ks-23
Scandium	Sc-44	440000000	488.4	Class A	10	0.164	d	4.48E-04		Ks-23
Scandium	Sc-46	440000000	488.4	Class A	10	83.8	d	2.30E-01		Ks-23
Scandium	Sc-47	440000000	488.4	Class A	10	3.349	d	9.18E-03		Ks-23
Selenium	Se-75	440000000	488.4	Class A	1	119.8	d	3.28E-01		Ks-23
Selenium	Se-79	69700000000	77367	SA	1	65000	y	6.50E+04	✓	
Selenium	Se-85	440000000	488.4	Class A	1	31.7	s	1.01E-06		Ks-23
Silicon	Si-32	65000000000000	72150000	SA	0.35	172	y	1.72E+02	✓	
Samarium	Sm-145	440000000	488.4	Class A	2.45	340	d	9.32E-01		Ks-23
Samarium	Sm-151	26320000000000	29215200	SA	2.45	90	y	9.00E+01	✓	
Samarium	Sm-153	440000000	488.4	Class A	2.45	1.928	d	5.28E-03		Ks-23
Tin	Sn-113	440000000	488.4	Class A	50	115.1	d	3.15E-01		Ks-24
Tin	Sn-117m	440000000	488.4	Class A	50	13.6	d	3.73E-02		Ks-24
Tin	Sn-119m	440000000	488.4	Class A	50	293.1	d	8.03E-01		Ks-24
Tin	Sn-121	440000000	488.4	Class A	50	1.128	d	3.09E-03		Ks-24
Tin	Sn-121m	53754000000000	59666940	SA	50	55	y	5.50E+01	✓	
Tin	Sn-126	28391000000	31514.01	SA	50	100000	y	1.00E+05	✓	
Strontium	Sr-81	440000000	488.4	Class A	0.05	22.3	m	4.24E-05		Ks-21
Strontium	Sr-82	440000000	488.4	Class A	0.05	25.55	d	7.00E-02		Ks-21
Strontium	Sr-85	440000000	488.4	Class A	0.05	64.8	d	1.78E-01		Ks-21
Strontium	Sr-87m	440000000	488.4	Class A	0.05	168.18	m	3.20E-04		Ks-21
Strontium	Sr-89	440000000	488.4	Class A	0.05	50.53	d	1.38E-01		Ks-21
Strontium	Sr-90	25000	0.02775	Class A	0.05	28.78	y	2.88E+01	✓	
Tantalum	Ta-182	440000000	488.4	Class A	2.2	114.43	d	3.14E-01		Ks-23
Terbium	Tb-157	150000000000000	16650000	SA	6.5	71	y	7.10E+01	✓	
Terbium	Tb-158	150000000000000	16650000	SA	6.5	180	y	1.80E+02	✓	
Terbium	Tb-160	440000000	488.4	Class A	6.5	72.3	d	1.98E-01		Ks-23
Technetium	Tc-95	440000000	488.4	Class A	0.11	0.833	d	2.28E-03		Ks-22
Technetium	Tc-95m	440000000	488.4	Class A	0.11	61	d	1.67E-01		Ks-22
Technetium	Tc-99	187500	0.208125	Class A	0.11	211100	y	2.11E+05	✓	
Technetium	Tc-99m	440000000	488.4	Class A	0.11	0.250	d	6.86E-04		Ks-22
Tellurium	Te-123	291	0.00032301	SA	1.25	1E+13	y	1.00E+13	✓	
Tellurium	Te-123m	440000000	488.4	Class A	1.25	119.7	d	3.28E-01		Ks-23
Tellurium	Te-125m	440000000	488.4	Class A	1.25	57.4	d	1.57E-01		Ks-23
Tellurium	Te-129	440000000	488.4	Class A	1.25	0.048	d	1.32E-04		Ks-23
Tellurium	Te-129m	440000000	488.4	Class A	1.25	33.6	d	9.21E-02		Ks-23
Thorium	Th-229	212830000000	236241.3	SA	10	7880	y	7.88E+03	✓	
Thorium	Th-230	20628000000	22897.08	SA	10	75380	y	7.54E+04	✓	
Thorium	Th-231	440000000	488.4	Class A	10	1.063	d	2.91E-03		Ks-23
Thorium	Th-232	110000	0.1221	SA	10	14050000000	y	1.41E+10	✓	
Thorium	Th-234	440000000	488.4	Class A	10	24.1	d	6.60E-02		Ks-23
Titanium	Ti-44	156350000000000	173548500	SA	10	63	y	6.30E+01	✓	
Thallium	Tl-201	440000000	488.4	Class A	0.15	3.038	d	8.32E-03		Ks-22
Thallium	Tl-202	440000000	488.4	Class A	0.15	12.23	d	3.35E-02		Ks-22
Thallium	Tl-204	440000000	488.4	Class A	0.15	3.78	y	3.78E+00	✓	
Thallium	Tl-210	440000000	488.4	Class A	0.15	1.3	m	2.47E-06		Ks-22
Thulium	Tm-170	440000000	488.4	Class A	6.5	128.6	d	3.52E-01	✓	
Thulium	Tm-171	440000000	488.4	Class A	6.5	1.92	y	1.92E+00		Ks-26
Uranium	U-228	440000000	488.4	Class A	6	9.1	m	1.73E-05		Ks-23
Uranium	U-230	440000000	488.4	Class A	6	20.8	d	5.70E-02		Ks-23
Uranium	U-232	22028000000000	24451080	SA	6	68.9	y	6.89E+01	✓	
Uranium	U-233	75000	0.08325	Class A	6	159200	y	1.59E+05	✓	
Uranium	U-234	6210000000	6893.1	SA	6	245500	y	2.46E+05	✓	
Uranium	U-235	15500	0.0279	Class A	6	703800000	y	7.04E+08	✓	
Uranium	U-236	64720000	71.8392	SA	6	23420000	y	2.34E+07	✓	
Uranium	U-238	336260	0.3732486	SA	6	4470000000	y	4.47E+09	✓	
Uranium	U-depleted	370000	0.4107	A+ (Class A)	6					U-isotopes

Table 22. List of Class A Radionuclides and Model Surrogates (Part 4)

ELEMENT	NUCLIDE	Maximum Concent. (pCi/gm)	Maximum Concentration (Ci/m3)	Concentration Data Source	Distribution Coefficient (K_d) (L/Kg)	1/2 life		1/2 life (Years)	Isotope to be Modeled	Model Surrogate
Uranium	U-natural	680000	0.7548	SA	6					U-isotopes
Vanadium	V-48	440000000	488.4	Class A	10	15.98	d	4.38E-02		Ks-23
Vanadium	V-50	0.0511	5.6721E-08	SA	10	1.4E+17	y	1.40E+17	✓	
Tungsten	W-181	440000000	488.4	Class A	1.5	121.2	d	3.32E-01		Ks-23
Tungsten	W-185	440000000	488.4	Class A	1.5	75.1	d	2.06E-01		Ks-23
Tungsten	W-187	440000000	488.4	Class A	1.5	23.72	h	2.71E-03		Ks-23
Tungsten	W-188	440000000	488.4	Class A	1.5	69.4	d	1.90E-01		Ks-23
Xenon	Xe-127	440000000	488.4	Class A	0.001	36.4	d	9.97E-02		Ks-20
Xenon	Xe-131m	440000000	488.4	Class A	0.001	11.934	d	3.27E-02		Ks-20
Xenon	Xe-133	440000000	488.4	Class A	0.001	5.245	d	1.44E-02		Ks-20
Xenon	Xe-133m	440000000	488.4	Class A	0.001	2.19	d	6.00E-03		Ks-20
Yttrium	Y-88	440000000	488.4	Class A	1.7	106.7	d	2.92E-01		Ks-23
Yttrium	Y-91	440000000	488.4	Class A	1.7	58.5	d	1.60E-01		Ks-23
Yttrium	Y-99	440000000	488.4	Class A	1.7	1.47	s	4.66E-08		Ks-23
Ytterbium	Yb-169	440000000	488.4	Class A	6.5	32.03	d	8.78E-02		Ks-23
Zinc	Zn-65	440000000	488.4	Class A	0.1	244.3	d	6.69E-01		Ks-22
Zirconium	Zr-88	440000000	488.4	Class A	10	83.4	d	2.28E-01		Ks-23
Zirconium	Zr-93	2514100000	2790.651	SA	10	1530000	y	1.53E+06	✓	
Zirconium	Zr-95	440000000	488.4	Class A	10	64.02	d	1.75E-01		Ks-23
SYNTHETIC (DUMMY) NUCLIDES:										
Surrogate	Ks-20	440000000	488.4		0.001	1	y	1.00E+00	✓	
Surrogate	Ks-21	440000000	488.4		0.01	1	y	1.00E+00	✓	
Surrogate	Ks-22	440000000	488.4		0.1	1	y	1.00E+00	✓	
Surrogate	Ks-23	440000000	488.4		1	1	y	1.00E+00	✓	
Surrogate	Ks-24	440000000	488.4		50	4	y	4.00E+00	✓	
Surrogate	Ks-25	440000000	488.4		100	4	y	4.00E+00	✓	
Surrogate	Ks-26	440000000	488.4		1	2	y	2.00E+00	✓	

NOTES: Class A = Class A limits
SA = Concentration represents the Specific Activity (maximum possible concentration) of the nuclide, rounded to ≈ 4 significant digits

The radionuclide concentrations in pCi/g were converted to Ci/m^3 using the waste bulk density of 1.8 gm/cm^3 for input to the PATHRAE model. The initial source term concentrations for the 0.238 cm/yr top slope and 0.335 cm/yr side slope models are shown in Table 24 and Table 25, respectively.

Table 23. Limiting Radionuclide Concentrations in CAW Cell Top Slope and Side Slope

	Model Results for 0.238 cm/yr Top Slope		Model Results for 0.335 cm/yr Side Slope	
NUCLIDE	Concentration that meets GWPL at the Water Table	Concentration that meets GWPL at the Compliance Well	Concentration that meets GWPL at the Water Table	Concentration that meets GWPL at the Compliance Well
Bk-247	4.93E-01	1.92E+00	3.39E+03	---
Cl-36	2.12E+03	7.39E+04	1.92E+07	1.06E+08

NOTES: Waste concentration shown in units of pCi/g
--- indicates no reduction from Class A concentration was necessary to meet GWPLs

Table 24. Waste Maximum Radionuclide Source Concentrations, K_ds, and Fractional Release Rates, based on 0.238 cm/year Infiltration

Waste Characteristics:	Infiltration Rate:	0.00238	m/yr
	Waste Thickness:	1	m
	Waste Moisture Content:	0.0573	cm^3/cm^3
	Waste Bulk Density:	1.8	gm/cm^3
Soil Characteristics:	Soil Thickness:	4.0725	m
	Soil Moisture Content:	0.100	cm^3/cm^3
	Soil Bulk Density:	1.563	gm/cm^3

Pathrae Isotope Number	ELEMENT	NUCLIDE	Maximum Concentration (pCi/gm)	Maximum Concentr. (Ci/m3)	Distribution Coefficient (K_d) (L/Kg)	Fractional Release Rate (1/yr)	Soil Retardation Factor	1/2 life		1/2 life (Years)
101	Actinium	Ac-227	7.23E+13	1.30E+08	4.5	2.92E-04	71.641	21.77	y	2.18E+01
102	Silver	Ag-108m	2.61E+13	4.69E+07	2.7	4.84E-04	43.384	418	y	4.18E+02
103	Aluminum	Al-26	1.86E+10	3.35E+04	15	8.80E-05	236.468	740,000	y	7.40E+05
48	Americium	Am-241	1.00E+04	1.80E-02	1	1.28E-03	16.698	432.2	y	4.32E+02
104	Americium	Am-242m	1.00E+04	1.80E-02	1	1.28E-03	16.698	141	y	1.41E+02
105	Americium	Am-243	1.00E+04	1.80E-02	1	1.28E-03	16.698	7,370	y	7.37E+03
106	Barium	Ba-133	2.56E+14	4.61E+08	10	1.32E-04	157.979	10.5	y	1.05E+01
107	Beryllium	Be-10	2.20E+10	3.96E+04	2.5	5.22E-04	40.245	1,510,000	y	1.51E+06
108	Bismuth	Bi-207	5.37E+13	9.66E+07	1	1.28E-03	16.698	31.55	y	3.16E+01
109	Bismuth	Bi-210m	5.68E+08	1.02E+03	1	1.28E-03	16.698	3,040,000	y	3.04E+06
110	Berkelium	Bk-247	***1.92E+00***	***3.46E-06***	0.001	4.03E-02	1.016	1,400	y	1.40E+03
111	Carbon	C-14	5.00E+06	9.00E+00	8.52	1.55E-04	134.746	5,730	y	5.73E+03
112	Calcium	Ca-41	8.67E+10	1.56E+05	0.05	1.62E-02	1.785	103,000	y	1.03E+05
113	Cadmium	Cd-113	4.30E-01	7.75E-07	1	1.28E-03	16.698	9.3.E+15	y	9.30E+15
114	Cadmium	Cd-113m	2.25E+14	4.04E+08	1	1.28E-03	16.698	14.1	y	1.41E+01
115	Californium	Cf-249	1.00E+04	1.80E-02	2	6.51E-04	32.396	351	y	3.51E+02
116	Californium	Cf-250	1.00E+04	1.80E-02	2	6.51E-04	32.396	13.08	y	1.31E+01
117	Californium	Cf-251	1.00E+04	1.80E-02	2	6.51E-04	32.396	898	y	8.98E+02
118	Californium	Cf-252	4.40E+08	7.92E+02	2	6.51E-04	32.396	2.65	y	2.65E+00
119	Chlorine	Cl-36	***7.39E+04***	***1.33E-01***	0.0025	3.85E-02	1.039	301,000	y	3.01E+05
120	Curium	Cm-243	1.00E+04	1.80E-02	93.3	1.42E-05	1465.613	29	y	2.91E+01
50	Curium	Cm-244	1.00E+04	1.80E-02	93.3	1.42E-05	1465.613	18	y	1.81E+01
121	Curium	Cm-245	1.00E+04	1.80E-02	93.3	1.42E-05	1465.613	8,500	y	8.50E+03
122	Curium	Cm-246	1.00E+04	1.80E-02	93.3	1.42E-05	1465.613	4730	y	4.73E+03
123	Curium	Cm-247	1.00E+04	1.80E-02	93.3	1.42E-05	1465.613	15,600,000	y	1.56E+07
124	Curium	Cm-248	1.00E+04	1.80E-02	93.3	1.42E-05	1465.613	340,000	y	3.40E+05
125	Cobalt	Co-60	4.40E+08	7.92E+02	370	3.57E-06	5809.221	5	y	5.27E+00
126	Cesium	Cs-135	1.15E+09	2.07E+03	133	9.94E-06	2088.820	2,300,000	y	2.30E+06
127	Cesium	Cs-137	6.30E+05	1.13E+00	133	9.94E-06	2088.820	30.07	y	3.01E+01
128	Europium	Eu-152	1.73E+14	3.11E+08	6.5	2.02E-04	103.036	14	y	1.35E+01
129	Europium	Eu-154	2.70E+14	4.87E+08	6.5	2.02E-04	103.036	8.6	y	8.59E+00
130	Europium	Eu-155	4.40E+08	7.92E+02	6.5	2.02E-04	103.036	4.76	y	4.76E+00
131	Iron	Fe-55	4.40E+08	7.92E+02	1.4	9.23E-04	22.977	2.73	y	2.73E+00
132	Iron	Fe-60	3.97E+09	7.15E+03	1.4	9.23E-04	22.977	1,500,000	y	1.50E+06
133	Gadolinium	Gd-148	3.22E+13	5.80E+07	6.5	2.02E-04	103.036	74.6	y	7.46E+01
134	Hydrogen	H-3	2.50E+07	4.50E+01	0.04	1.84E-02	1.628	12.3	y	1.23E+01
135	Mercury	Hg-194	3.55E+12	6.38E+06	10	1.32E-04	157.979	444	y	4.44E+02
136	Holmium	Ho-166m	1.80E+12	3.24E+06	2.5	5.22E-04	40.245	1,200	y	1.20E+03
137	Iodine	I-129	5.00E+03	9.00E-03	0.12	8.71E-03	2.884	15,700,000	y	1.57E+07
139	Manganese	Mn-53	1.80E+09	3.24E+03	6.4	2.06E-04	101.467	3,740,000.00	y	3.74E+06
140	Sodium	Na-22	4.40E+08	7.92E+02	1	1.28E-03	16.698	2.6	y	2.60E+00
141	Niobium	Nb-91	5.78E+12	1.04E+07	1.6	8.10E-04	26.117	680	y	6.80E+02
142	Niobium	Nb-92	1.12E+08	2.02E+02	1.6	8.10E-04	26.117	34,700,000	y	3.47E+07
143	Niobium	Nb-93m	2.63E+14	4.74E+08	1.6	8.10E-04	26.117	16.13	y	1.61E+01
144	Niobium	Nb-94	1.30E+04	2.34E-02	1.6	8.10E-04	26.117	20,300	y	2.03E+04
146	Nickel	Ni-59	1.40E+07	2.52E+01	10	1.32E-04	157.979	76,000	y	7.60E+04
147	Nickel	Ni-63	2.20E+06	3.96E+00	10	1.32E-04	157.979	100.1	y	1.00E+02
42	Neptunium	Np-237	1.00E+04	1.80E-02	3	4.36E-04	48.094	2,144,000	y	2.14E+06
148	Osmium	Os-194	3.07E+14	5.53E+08	4.5	2.92E-04	71.641	6	y	6.00E+00
149	Protactinium	Pa-231	4.70E+10	8.46E+04	5.5	2.39E-04	87.338	32,760	y	3.28E+04
150	Lead	Pb-202	3.40E+09	6.12E+03	19	6.95E-05	299.260	52,500	y	5.25E+04
151	Lead	Pb-210	7.60E+13	1.37E+08	19	6.95E-05	299.260	22.3	y	2.23E+01
152	Palladium	Pd-107	5.10E+08	9.18E+02	0.55	2.27E-03	9.634	6,500,000	y	6.50E+06
153	Promethium	Pm-145	1.40E+14	2.52E+08	6.5	2.02E-04	103.036	17.7	y	1.77E+01

Table 24. Waste Maximum Radionuclide Source Concentrations, Kds, and Fractional Release Rates, based on 0.238 cm/year Infiltration (Part 2)

Pathrae Isotope Number	ELEMENT	NUCLIDE	Maximum Concentration (pCi/gm)	Maximum Concentr. (Ci/m3)	Distribution Coefficient (K_d) (L/Kg)	Fractional Release Rate (1/yr)	Soil Retardation Factor	1/2 life		1/2 life (Years)
154	Promethium	Pm-147	4.40E+08	7.92E+02	6.5	2.02E-04	103.036	2.6234	y	2.62E+00
155	Polonium	Po-208	4.40E+08	7.92E+02	9	1.46E-04	142.281	2.9	y	2.90E+00
156	Polonium	Po-209	1.68E+13	3.02E+07	9	1.46E-04	142.281	102	y	1.02E+02
157	Platinum	Pt-193	3.70E+13	6.66E+07	0.9	1.42E-03	15.128	50	y	5.00E+01
158	Plutonium	Pu-236	5.00E+02	9.00E-04	10	1.32E-04	157.979	2.86	y	2.86E+00
159	Plutonium	Pu-238	1.00E+04	1.80E-02	10	1.32E-04	157.979	87.7	y	8.77E+01
160	Plutonium	Pu-239	1.00E+04	1.80E-02	10	1.32E-04	157.979	24,110	y	2.41E+04
45	Plutonium	Pu-240	1.00E+04	1.80E-02	10	1.32E-04	157.979	6,564	y	6.56E+03
46	Plutonium	Pu-241	3.50E+05	6.30E-01	10	1.32E-04	157.979	14.35	y	1.44E+01
161	Plutonium	Pu-242	1.00E+04	1.80E-02	10	1.32E-04	157.979	373,300	y	3.73E+05
162	Plutonium	Pu-244	5.00E+02	9.00E-04	10	1.32E-04	157.979	80,800,000	y	8.08E+07
55	Radium	Ra-226	1.00E+04	1.80E-02	10	1.32E-04	157.979	1,600	y	1.60E+03
163	Radium	Ra-228	2.72E+14	4.90E+08	10	1.32E-04	157.979	5.75	y	5.75E+00
164	Rhenium	Re-187	3.80E+04	6.84E-02	0.075	1.24E-02	2.177	43,500,000,000	y	4.35E+10
165	Selenium	Se-79	6.97E+10	1.25E+05	1	1.28E-03	16.698	65,000	y	6.50E+04
166	Silicon	Si-32	6.50E+13	1.17E+08	0.35	3.46E-03	6.494	172	y	1.72E+02
167	Samarium	Sm-151	2.63E+13	4.74E+07	2.45	5.33E-04	39.460	90	y	9.00E+01
168	Tin	Sn-121m	5.38E+13	9.68E+07	50	2.64E-05	785.895	55	y	5.50E+01
169	Tin	Sn-126	2.84E+10	5.11E+04	50	2.64E-05	785.895	100,000	y	1.00E+05
170	Strontium	Sr-90	2.50E+04	4.50E-02	0.05	1.62E-02	1.785	28.78	y	2.88E+01
171	Terbium	Tb-157	1.50E+13	2.70E+07	6.5	2.02E-04	103.036	71	y	7.10E+01
172	Terbium	Tb-158	1.50E+13	2.70E+07	6.5	2.02E-04	103.036	180	y	1.80E+02
173	Technetium	Tc-99	1.88E+05	3.38E-01	0.11	9.32E-03	2.727	211,100	y	2.11E+05
174	Tellurium	Te-123	2.91E+02	5.24E-04	1.25	1.03E-03	20.622	1E+13	y	1.00E+13
175	Thorium	Th-229	2.13E+11	3.83E+05	10	1.32E-04	157.979	7,880	y	7.88E+03
36	Thorium	Th-230	2.06E+10	3.71E+04	10	1.32E-04	157.979	75,380	y	7.54E+04
176	Thorium	Th-232	1.10E+05	1.98E-01	10	1.32E-04	157.979	14,050,000,000	y	1.41E+10
177	Titanium	Ti-44	1.56E+14	2.81E+08	10	1.32E-04	157.979	63	y	6.30E+01
178	Thallium	Tl-204	4.40E+08	7.92E+02	0.15	7.27E-03	3.355	3.78	y	3.78E+00
179	Thulium	Tm-170	4.40E+08	7.92E+02	6.5	2.02E-04	103.036	128.6	d	3.52E-01
180	Uranium	U-232	2.20E+13	3.97E+07	6	2.19E-04	95.187	68.9	y	6.89E+01
181	Uranium	U-233	7.50E+04	1.35E-01	6	2.19E-04	95.187	159,200	y	1.59E+05
182	Uranium	U-234	6.21E+09	1.12E+04	6	2.19E-04	95.187	245,500	y	2.46E+05
183	Uranium	U-235	1.55E+04	2.79E-02	6	2.19E-04	95.187	703,800,000	y	7.04E+08
40	Uranium	U-236	6.47E+07	1.16E+02	6	2.19E-04	95.187	23,420,000	y	2.34E+07
41	Uranium	U-238	3.36E+05	6.05E-01	6	2.19E-04	95.187	4,470,000,000	y	4.47E+09
184	Vanadium	V-50	5.11E-02	9.20E-08	10	1.32E-04	157.979	1.4E+17	y	1.40E+17
185	Zirconium	Zr-93	2.51E+09	4.53E+03	10	1.32E-04	157.979	1,530,000	y	1.53E+06
186	Surrogate	Ks-20	4.40E+08	7.92E+02	0.001	4.03E-02	1.016	1	y	1.00E+00
187	Surrogate	Ks-21	4.40E+08	7.92E+02	0.01	3.16E-02	1.157	1	y	1.00E+00
188	Surrogate	Ks-22	4.40E+08	7.92E+02	0.1	1.00E-02	2.570	1	y	1.00E+00
189	Surrogate	Ks-23	4.40E+08	7.92E+02	1	1.28E-03	16.698	1	y	1.00E+00
190	Surrogate	Ks-24	4.40E+08	7.92E+02	50	2.64E-05	785.895	4	y	4.00E+00
191	Surrogate	Ks-25	4.40E+08	7.92E+02	100	1.32E-05	1570.789	4	y	4.00E+00
192	Surrogate	Ks-26	4.40E+08	7.92E+02	1	1.28E-03	16.698	2	y	2.00E+00

Note: Concentrations shown in bold and italics are model-calculated concentrations that meet on GWPLs at the water table

Table 25. Waste Maximum Radionuclide Source Concentrations, K_ds, and Fractional Release Rates, based on 0.335 cm/year Infiltration

Waste Characteristics:	Infiltration Rate:	0.00335	m/yr
	Waste Thickness:	1	m
	Waste Moisture Content:	0.0564	cm^3/cm^3
	Waste Bulk Density:	1.8	gm/cm^3
Soil Characteristics:	Soil Thickness:	4.072	m
	Soil Moisture Content:	0.101	cm^3/cm^3
	Soil Bulk Density:	1.563	gm/cm^3

Pathrae Isotope Number	ELEMENT	NUCLIDE	Maximum Concentration (pCi/gm)	Maximum Concentr. (Ci/m3)	Distribution Coefficient (K_d) (L/Kg)	Fractional Release Rate (1/yr)	Soil Retardation Factor	1/2 life		1/2 life (Years)
101	Actinium	Ac-227	7.23E+13	1.30E+08	4.5	4.11E-04	70.619	21.77	y	2.18E+01
102	Silver	Ag-108m	2.61E+13	4.69E+07	2.7	6.81E-04	42.771	418	y	4.18E+02
103	Aluminum	Al-26	1.86E+10	3.35E+04	15	1.24E-04	233.062	740,000	y	7.40E+05
48	Americium	Am-241	1.00E+04	1.80E-02	1	1.80E-03	16.471	432.2	y	4.32E+02
104	Americium	Am-242m	1.00E+04	1.80E-02	1	1.80E-03	16.471	141	y	1.41E+02
105	Americium	Am-243	1.00E+04	1.80E-02	1	1.80E-03	16.471	7,370	y	7.37E+03
106	Barium	Ba-133	2.56E+14	4.61E+08	10	1.86E-04	155.708	10.5	y	1.05E+01
107	Beryllium	Be-10	2.20E+10	3.96E+04	2.5	7.35E-04	39.677	1,510,000	y	1.51E+06
108	Bismuth	Bi-207	5.37E+13	9.66E+07	1	1.80E-03	16.471	31.55	y	3.16E+01
109	Bismuth	Bi-210m	5.68E+08	1.02E+03	1	1.80E-03	16.471	3,040,000	y	3.04E+06
110	Berkelium	Bk-247	1.00E+04	1.80E-02	0.001	5.76E-02	1.015	1,400	y	1.40E+03
111	Carbon	C-14	5.00E+06	9.00E+00	8.52	2.18E-04	132.811	5,730	y	5.73E+03
112	Calcium	Ca-41	8.67E+10	1.56E+05	0.05	2.29E-02	1.774	103,000	y	1.03E+05
113	Cadmium	Cd-113	4.30E-01	7.75E-07	1	1.80E-03	16.471	9.3.E+15	y	9.30E+15
114	Cadmium	Cd-113m	2.25E+14	4.04E+08	1	1.80E-03	16.471	14.1	y	1.41E+01
115	Californium	Cf-249	1.00E+04	1.80E-02	2	9.16E-04	31.942	351	y	3.51E+02
116	Californium	Cf-250	1.00E+04	1.80E-02	2	9.16E-04	31.942	13.08	y	1.31E+01
117	Californium	Cf-251	1.00E+04	1.80E-02	2	9.16E-04	31.942	898	y	8.98E+02
118	Californium	Cf-252	4.40E+08	7.92E+02	2	9.16E-04	31.942	2.65	y	2.65E+00
119	Chlorine	Cl-36	***1.06E+08***	***1.90E+02***	0.0025	5.50E-02	1.039	301,000	y	3.01E+05
120	Curium	Cm-243	1.00E+04	1.80E-02	93.3	1.99E-05	1444.429	29	y	2.91E+01
50	Curium	Cm-244	1.00E+04	1.80E-02	93.3	1.99E-05	1444.429	18	y	1.81E+01
121	Curium	Cm-245	1.00E+04	1.80E-02	93.3	1.99E-05	1444.429	8,500	y	8.50E+03
122	Curium	Cm-246	1.00E+04	1.80E-02	93.3	1.99E-05	1444.429	4730	y	4.73E+03
123	Curium	Cm-247	1.00E+04	1.80E-02	93.3	1.99E-05	1444.429	15,600,000	y	1.56E+07
124	Curium	Cm-248	1.00E+04	1.80E-02	93.3	1.99E-05	1444.429	340,000	y	3.40E+05
125	Cobalt	Co-60	4.40E+08	7.92E+02	370	5.03E-06	5725.208	5	y	5.27E+00
126	Cesium	Cs-135	1.15E+09	2.07E+03	133	1.40E-05	2058.621	2,300,000	y	2.30E+06
127	Cesium	Cs-137	6.30E+05	1.13E+00	133	1.40E-05	2058.621	30.07	y	3.01E+01
128	Europium	Eu-152	1.73E+14	3.11E+08	6.5	2.85E-04	101.560	14	y	1.35E+01
129	Europium	Eu-154	2.70E+14	4.87E+08	6.5	2.85E-04	101.560	8.6	y	8.59E+00
130	Europium	Eu-155	4.40E+08	7.92E+02	6.5	2.85E-04	101.560	4.76	y	4.76E+00
131	Iron	Fe-55	4.40E+08	7.92E+02	1.4	1.30E-03	22.659	2.73	y	2.73E+00
132	Iron	Fe-60	3.97E+09	7.15E+03	1.4	1.30E-03	22.659	1,500,000	y	1.50E+06
133	Gadolinium	Gd-148	3.22E+13	5.80E+07	6.5	2.85E-04	101.560	74.6	y	7.46E+01
134	Hydrogen	H-3	2.50E+07	4.50E+01	0.04	2.61E-02	1.619	12.3	y	1.23E+01
135	Mercury	Hg-194	3.55E+12	6.38E+06	10	1.86E-04	155.708	444	y	4.44E+02
136	Holmium	Ho-166m	1.80E+12	3.24E+06	2.5	7.35E-04	39.677	1,200	y	1.20E+03
137	Iodine	I-129	5.00E+03	9.00E-03	0.12	1.23E-02	2.856	15,700,000	y	1.57E+07
138	Potassium	K-40	1.80E+09	3.24E+03	6.4	2.89E-04	100.013	1,277,000,000	y	1.28E+09
139	Manganese	Mn-53	4.40E+08	7.92E+02	1	1.80E-03	16.471	3,740,000.00	y	3.74E+06
140	Sodium	Na-22	5.78E+12	1.04E+07	1.6	1.14E-03	25.753	2.6	y	2.60E+00
141	Niobium	Nb-91	1.12E+08	2.02E+02	1.6	1.14E-03	25.753	680	y	6.80E+02
142	Niobium	Nb-92	2.63E+14	4.74E+08	1.6	1.14E-03	25.753	34,700,000	y	3.47E+07
143	Niobium	Nb-93m	1.30E+04	2.34E-02	1.6	1.14E-03	25.753	16.13	y	1.61E+01
144	Niobium	Nb-94	1.40E+07	2.52E+01	10	1.86E-04	155.708	20,300	y	2.03E+04
146	Nickel	Ni-59	2.20E+06	3.96E+00	10	1.86E-04	155.708	76,000	y	7.60E+04
147	Nickel	Ni-63	1.00E+04	1.80E-02	3	6.14E-04	47.412	100.1	y	1.00E+02
42	Neptunium	Np-237	3.07E+14	5.53E+08	4.5	4.11E-04	70.619	2,144,000	y	2.14E+06
148	Osmium	Os-194	4.70E+10	8.46E+04	5.5	3.36E-04	86.090	6	y	6.00E+00
149	Protactinium	Pa-231	3.40E+09	6.12E+03	19	9.78E-05	294.946	32,760	y	3.28E+04
150	Lead	Pb-202	7.60E+13	1.37E+08	19	9.78E-05	294.946	52,500	y	5.25E+04
151	Lead	Pb-210	5.10E+08	9.18E+02	0.55	3.20E-03	9.509	22.3	y	2.23E+01
152	Palladium	Pd-107	1.40E+14	2.52E+08	6.5	2.85E-04	101.560	6,500,000	y	6.50E+06
153	Promethium	Pm-145	4.40E+08	7.92E+02	6.5	2.85E-04	101.560	17.7	y	1.77E+01
154	Promethium	Pm-147	4.40E+08	7.92E+02	9	2.06E-04	140.237	2.6234	y	2.62E+00
155	Polonium	Po-208	7.23E+13	1.30E+08	4.5	4.11E-04	70.619	2.9	y	2.90E+00

Table 25. Waste Maximum Radionuclide Source Concentrations, Kds, and Fractional Release Rates, based on 0.335 cm/year Infiltration (Part 2)

Pathrae Isotope Number	ELEMENT	NUCLIDE	Maximum Concentration (pCi/gm)	Maximum Concentr. (Ci/m3)	Distribution Coefficient (K_d) (L/Kg)	Fractional Release Rate (1/yr)	Soil Retardation Factor	1/2 life		1/2 life (Years)
156	Polonium	Po-209	1.68E+13	3.02E+07	9	1.37E-04	140.237	102	y	1.02E+02
157	Platinum	Pt-193	3.70E+13	6.66E+07	0.9	1.33E-03	14.924	50	y	5.00E+01
158	Plutonium	Pu-236	5.00E+02	9.00E-04	10	1.24E-04	155.708	2.86	y	2.86E+00
159	Plutonium	Pu-238	1.00E+04	1.80E-02	10	1.24E-04	155.708	87.7	y	8.77E+01
160	Plutonium	Pu-239	1.00E+04	1.80E-02	10	1.24E-04	155.708	24,110	y	2.41E+04
45	Plutonium	Pu-240	1.00E+04	1.80E-02	10	1.24E-04	155.708	6,564	y	6.56E+03
46	Plutonium	Pu-241	3.50E+05	6.30E-01	10	1.24E-04	155.708	14.35	y	1.44E+01
161	Plutonium	Pu-242	1.00E+04	1.80E-02	10	1.24E-04	155.708	373,300	y	3.73E+05
162	Plutonium	Pu-244	5.00E+02	9.00E-04	10	1.24E-04	155.708	80,800,000	y	8.08E+07
55	Radium	Ra-226	1.00E+04	1.80E-02	10	1.24E-04	155.708	1,600	y	1.60E+03
163	Radium	Ra-228	2.72E+14	4.90E+08	10	1.24E-04	155.708	5.75	y	5.75E+00
164	Rhenium	Re-187	3.80E+04	6.84E-02	0.075	1.17E-02	2.160	43,500,000,000	y	4.35E+10
165	Selenium	Se-79	6.97E+10	1.25E+05	1	1.20E-03	16.471	65,000	y	6.50E+04
166	Silicon	Si-32	6.50E+13	1.17E+08	0.35	3.25E-03	6.415	172	y	1.72E+02
167	Samarium	Sm-151	2.63E+13	4.74E+07	2.45	4.99E-04	38.904	90	y	9.00E+01
168	Tin	Sn-121m	5.38E+13	9.68E+07	50	2.48E-05	774.542	55	y	5.50E+01
169	Tin	Sn-126	2.84E+10	5.11E+04	50	2.48E-05	774.542	100,000	y	1.00E+05
170	Strontium	Sr-90	2.50E+04	4.50E-02	0.05	1.52E-02	1.774	28.78	y	2.88E+01
171	Terbium	Tb-157	1.50E+13	2.70E+07	6.5	1.90E-04	101.560	71	y	7.10E+01
172	Terbium	Tb-158	1.50E+13	2.70E+07	6.5	1.90E-04	101.560	180	y	1.80E+02
173	Technetium	Tc-99	1.88E+05	3.38E-01	0.11	8.77E-03	2.702	211,100	y	2.11E+05
174	Tellurium	Te-123	2.91E+02	5.24E-04	1.25	9.67E-04	20.339	1E+13	y	1.00E+13
175	Thorium	Th-229	2.13E+11	3.83E+05	10	1.24E-04	155.708	7,880	y	7.88E+03
36	Thorium	Th-230	2.06E+10	3.71E+04	10	1.24E-04	155.708	75,380	y	7.54E+04
176	Thorium	Th-232	1.10E+05	1.98E-01	10	1.24E-04	155.708	14,050,000,000	y	1.41E+10
177	Titanium	Ti-44	1.56E+14	2.81E+08	10	1.24E-04	155.708	63	y	6.30E+01
178	Thallium	Tl-204	4.40E+08	7.92E+02	0.15	6.83E-03	3.321	3.78	y	3.78E+00
179	Thulium	Tm-170	4.40E+08	7.92E+02	6.5	1.90E-04	101.560	128.6	d	3.52E-01
180	Uranium	U-232	2.20E+13	3.97E+07	6	2.05E-04	93.825	68.9	y	6.89E+01
181	Uranium	U-233	7.50E+04	1.35E-01	6	2.05E-04	93.825	159,200	y	1.59E+05
182	Uranium	U-234	6.21E+09	1.12E+04	6	2.05E-04	93.825	245,500	y	2.46E+05
183	Uranium	U-235	1.55E+04	2.79E-02	6	2.05E-04	93.825	703,800,000	y	7.04E+08
40	Uranium	U-236	6.47E+07	1.16E+02	6	2.05E-04	93.825	23,420,000	y	2.34E+07
41	Uranium	U-238	3.36E+05	6.05E-01	6	2.05E-04	93.825	4,470,000,000	y	4.47E+09
184	Vanadium	V-50	5.11E-02	9.20E-08	10	1.24E-04	155.708	1.4E+17	y	1.40E+17
185	Zirconium	Zr-93	2.51E+09	4.53E+03	10	1.24E-04	155.708	1,530,000	y	1.53E+06
186	Surrogate	Ks-20	4.40E+08	7.92E+02	0.001	3.83E-02	1.015	1	y	1.00E+00
187	Surrogate	Ks-21	4.40E+08	7.92E+02	0.01	3.00E-02	1.155	1	y	1.00E+00
188	Surrogate	Ks-22	4.40E+08	7.92E+02	0.1	9.43E-03	2.547	1	y	1.00E+00
189	Surrogate	Ks-23	4.40E+08	7.92E+02	1	1.20E-03	16.471	1	y	1.00E+00
190	Surrogate	Ks-24	4.40E+08	7.92E+02	50	2.48E-05	774.542	4	y	4.00E+00
191	Surrogate	Ks-25	4.40E+08	7.92E+02	100	1.24E-05	1548.083	4	y	4.00E+00
192	Surrogate	Ks-26	4.40E+08	7.92E+02	1	1.20E-03	16.471	2	y	2.00E+00

Note: Concentrations shown in bold and italics are model-calculated concentrations that meet on GWPLs at the water table

5.1.1.2 Heavy Metals Concentrations

The starting metals concentrations in the model were determined by calculating the maximum possible metals concentration, based on the density of each metal. Those metal densities, and corresponding concentrations in mg/m^3 are given in Table 26. The PATHRAE model was run using these source term concentrations in the vertical (unsaturated) model domain.

Table 26. Maximum Possible Metals Concentrations Based on Density

Element	Symbol	Density (gm/cc)	Maximum Possible Metal Concentration (mg/m^3)
Silver	Ag	10.5	1.05E+10
Arsenic	As	5.73	5.73E+09
Barium	Ba	3.5	3.50E+09
Beryllium	Be	1.848	1.85E+09
Cadmium	Cd	8.65	8.65E+09
Chromium	Cr	8.96	8.96E+09
Copper	Cu	8.92	8.92E+09
Mercury	Hg	13.54	1.35E+10
Molybdenum	Mo	10.22	1.02E+10
Nickel	Ni	8.4	8.40E+09
Lead	Pb	11.35	1.14E+10
Selenium	Se	4.79	4.79E+09
Zinc	Zn	7.13	7.13E+09

5.1.2 Waste Bulk Density

A value of 1.8 gm/cm^3 was used for the bulk density of the waste. This value is consistent with previous modeling and the range of density determined by Energy*Solutions* (1.75 to 1.80 gm/cm^3) for the compacted, in-place waste.

5.1.3 Partitioning Coefficients (K_d)

The partitioning coefficient (a.k.a. distribution coefficient, sorption coefficient, or K_d) is the equilibrium ratio of the adsorbed contaminant concentration in soil or waste (mg/kg) to the concentration in the pore water or leachate (mg/l). Higher K_d values indicate that the constituent is more likely to partition to the soil and less likely to be released into groundwater.

The K_d values used in modeling the fate and transport of isotopes at the Energy*Solutions* site have evolved over time, as radionuclide inventories changed and more information was obtained from the literature and from site-specific K_d testing. The modeling performed for the CAW cell incorporates the current approved K_d values for the site. The modeling preferentially uses 1) approved site-specific K_d values, 2) the lowest measured soil K_d values published in the literature, and 3) published K_d values calculated from the soil:plant ratio. Approved site-specific K_d values were available for Cs, Co, C-14, I-129, Np-237, Tc-99, U and Zn. The most conservative (lowest) K_d values found in the literature were used for nuclides that did not have site-specific K_d values, as indicated in Table 27. The soil:plant ratio was only used where actual measured soil K_d values are not available, and the published K_d value from the soil:plant ratio was decreased by two orders of magnitude to be conservative. The K_d values and data sources for radionuclides and metals are listed in Table 27.

Table 27. Sorption Coefficient (K_d) Values for Radionuclides and Metals

(See large tables at end of report document)

5.1.4 Half Lives

The half lives used in the modeling are shown in Table 24 and Table 25. Radionuclides were modeled using half lives identical to those used in the previous Class A cell modeling (Whetstone, 2000e). The source of the radionuclide half lives are provided in Table 28. All of the metals were modeled using a half life of 10^{14} years, which essentially allowed no degradation.

5.1.5 Fractional Release Rate

The annual fractional release rate, or "leach rate", was calculated using the following equation (Kozak 1990):

$$L = \frac{q_{in}}{d\theta\left(1 + \frac{\rho K_d}{\theta}\right)}$$

where L = fractional annual contaminant release rate (yr^{-1})
q_{in} = water infiltration rate (m/yr)
θ = volumetric moisture content of waste
d = waste layer thickness (meters)
ρ = waste density (g/cm^3)
K_d = waste distribution coefficient (ml/g)

This method of determining the leachate concentration is environmentally-conservative for several reasons. First, PATHRAE assumes that the release rate is constant throughout time. The constituent is leached from the waste at a constant rate, until the initial source concentration is totally mobilized. In reality, the leach rate will decrease as the source concentration decreases. Second, the use of K_d to determine contaminant release rates assumes that all of the constituent is adsorbed and will eventually be completely desorbed (or leached out) by percolating water. In reality, some of the constituent may occur in the refractory phase, which would render it less mobile. Last, the CAW cell modeling used the lowest literature K_d values, for constituents without site-specific K_ds.

The annual fractional release rates from the waste (vertical simulation) were calculated based on the infiltration rate (q_{in}) from the HELP3 modeling and the moisture content (θ) from the UNSAT-H modeling. The annual fractional release rates for each nuclide are shown in Table 24 for the top slope and Table 25 for the side slope.

5.1.6 Container Life

The container life was set to zero, in both the horizontal and vertical PATHRAE modeling. The CAW cell modeling disregards the time required for the water to percolate through the cover, and assumes that the clay cover is immediately degraded and that water moves through the cover instantaneously.

In reality, a significant delay will occur for the time required to wet the cover and the waste, and for moisture to travel through the cell cover, waste, and liner. Although the initial waste moisture contents cannot be known with certainty due to the inherent variability in the waste and in climatic conditions while the cell is open, previous open-cell modeling suggests that drying of the waste may occur and that the moisture content in the waste at the time of cell closure may be well below the levels assumed at the start of the closed cell modeling.

Table 28. Radionuclide Half-Lives and Data Sources

Nuclide	HALF-LIFE (Years)	DATA SOURCE
Ag-108	4.5E-06	National Nuclear Data Center, Brookhaven National Laboratory, August 1996
Ag-110m	0.684	Chart of the Nuclides Knolls Atomic Power Laboratory Naval Reactors, DOE, Rev. 1996.
Al-26	740,000	National Nuclear Data Center, Brookhaven National Laboratory, August 1996
Am-241	432.2	National Nuclear Data Center, Brookhaven National Laboratory, August 1996
Am-243	7,370	National Nuclear Data Center, Brookhaven National Laboratory, August 1996
Au-195	0.510	Chart of the Nuclides Knolls Atomic Power Laboratory Naval Reactors, DOE, Rev. 1996.
Ba-133	10.51	National Nuclear Data Center, Brookhaven National Laboratory, August 1996
Be-7	1.46E-01	Chart of the Nuclides Knolls Atomic Power Laboratory Naval Reactors, DOE, Rev. 1996.
Bi-207	32	National Nuclear Data Center, Brookhaven National Laboratory, August 1996
Bi-210m	3,040,000	National Nuclear Data Center, Brookhaven National Laboratory, August 1996
Bk-247	1,400	F.W. Walker, et. al., "Nuclides and Isotopes, Fourteenth Edition", General Electric Co. (1989)
C-14	5730	National Nuclear Data Center, Brookhaven National Laboratory, August 1996
Ca-45	0.446	Chart of the Nuclides Knolls Atomic Power Laboratory Naval Reactors, DOE, Rev. 1996.
Cd-109	1.267	Chart of the Nuclides Knolls Atomic Power Laboratory Naval Reactors, DOE, Rev. 1996.
Cd-113m	14.1	F.W. Walker, et. al., "Nuclides and Isotopes, Fourteenth Edition", General Electric Co. (1989)
Ce-139	0.377	Chart of the Nuclides Knolls Atomic Power Laboratory Naval Reactors, DOE, Rev. 1996.
Ce-141	0.089	Chart of the Nuclides Knolls Atomic Power Laboratory Naval Reactors, DOE, Rev. 1996.
Ce-144	0.781	Chart of the Nuclides Knolls Atomic Power Laboratory Naval Reactors, DOE, Rev. 1996.
Cf-249	351	National Nuclear Data Center, Brookhaven National Laboratory, August 1996
Cf-250	13.08	F.W. Walker, et. al., "Nuclides and Isotopes, Fourteenth Edition", General Electric Co. (1989)
Cf-251	898	National Nuclear Data Center, Brookhaven National Laboratory, August 1996
Cl-36	301,000	Chart of the Nuclides Knolls Atomic Power Laboratory Naval Reactors, DOE, Rev. 1996.
Cm-242	0.446	Chart of the Nuclides Knolls Atomic Power Laboratory Naval Reactors, DOE, Rev. 1996.
Cm-243	29.10	National Nuclear Data Center, Brookhaven National Laboratory, August 1996
Cm-244	18.10	National Nuclear Data Center, Brookhaven National Laboratory, August 1996
Cm-245	8,500	F.W. Walker, et. al., "Nuclides and Isotopes, Fourteenth Edition", General Electric Co. (1989)
Cm-246	4,730	National Nuclear Data Center, Brookhaven National Laboratory, August 1996
Cm-247	15,600,000	Kocher, David C. Radioactive Decay Data Tables, A Handbook of Decay Data for Application to Radiation Dosimetry and Radiological Assessments, Technical Information Center, US DOE
Cm-248	340,000	National Nuclear Data Center, Brookhaven National Laboratory, August 1996
Co-56	0.212	Chart of the Nuclides Knolls Atomic Power Laboratory Naval Reactors, DOE, Rev. 1996.
Co-57	0.745	Chart of the Nuclides Knolls Atomic Power Laboratory Naval Reactors, DOE, Rev. 1996.
Co-58	0.194	Chart of the Nuclides Knolls Atomic Power Laboratory Naval Reactors, DOE, Rev. 1996.
Co-60	5.270	National Nuclear Data Center, Brookhaven National Laboratory, August 1996
Cr-51	0.076	Chart of the Nuclides Knolls Atomic Power Laboratory Naval Reactors, DOE, Rev. 1996.
Cs-134	2.065	Chart of the Nuclides Knolls Atomic Power Laboratory Naval Reactors, DOE, Rev. 1996.
Cs-135	2,300,000	Chart of the Nuclides Knolls Atomic Power Laboratory Naval Reactors, DOE, Rev. 1996.
Cs-137	30.07	Chart of the Nuclides Knolls Atomic Power Laboratory Naval Reactors, DOE, Rev. 1996.
Cu-67	0.169	Chart of the Nuclides Knolls Atomic Power Laboratory Naval Reactors, DOE, Rev. 1996.
Eu-152	13.54	Chart of the Nuclides Knolls Atomic Power Laboratory Naval Reactors, DOE, Rev. 1996.
Eu-154	8.59	National Nuclear Data Center, Brookhaven National Laboratory, August 1996
Eu-155	4.76	Chart of the Nuclides Knolls Atomic Power Laboratory Naval Reactors, DOE, Rev. 1996.
Fe-55	2.73	Chart of the Nuclides Knolls Atomic Power Laboratory Naval Reactors, DOE, Rev. 1996.
Fe-59	0.122	Chart of the Nuclides Knolls Atomic Power Laboratory Naval Reactors, DOE, Rev. 1996.
Fe-60	1,500,000	F.W. Walker, et. al., "Nuclides and Isotopes, Fourteenth Edition", General Electric Co. (1989)
Gd-148	74.6	National Nuclear Data Center, Brookhaven National Laboratory, August 1996
Gd-153	0.662	Chart of the Nuclides Knolls Atomic Power Laboratory Naval Reactors, DOE, Rev. 1996.
Ge-68	0.742	Chart of the Nuclides Knolls Atomic Power Laboratory Naval Reactors, DOE, Rev. 1996.
H-3	12.33	National Nuclear Data Center, Brookhaven National Laboratory, August 1996
Hf-181	0.116	Chart of the Nuclides Knolls Atomic Power Laboratory Naval Reactors, DOE, Rev. 1996.
Hg-194	444	National Nuclear Data Center, Brookhaven National Laboratory, August 1996
Hg-203	0.128	Chart of the Nuclides Knolls Atomic Power Laboratory Naval Reactors, DOE, Rev. 1996.
Ho-166m	1,200	F.W. Walker, et. al., "Nuclides and Isotopes, Fourteenth Edition", General Electric Co. (1989)
I-125	0.163	Chart of the Nuclides Knolls Atomic Power Laboratory Naval Reactors, DOE, Rev. 1996.
I-129	1.57E+07	Chart of the Nuclides Knolls Atomic Power Laboratory Naval Reactors, DOE, Rev. 1996.
Ir-192	0.202	Chart of the Nuclides Knolls Atomic Power Laboratory Naval Reactors, DOE, Rev. 1996.
K-40	1.28E+09	National Nuclear Data Center, Brookhaven National Laboratory, August 1996
Mn-54	0.856	Chart of the Nuclides Knolls Atomic Power Laboratory Naval Reactors, DOE, Rev. 1996.
Na-22	2.6	Chart of the Nuclides Knolls Atomic Power Laboratory Naval Reactors, DOE, Rev. 1996.
Nb-93m	16.13	National Nuclear Data Center, Brookhaven National Laboratory, August 1996
Nb-94	20,300	National Nuclear Data Center, Brookhaven National Laboratory, August 1996
Ni-59	76,000	Chart of the Nuclides Knolls Atomic Power Laboratory Naval Reactors, DOE, Rev. 1996.

Table 28. Radionuclide Half-Lives and Data Sources (Part 2)

Nuclide	HALF-LIFE (Years)	DATA SOURCE
Ni-63	100	National Nuclear Data Center, Brookhaven National Laboratory, August 1996
Np-237	2,144,000	National Nuclear Data Center, Brookhaven National Laboratory, August 1996
Os-194	6	F.W. Walker, et. al., "Nuclides and Isotopes, Fourteenth Edition", General Electric Co. (1989)
Pb-210	22.30	National Nuclear Data Center, Brookhaven National Laboratory, August 1996
Pm-147	2.62	Chart of the Nuclides Knolls Atomic Power Laboratory Naval Reactors, DOE, Rev. 1996.
Po-209	102	F.W. Walker, et. al., "Nuclides and Isotopes, Fourteenth Edition", General Electric Co. (1989)
Po-210	0.379	Chart of the Nuclides Knolls Atomic Power Laboratory Naval Reactors, DOE, Rev. 1996.
Pu-236	2.86	National Nuclear Data Center, Brookhaven National Laboratory, August 1996
Pu-238	87.70	National Nuclear Data Center, Brookhaven National Laboratory, August 1996
Pu-239	24,110	National Nuclear Data Center, Brookhaven National Laboratory, August 1996
Pu-240	6,564	National Nuclear Data Center, Brookhaven National Laboratory, August 1996
Pu-241	14.35	National Nuclear Data Center, Brookhaven National Laboratory, August 1996
Pu-242	373,300	National Nuclear Data Center, Brookhaven National Laboratory, August 1996
Pu-243	0.00057	Kocher, David C. Radioactive Decay Data Tables, A Handbook of Decay Data for Application to Radiation Dosimetry and Radiological Assessments, Technical Information Center, US DOE
Pu-244	80,800,000	National Nuclear Data Center, Brookhaven National Laboratory, August 1996
Ra-226	1,600	Chart of the Nuclides Knolls Atomic Power Laboratory Naval Reactors, DOE, Rev. 1996.
Ra-228	5.75	Chart of the Nuclides Knolls Atomic Power Laboratory Naval Reactors, DOE, Rev. 1996.
Rb-83	0.236	Chart of the Nuclides Knolls Atomic Power Laboratory Naval Reactors, DOE, Rev. 1996.
Ru-106	1.02	Chart of the Nuclides Knolls Atomic Power Laboratory Naval Reactors, DOE, Rev. 1996.
S-35	0.240	Chart of the Nuclides Knolls Atomic Power Laboratory Naval Reactors, DOE, Rev. 1996.
Sb-124	1.65E-01	Chart of the Nuclides Knolls Atomic Power Laboratory Naval Reactors, DOE, Rev. 1996.
Sb-125	2.76	National Nuclear Data Center, Brookhaven National Laboratory, August 1996
Sc-46	0.230	Chart of the Nuclides Knolls Atomic Power Laboratory Naval Reactors, DOE, Rev. 1996.
Se-75	0.328	Chart of the Nuclides Knolls Atomic Power Laboratory Naval Reactors, DOE, Rev. 1996.
Se-79	65,000	F.W. Walker, et. al., "Nuclides and Isotopes, Fourteenth Edition", General Electric Co. (1989)
Si-32	172	National Nuclear Data Center, Brookhaven National Laboratory, August 1996
Sm-151	90	Chart of the Nuclides Knolls Atomic Power Laboratory Naval Reactors, DOE, Rev. 1996.
Sn-113	0.315	Chart of the Nuclides Knolls Atomic Power Laboratory Naval Reactors, DOE, Rev. 1996.
Sn-121m	55	F.W. Walker, et. al., "Nuclides and Isotopes, Fourteenth Edition", General Electric Co. (1989)
Sn-126	100,000	F.W. Walker, et. al., "Nuclides and Isotopes, Fourteenth Edition", General Electric Co. (1989)
Sr-85	0.178	Chart of the Nuclides Knolls Atomic Power Laboratory Naval Reactors, DOE, Rev. 1996.
Sr-89	0.138	Chart of the Nuclides Knolls Atomic Power Laboratory Naval Reactors, DOE, Rev. 1996.
Sr-90	28.8	National Nuclear Data Center, Brookhaven National Laboratory, August 1996
Ta-182	0.314	Chart of the Nuclides Knolls Atomic Power Laboratory Naval Reactors, DOE, Rev. 1996.
Tc-99	211,100	National Nuclear Data Center, Brookhaven National Laboratory, August 1996
Th-229	7,880	National Nuclear Data Center, Brookhaven National Laboratory, August 1996
Th-230	75,380	National Nuclear Data Center, Brookhaven National Laboratory, August 1996
Th-232	1.41E+10	National Nuclear Data Center, Brookhaven National Laboratory, August 1996
Ti-44	63	National Nuclear Data Center, Brookhaven National Laboratory, August 1996
Tl-204	3.78	Integrated Data Base for 1989, Spent Fuel and Radioactive Waste Inventories, Projections, and Characteristics, Prepared for U.S. Dept. of Energy. Nov. 1989.
Tm-170	0.352	F.W. Walker, et. al., "Nuclides and Isotopes, Fourteenth Edition", General Electric Co. (1989)
U-232	68.9	National Nuclear Data Center, Brookhaven National Laboratory, August 1996
U-233	159,200	National Nuclear Data Center, Brookhaven National Laboratory, August 1996
U-234	245,500	National Nuclear Data Center, Brookhaven National Laboratory, August 1996
U-235	7.04E+08	National Nuclear Data Center, Brookhaven National Laboratory, August 1996
U-236	2.34E+07	National Nuclear Data Center, Brookhaven National Laboratory, August 1996
U-238	4.47E+09	F.W. Walker, et. al., "Nuclides and Isotopes, Fourteenth Edition", General Electric Co. (1989)
Y-88	0.292	F.W. Walker, et. al., "Nuclides and Isotopes, Fourteenth Edition", General Electric Co. (1989)
Y-91	0.160	Chart of the Nuclides Knolls Atomic Power Laboratory Naval Reactors, DOE, Rev. 1996.
Zn-65	0.669	Chart of the Nuclides Knolls Atomic Power Laboratory Naval Reactors, DOE, Rev. 1996.
Zr-95	0.175	Chart of the Nuclides Knolls Atomic Power Laboratory Naval Reactors, DOE, Rev. 1996.

5.1.7 Decay Chain Computation

The natural uranium decay chain (U-238→Th-230→U-234) and the plutonium-241 decay chain (Pu-241→Am-241→Np-237) were calculated by the model. PATHRAE has the ability to model five other decay chains, but this option was not invoked.

The simulation of decay chains for Pu-241→Am-241→Np-237 and U-238→Th-230→Ra-226 requires that all decay chain isotopes be contained in a single model run. The vertical model run with decay contained a total of 65 isotopes. The remaining 35 isotopes were modeled in a separate run, which did not invoke the decay chain option. Also, because the decay chain calculations require each isotope in the decay chain to have a different retardation, the Ra-226 K_d was changed from 10.0 to 9.99 in the vertical PathRAE input files.

5.2 Vertical Input Parameters for Flow and Transport

5.2.1 Infiltration

The infiltration rate through the CAW cell was determined from the HELP3 modeling described in Section 2.0 above. Two infiltration rates were used to evaluate transport. The 0.238 cm/yr infiltration rate was used to evaluate transport from the top slope, while the 0.335 cm/yr infiltration rate was used to evaluate transport from the side slope (Table 29).

Table 29. Infiltration Rates Input to PATHRAE Model

MODEL CASE	INFILTRATION RATE
Top Slope – Base Case	0.238 cm/yr
Side Slope – Base Case	0.335 cm/yr

5.2.2 Single Homogeneous Medium

PATHRAE is limited to solving the contaminant transport equation in one homogeneous medium for the vertical zone and one for the horizontal zone. In reality, particles migrating out of the landfill cell along the vertical pathway may travel through the waste, the bottom clay liner, the Unit 3 sand, and potentially the Unit 2 clay, all of which have differing hydraulic properties.

For the vertical pathway, the characteristics of individual units were converted to a single equivalent porous medium based on the methods described below. The equivalent moisture content and soil moisture velocities were calculated using the infiltration rate from the HELP3 modeling and UNSAT-H modeling. The characteristics of the equivalent porous media for the top slope and side slope are given in Table 30 and Table 31, respectively.

The soil bulk density for the equivalent porous media (clay liner and Unit 3 sand) below the CAW cell was calculated as the thickness-weighted average using the following equation:

$$\rho_{eq} = \frac{\left(\rho_{clay} \cdot d_{clay}\right) + \left(\rho_{sand} \cdot d_{sand}\right)}{\left(d_{clay} + d_{sand}\right)}$$

Where ρ = density
d = thickness

The volumetric water content for the equivalent porous media (clay liner and Unit 3 sand) below the CAW cell was calculated as the thickness-weighted average using the following equation:

$$\theta_{eq} = \frac{(\theta_{clay} \cdot d_{clay}) + (\theta_{sand} \cdot d_{sand})}{(d_{clay} + d_{sand})}$$

Where θ = volumetric water content
d = thickness

Table 30. Calculation of Equivalent Porous Media Properties based on CAW Cell Top Slope Design (0.238 cm/year Infiltration)

Layer	Material Type	Soil Bulk Density (g/cm^3)	Layer Thickness (cm)	Volumetric Water Content	Infiltration (cm/day)	Vadose Velocity (cm/yr)	Vadose Velocity (m/yr)	Saturated Hydraulic Conductivity (cm/sec)	Saturated Hydraulic Conductivity (m/yr)
0	Waste	1.8	50	0.0573	0.00065	0.24	0.002	5.00E-04	157.7
1	Clay Liner	1.35	61	0.4182	0.00065	1.76	0.018	1.00E-06	0.315
2	Unit 3 Sand	1.6	346.25	0.0434	0.00065	0.18	0.002	7.53E-04	237.5
1+2	Weighted average	1.563	407.25	0.100		0.418	0.0042	6.63E-06	2.09

Notes: Waste thickness is based on midpoint of unit (1 m^3) block of waste above liner.
Volumetric water content from UNSAT-H model run T6E_21
Infiltration from HELP3 model, Class A West cell top slope run MT6
Vadose velocity = Infiltration/effective porosity
Vadose velocity for Clay+Unit 3 = (infiltration) / (weighted average effective porosity)
Saturated hydraulic conductivity of Unit 3 sand is site-wide geometric mean K from Table 16.

Table 31. Calculation of Equivalent Porous Media Properties based on CAW Cell Side Slope Design (0.335 cm/year Infiltration)

Layer	Material Type	Soil Bulk Density (gm/cm^3)	Layer Thickness (cm)	Volumetric Water Content	Infiltration (cm/day)	Vadose Velocity (cm/yr)	Vadose Velocity (m/yr)	Saturated Hydraulic Conductivity (cm/sec)	Saturated Hydraulic Conductivity (m/yr)
0	Waste	1.8	50	0.0599	0.00092	0.18	0.002	5.00E-04	157.7
1	Clay Liner	1.35	61	0.4191	0.00092	1.25	0.013	1.00E-06	0.315
2	Unit 3 Sand	1.6	346.25	0.0451	0.00092	0.13	0.001	7.53E-04	237.5
1+2	Weighted average	1.563	407.25	0.101		0.302	0.0030	6.63E-06	2.09

Notes: Waste thickness is based on midpoint of unit (1 m^3) block of waste above liner.
Volumetric water content from UNSAT-H model run S6E_08
Infiltration from HELP3 model, Class A West cell side slope run M6S6-R3
Vadose velocity = Infiltration/effective porosity
Vadose velocity for Clay+Unit 3 = (infiltration) / (weighted average effective porosity)
Saturated hydraulic conductivity of Unit 3 sand is site-wide geometric mean K from Table 16.

The saturated hydraulic conductivity of the equivalent porous media representing the clay liner and Unit 3 sand was calculated using method to calculate an equivalent vertical hydraulic conductivity for a system of layers described in Freeze and Cherry (1979):

$$K_z = \frac{d}{\sum_{i=1}^{n} d_i / K_i} = \frac{d_1 + d_2 + d_3 + \ldots d_n}{\left(\frac{d_1}{K_1} + \frac{d_2}{K_2} + \frac{d_3}{K_3} \ldots + \frac{d_n}{K_n} \right)}$$

Where K_z = equivalent vertical hydraulic conductivity (L/T)
d_i = thickness of the given layer (L)
K_i = hydraulic conductivity of the given layer (L/T)

Applying this equation to the layered media below the CAW waste and above the capillary fringe, the equivalent saturated vertical hydraulic conductivity was calculated as follows:

$$K_{eq} = \frac{d_c + d_s}{\left(\frac{d_c}{K_c} + \frac{d_s}{K_s} \right)}$$

Where K_{eq} = equivalent vertical hydraulic conductivity (L/T)
d_c = thickness of the clay layer (L)
K_c = saturated hydraulic conductivity of the clay layer (L/T)
d_s = thickness of the Unit 3 Sand layer to the top of the capillary fringe (L)
K_c = saturated hydraulic conductivity of the Unit 3 Sand layer (L/T)

The saturated hydraulic conductivity of the clay layer is 1×10^{-6} cm/sec while the saturated hydraulic conductivity of the Unit 3 sand is 7.53×10^{-4} cm/sec, as described in Section 3.5. The thickness of the Unit 3 Sand from the bottom of the waste to the top of the capillary zone was determined from UNSAT-H modeling, as described in Section 3.6.2. The calculated saturated vertical hydraulic conductivity values for the equivalent porous media are shown in Table 30 and Table 31.

5.2.3 Aquifer Velocity

The aquifer velocity in the vertical model was calculated according to the equation for average linear velocity in the vadose zone (Stephens, 1996):

$$v = q / \theta_e$$

where v = average linear velocity (L/T)
q = infiltration rate (L/T)
θ_e = effective water content that participates in carrying the flow (L^3/L^3)

In this equation, the infiltration rate (q) was determined using the HELP3 model. The moisture content (θ) was determined for each material using the UNSAT-H model, as described in Section 3.6.1.

The velocity for the layered vertical profile was calculated as a thickness-weighted average of the layered profile which included the clay liner and Unit 3 sand to the top of the capillary fringe. The velocity through the layered profile was calculated as follows:

$$v_{eq} = \frac{v_c \cdot d_c + v_s \cdot d_s}{(d_c + d_s)} = \frac{q/\theta_c \cdot d_c + q/\theta_s \cdot d_s}{(d_c + d_s)}$$

Where v_{eq} = average linear velocity of the layered system represented by an equivalent porous medium (L/T)
v_c = average linear velocity of the clay layer (L/T)
d_c = thickness of the clay layer (L)
v_s = average linear velocity of the Unit 3 Sand layer (L/T)
d_s = thickness of the Unit 3 Sand layer to the top of the capillary fringe (L)
q = infiltration rate (L/T)
θ_c = effective water content in the clay (L^3/L^3)
θ_s = effective water content in the Unit 3 Sand (L^3/L^3)

The vadose zone velocities calculated for the equivalent porous media (liner and silty sand) underlying the top slope and side slope simulations are 0.418 and 0.302 cm/yr, as shown in Table 30 and Table 31.

5.2.4 Vertical Transport Distance

The vertical pathway represents the distance from the bottom of the waste to the aquifer, including the 2-foot thick clay liner and excluding the capillary fringe. The distance from the bottom of the waste to the top of the aquifer is 15.40 feet, based on the cell design and the measured water levels in August 2010. Using the measured elevations adjusted for freshwater head (Table 13), and the capillary fringe height predicted by the UNSAT-H modeling (Section 3.6.2), the distance was calculated as follows:

$$\text{Adjusted Distance} = H_{clay} - H_{aq} - cf$$

$$\text{Adjusted Distance} = 4265.0 - 4249.6 - 2.04 = 13.36 \text{ feet}$$

where H_{clay} = Elevation of the top of the clay (4265.0, based on engineering drawing 10014 C01)
H_{aq} = Elevation of the top of the aquifer (4249.6, see Table 13)
cf = Capillary fringe (2.04 feet, determined from UNSAT-H modeling)

The PATHRAE model requires distances in meters. The 13.36 feet was converted to 4.072 meters, for the vertical transport distance.

Table 32. Calculation of Vertical Transport Distance

Top of clay elevation	4265.00	ft amsl
Water table elevation	4249.60	ft amsl
Distance to water table	15.40	
Height of capillary fringe	2.04	ft
Vertical transport distance	13.36	ft
Vertical transport distance	4.07	meters

5.2.5 Dispersivity

Dispersivity is an empirical index of the magnitude of variations of the pore velocities in the soil. Dispersivity in the vadose zone tends to be lower than that in the saturated zone because 1) the pore spaces through which water moves are generally of about the same size – larger and smaller pores do not participate in transport, and 2) layered heterogeneity may have an averaging effect on solute transport in the vadose zone.

- Soils with a small range of pore sizes have smaller values than those with a wide range of pore sizes (Nofziger et al, 1989). The Unit 3 soils below the CAW cell are moderately well sorted, indicating that dispersivity will be low.
- Values are generally less than 1 cm for laboratory columns and less than 10 cm for field soils (Rao, et al., 1987; Nofziger et al, 1989)
- Local differences in fluid velocity are evened out by layering or vertical heterogeneity (Wierenga, 1995). Dispersivity in a column filled with layered soils is half of the dispersivity measured in a column of uniformly filled with soil, as measured during unsaturated transport through 6 m deep columns (Porro and Wierenga, 1993). Similar observations were made by Roth, et al. (1991.)
- Dispersivity is dependent on the water content of the material and any change in water content which may be occurring. The highest dispersivities have been measured in soils which were fully saturated and are draining. The lowest dispersivities have been measured in soils with relatively stable moisture contents, as is expected in the long term below the CAW cell.
- Dispersivity is lower in layered systems.

For these reasons, the dispersivity of 0.1 meters was applied to the 4.07 meter transport distance in the vertical PATHRAE model runs. Previous modeling performed for the LARW cell (ABC, 1997) included sensitivity analyses using 0.2 and 0.4 meter dispersivity values. The vertical dispersivity value of 0.1 is consistent with the previously submitted and approved modeling at the site.

5.2.6 River Flow Rate

The river flow rate in the vertical model was set equal to the infiltration rate, in order to prevent any dilution of concentrations. The river flow rate was set to 0.00238 and 0.00335 m^3/yr for the top slope and side slope PATHRAE simulations.

5.3 Vertical Transport Model Results

5.3.1 Vertical Top Slope Analysis (0.238 cm/yr)

Two of the 99 nuclides[6] modeled exceeded the GWPLs at the water table in less than 500 years (Bk-247 and Cl-36), based on the top slope cover design infiltration rate of 0.238 cm/yr (0.094 in/yr), as shown in Table 33. A summary of peak concentrations and the year in which the GWPLs were exceeded are provided in Table 34. A complete listing of output times and concentrations for all nuclides that arrived at the water table is provided in Table 35. In all tables, the "Year To Exceed" is conservatively reported as the next *lowest* model output time. None of the surrogate nuclides exceeded a benchmark standard of 1 pCi/L.

Starting concentrations that would meet GWPLs at the water table were calculated for Bk-247 and Cl-36 and are shown in Table 23. A total of 16 nuclides were carried through to the horizontal PATHRAE modeling (described in Section 6) to determine the concentrations that would meet GWPLs at a compliance well (Section 6.3.1). The 16 nuclides that were carried forward to the horizontal PATHRAE modeling included Bk-247 and Cl-36 and 14 additional nuclides that met GWPLs at the water table.

[6] 92 real nuclides and 7 synthetic surrogate nuclides

Table 33. Summary of Peak Concentrations and Exceedences at the Water Table, PATHRAE Vertical Model Results for Top Slope 0.238 cm/yr Case

Nuclide	Time To Exceed (Year)	Peak Concentration (Ci/m^3)	Peak Concentration (pCi/L)	Peak Year
Cl-36	290	4.47E+04	4.47E+13	1,072.7
Bk-247	340	8.20E-03	8.20E+06	1,024.9
Ca-41	500	6.68E+04	6.68E+13	1,846.7
Sr-90	-1	1.16E-14	1.16E-05	859.3
I-129	-1	2.42E-03	2.42E+06	2,986.8
Re-187	-1	2.43E-02	2.43E+07	2,255.8
Si-32	-1	5.10E-02	5.10E+07	3,764.9
Tc-99	-1	9.51E-02	9.51E+07	2,826.0

Note: -1 indicates nuclide did not exceed GWPLs at the water table within the 1,000 years modeled

Most of the nuclides did not exceed GWPLs at the water table, due to a high K_d value, low starting concentration, or short half-life.

Table 34. Peak Radionuclide Concentrations and Time to Exceed GWPL at the Water Table, Vertical PATHRAE Results for CAW Cell Top Slope (0.238 cm/year Infiltration)

(See large tables at end of report document.)

Table 35. Radionuclide Concentrations (pCi/L) at the Water Table, Vertical PATHRAE Model Results for the CAW Top Slope (0.238 cm/year Infiltration

(See large tables at end of report document.)

5.3.2 Vertical Side Slope Analysis (0.335 cm/yr)

Two of the 99 nuclides modeled exceeded the GWPLs at the water table in less than 500 years, based on the side slope cover design infiltration rate of 0.335 cm/yr (0.132 in/yr). A summary of peak concentrations and the year in which the GWPLs were exceeded are provided in Table 36. A complete listing of output times and concentrations for all nuclides that arrived at the water table is provided in Table 38. In all tables, the "Year to Exceed" is conservatively reported as the next *lowest* model output time. None of the surrogate nuclides exceeded a benchmark standard of 1 pCi/L.

Starting concentrations that would meet GWPLs at the water table were calculated for Bk-247 and Cl-36 and are shown in Table 23. A total of 16 nuclides were carried through to the horizontal PATHRAE modeling (described in Section 6) to determine the concentrations that would meet GWPLs at a compliance well (Section 6.3.1). The 16 nuclides that were carried forward to the horizontal PATHRAE modeling included Bk-247 and Cl-36 (which exceeded GWPLs at the water table) and 14 additional nuclides that met GWPLs at the water table.

Table 36. Summary of Peak Concentrations and Exceedences at the Water Table, PATHRAE Vertical Model Results for 0.335 cm/yr Side Slope Case

Nuclide	Time To Exceed (Year)	Peak Concentration (Ci/m^3)	Peak Concentration (pCi/L)	Peak Year
Cl-36	400	2.27E+04	2.27E+13	1,492.1
Bk-247	480	3.42E-03	3.42E+06	1,413.9
Ca-41	700	3.39E+04	3.39E+13	2,550.4
Sr-90	-1	4.36E-18	4.36E-09	1,037.3
Si-32	-1	1.42E-04	1.42E+05	4,583.8
I-129	-1	1.24E-03	1.24E+06	4,118.3
Re-187	-1	1.24E-02	1.24E+07	3,110
Tc-99	-1	4.84E-02	4.84E+07	3,891

Note: -1 indicates nuclide did not exceed GWPLs at the water table within the 1,000 years modeled

Table 37. Peak Radionuclide Concentrations and Time to Exceed GWPL at the Water Table, Vertical PATHRAE Model Results for CAW Cell Side Slope (0.335 cm/year Infiltration)

(See large tables at end of report document.)

Table 38. Radionuclide Concentrations (pCi/L) at the Water Table, Vertical PATHRAE Model Results for CAW Cell Side Slope (0.335 cm/year Infiltration)

(See large tables at end of report document.)

5.3.3 Vertical Analysis for Metals

Vertical PATHRAE modeling for metals was performed for the CAW top slope and side slope.

The top slope vertical model results indicate that none of the metals modeled would arrive or exceed GWPLs at the water within 200 years, based on an infiltration rate of 0.238 cm/yr. The concentrations at the water table predicted by the model are not subject to solubility controls. Therefore, the model results predicted by complete leaching using the lowest-literature K_d values may significantly exceed the solubility of metals in groundwater at the site.

The side slope vertical model results indicate that none of the metals modeled would arrive or exceed GWPLs at the water within 200 years. The metals modeling was not carried through to the horizontal PATHRAE modeling because all GWPLs were met at the water table.

6. HORIZONTAL PATHRAE FATE AND TRANSPORT MODELING

6.1 Horizontal Input Parameters for Contaminant Release

6.1.1 Waste Source Term Concentrations

The source term concentrations for the horizontal model were calculated from the output from the vertical model, as described in Section 4. The method involves calculating the concentration in each of the 116 "slices" using the following equation:

$$C = \frac{\left(C_t + C_{t+n}\right)}{2} \cdot \left(\left(t+n\right) - t\right)$$

where: C = Mass/activity of nuclide in a given time slice in a unit volume of fluid [Ci·yrs/m^3]
C_t = Output concentration at time t [Ci/m^3]
C_{t+n} = Output concentration at time t+n [Ci/m^3]
t = Time at beginning of "time slice" [years]
t+n = Time at end of "time slice" [years]
n = Duration of "time slice" [years]

The leachate concentration in water (Ci/m^3) was converted to a sorbate concentration on aquifer soil (Ci/m^3). The mass ascribed to one cubic meter of aquifer was determined using the following equation:

$$C_{aq} = \frac{C_l\left(q_{in}\right)}{V_{soil}} = \frac{C_l\left(q_{in}\right)}{\left(1\,m^3\right)}$$

where: C_{aq} = Concentration of constituent sorbed onto 1 m^3 of aquifer soil [Ci/yr/m^3 soil]
C_l = Concentration in leachate (output of vertical slice) [Ci/m^3 water]
V_{soil} = Volume of soil [m^3]
q_{in} = Infiltration rate [m/yr applied to 1 m^2 surface area = m^3/yr]

6.1.2 Aquifer Bulk Density

The aquifer bulk density in the horizontal model was set at the thickness weighted average bulk density shown in Table 30 (1.563 gm/cm^3.)

6.1.3 Aquifer Moisture Content

The aquifer is saturated, with a moisture content equal to the saturated porosity of 29%. The effective porosity value of 0.29 has been used in previous modeling (DEQ, 1994 August), and is based on site specific data.

6.1.4 Partitioning Coefficients (K_d)

The distribution coefficients (K_ds) used in the horizontal pathway were identical to those used in the vertical model. The radionuclide and metals K_d values used in the modeling were summarized in Table 27.

6.1.5 Fractional Release Rate

The contaminant release rate (or leach rate) for the horizontal simulation was set to 1/yr for all constituents modeled. In this manner, the entire waste concentration in each "time slice" was released "instantaneously". The K_d-limited leach rate was already accounted for in the vertical simulation and the resulting time offset for the "time slices" which was input to the horizontal model.

6.2 Horizontal Input Parameters for Flow and Transport

6.2.1 Hydraulic Conductivity

The geologic materials underlying the CAW cell include the Unit 3 sand and Unit 2 clay. As discussed in Section 3.5, the hydraulic conductivity of the shallow aquifer is 7.53 x 10^{-4} cm/sec, based on the 90% upper confidence level (UCL) for the Unit 3 sand calculated from 118 slug tests conducted site-wide (Table 16). The use of the 90% UCL is more conservative than using the geometric mean hydraulic conductivity (6.16 x 10^{-4} cm/sec) because aquifer velocity is directly proportional to hydraulic conductivity (Section 6.2.4).

6.2.2 Hydraulic Gradient

Hydraulic gradients have been calculated monthly for the unconfined shallow groundwater beneath the Energy*Solutions* site to determine compliance with the Ground Water Quality Discharge Permit (UGW450005). The Permit for the existing Class A and Class A North cells gives a maximum allowable hydraulic gradient $1.0x10^{-3}$ ft/ft for the shallow aquifer beneath the cells. Previous and current modeling is based on this hydraulic gradient.

6.2.3 Effective Porosity

The effective porosity value of 0.29 was used in the calculation of aquifer velocity for all calculations in the saturated zone / horizontal pathway.

6.2.4 Aquifer Average Linear Velocity

The aquifer velocity (v_a) is calculated based on the Darcy equation, such that:

$$\overline{v}_a = \frac{Ki}{n_e}$$

where v_a = average linear velocity in the aquifer (L/T)
K = hydraulic conductivity (L/T)
i = hydraulic gradient (L/L)
n_e = aquifer effective porosity (L^3/L^3)

Using the effective porosity (0.29), 90% UCL hydraulic conductivity ($7.53x10^{-4}$ cm/sec), and the average hydraulic gradient ($1.0x10^{-3}$) described in the previous sections, the average groundwater linear velocity is 0.819 m/yr (2.7 ft/yr), as shown below:

$$\overline{v} = \frac{Ki}{n_e} = \frac{\left(7.53x10^{-4}\ \text{cm/sec}\right)\left(1.0x10^{-3}\right)}{0.29} = 2.60x10^{-6}\ \text{cm/sec} = 0.819\ \text{m/yr}$$

6.2.5 Horizontal Transport Distance

The horizontal distance was modeled as the distance from the edge of the waste to the nearest compliance monitoring well. The side slope modeling used a horizontal distance of 90 ft (27.4 m).

The distance from the compliance well to the edge of the waste under the top slope was modeled using the side slope length (188 ft) plus the distance from the side slope to the well (90 ft) for a total distance of 278 feet from the waste to the compliance monitoring well. The top slope modeling used this 278 ft (84.7 m) horizontal transport distance.

6.2.6 River Flow Rate

The river flow rate in the horizontal model was set equal to the infiltration rate, in order to prevent any dilution of concentrations. The river flow rate was set to 0.00238 m^3/yr and 0.00335 m^3/yr for the top slope

and side slope PATHRAE simulations, respectively. This approach conservatively neglects any mixing or dilution that will occur in the aquifer.

6.3 Horizontal Transport Model Results

Horizontal PATHRAE modeling was conducted for the top slope and side slope infiltration rates. The model results are summarized in Table 39, which shows the time to exceed the GWPLs at the compliance well based on limited starting concentrations for Bk-247 (side slope and top slope) and Cl-36 (top slope only). The limiting concentrations were shown in Table 23. In the results tables below, the "Year To Exceed" is conservatively reported as the next *lowest* model output time.

Table 39. Summary of Horizontal PATHRAE Model Results—Time to Exceed GWPLs at the Compliance Monitoring Well, based on 0.238 and 0.335 cm/yr Infiltration

Nuclide	Top Slope 0.238 cm/yr Model Results YEAR TO EXCEED	Side Slope 0.335 cm/yr Model Results YEAR TO EXCEED
Bk-247	500	510
Ca-41	580	725
Cl-36	500	500
H-3	-1	---
I-129	-1	-1
Re-187	-1	-1
Sr-90	-1	-1
Tc-99	-1	-1

NOTES: Year to exceed GWPL reported to next lowest model output year.
-1 indicates nuclide does not exceed GWPL within the 2,000 years modeled
--- indicates nuclide was not modeled in the horizontal pathway or did not arrive at the compliance well
See Table 22 and Table 23 for starting concentrations for each model

Note that 16 nuclides from the vertical modeling were carried forward to the horizontal modeling. The PATHRAE code only produces output for nuclides that arrive at the compliance point. Therefore, several of the nuclides that were input to the horizontal model are not included by PATHRAE in the output files (described below). The output concentration of these nuclides is essentially zero.

6.3.1 Horizontal Top Slope Analysis (0.238 cm/yr)

None of the nuclides modeled exceeded the GWPLs at the compliance well within 500 years, based on horizontal modeling of the top slope cover design infiltration rate of 0.238 cm/yr (0.094 in/yr). The concentrations of each constituent at each model output time are given in Table 40.

As described in Section 5.1.1.1 and listed in Table 23, the source concentrations for Bk-247 and Cl-36 used in the top slope model were set to the limiting concentrations that met GWPLs for 500 years at the compliance well. All other radionuclides were modeled at Class A limits or Specific Activity and met the groundwater standard for at least 500 years.

Table 40. Radionuclide Concentrations (pCi/L) at Compliance Well, Horizontal PATHRAE Model Results for CAW Cell Top Slope (0.238 cm/year Infiltration

(See large tables at end of report document.)

6.3.2 Horizontal Side Slope Analysis (0.335 cm/yr)

None of the nuclides exceeded the GWPLs at the compliance well in less than 500 years, based on the side slope cover design infiltration rate of 0.335 cm/yr (0.132 in/yr). The concentrations of each constituent at each model output time are given in Table 41.

As described in Section 5.1.1 and listed in Table 23, the source concentrations for Cl-36 used in the side slope model were set to the limiting concentrations that met GWPLs for 500 years at the compliance well. All other radionuclides were modeled at Class A limits or Specific Activity and met the groundwater standard for at least 500 years.

Table 41. Radionuclide Concentrations (pCi/L) at Compliance Well, Horizontal PATHRAE Model Results for CAW Cell Side Slope (0.335 cm/year Infiltration)

(See large tables at end of report document.)

7. SUMMARY AND CONCLUSIONS

The infiltration, fate, and transport modeling for Energy*Solutions*' Class A West cell was based on previous modeling of the existing Class A cell. The input parameters have been selected to provide conservative (environmentally protective) estimates for infiltration through the cell and for fate and transport of constituents from the waste.

The HELP infiltration modeling results indicate that 0.238 cm/yr infiltration would occur through the CAW cell top slope, while 0.335 cm/yr would infiltrate through the side slope with 6-inch thick Type-B filter. Based on these infiltration rates, moisture contents would stabilize at 0.057 v/v in the waste and 0.043 v/v in the native soil below the top slope, at 0.0599 and 0.045 v/v in the waste and native soil below the side slope.

The PATHRAE fate and transport modeling for the top slope (0.238 cm/yr infiltration case) indicates that all radionuclides modeled would remain below the GWPLs for at least 500 years at a compliance well located 278 feet from the edge of the top slope waste, provided that the concentrations of two radionuclides, Bk-247 and Cl-36, are received in limited concentrations of 1.92 and 73,900 pCi/g, respectively. All other modeled constituents would meet the groundwater standard if placed in the top slope area at Class A limits.

The PATHRAE fate and transport modeling for the side slope with a 6-inch thick Type-B filter (0.335 cm/yr infiltration case) indicates that all radionuclides modeled would remain below the GWPLs for at least 500 years at a compliance well located 90 feet from the edge of the waste, provided that Cl-36 is received in limited concentrations of 106,000,000 pCi/g. All other modeled constituents would meet the groundwater standard if placed under the side slope at Class A limits.

The transport of heavy metals from the top slope and side slope areas was modeled using separate vertical PATHRAE model runs. The results indicated that all thirteen metals could be placed in the top slope or side slope at the maximum possible concentration based on density, and would meet GWPLs at a the water table and, by extension, at a compliance well located 90 feet from the edge of the waste for the 200-year compliance period established for heavy metals.

April 19, 2011

Prepared and submitted by:

Whetstone Associates, Inc.

Susan A. Wyman, P.E., P.G.
Principal Hydrologist / Civil Engineer

8. REFERENCES

Adrian Brown Consultants, Inc. (ABC), 1997. Volume I. LARW Infiltration Modeling Input Parameters and Results, prepared for Envirocare of Utah, Inc. 41 pp plus tables, figures, and attachments. May 15, 1997.

Adrian Brown Consultants, Inc., 1998. Volume II. LARW Groundwater Fate and Transport Modeling Input Parameters and Results, prepared for Envirocare of Utah, Inc. 44 pp. plus tables, figures and attachments. February 12, 1998.

Adrian Brown Consultants, Inc., 1999. 11e.(2) Disposal Cell Infiltration and Transport Model Input Parameters, prepared for Envirocare of Utah, Inc. 19 pp. plus tables and figures. July 16, 1999.

Baes, C. F. III, Sharp, R.D, Sjoreen, A.L, and Shor, R.W. , 1984. "A Review and Analysis of Parameters for Assessing Transport of Environmentally Released Radionuclides Through Agriculture". Oak Ridge National Laboratory for US DOE. ORNL-5786.

Bingham Environmental, 1995. Memorandum to George Hellstrom, Envirocare of Utah, Inc. from David Cline and David Waite, Regarding Summary of Results Radionuclide K_d Tests, Envirocare Disposal Landfills, Clive, Utah, 14 pp plus figures and appendices.

Cheng, Jing-Jy, 2001. E-mail correspondence to Susan Wyman (Whetstone Associates) from Jing-Jy Cheng (Environmental Systems Engineer, Environmental Assessment Division, Argonne National Laboratory), RE: Question about RESRAD Default K_d Value. August 17, 2001.

Del Debbio, J.A. (1991) Sorption of Strontium, Selenium, Cadmium, and Mercury in Soil. Radiochimica Acta, Vol. 52/53, pp. 181-186

Division of Radiation Control (DRC), 1997. Memorandum from Loren Morton (DRC) to Envirocare RE-Licensing File through Dane Finerfrock, regarding Envirocare HELP Model Weather Data: Staff Evaluation of Precipitation and Temperature Analog for Clive, Utah. 12 pp. plus attachments. September 19, 1997.

Division of Radiation Control (DRC), 2001. "Re-Modeling Results of Californium-251 for the Class A Cell - DRC Approval", letter to Kenneth L. Alkema (Envirocare) from William J. Sinclair (DRC), Sept. 5, 2001. 3 pp.

DRC, 2001. "Re-Modeling Results of Californium-251 for the Class A Cell - DRC Approval", letter from William J. Sinclair (DRC) to Kenneth L. Alkema (Envirocare), Sept. 5, 2001. 3 pp.

Enchemica, LLC, 2002. In Situ Metals Kd Values at the Envirocare Site, prepared for Envirocare of Utah of Utah, Inc., 8 pp with 2 tables and 3 appendices. May 2, 2002.

Environmental Assessment Division (EAD), 2001. The RESRAD Family of Codes website, Argonne National Laboratory Environmental Assessment Division, http://web.ead.anl.gov/resrad.

Fayer, M.J., 1999 (April). UNSAT-H version 2.05, available for down load from website http://etd.pnl.gov:2080/~mj_fayer/topv205.htm, updated April 23, 1999.

Fayer, M.J., and Jones, T.L., 1990 (April). UNSAT-H version 2.0: Unsaturated Soil Water and Heat Flow Model, PNL-6779, Battelle Memorial Institute.

Freeze, R.A., and Cherry, J.A., 1979. Groundwater, Prentice-Hall, Inc, Englewood Cliffs, New Jersey, 603 pp.

Isherwood, Dana, 1981. Geoscience Data Base Handbook for Modeling a Nuclear Waste Repository, Lawrence Livermore Laboratory, prepared for U.S. Nuclear Regulatory Commission, NUREG/CR-0912, Volume I. January, 1981.

Kozak, M.W., et al., 1990. "Background Information for the Development of a Low-Level Waste Performance Assessment Methodology — Computer Code Implementation and Assessment," U.S. Nuclear Regulatory Commission, NUREG/CR-5453, Vol. 5, August 1990.

Looney, BB., Grant, M.W., and King, C.M., 1987 (March). "Estimation of Geochemical Parameters for Assessing Subsurface Transport at the Savannah River Plant", DuPont DPST-85-904.

McKinley, I.G., Grogan, H.A., 1991. Radionuclide Sorption Database for Swiss Repository Safety Assessments. Radiochimica Acta, Vol. 52/53, pp. 415-420

Merrell, G.B., Rogers, V.C., and Chau, T.K., 1995. The PATHRAE-RAD Performance Assessment Code for the Land Disposal of Radioactive Wastes, Rogers & Associates Engineering Corporation, RAE-9500/2-1. March 1995.

Meteorological Solutions, Inc. (MSI), 2010. "January 2009 Through December 2009 and January 1993 Through December 2009 Summary Report of Meteorological Data Collected at Energy*Solutions*' Clive, Utah Facility", prepared for: Energy*Solutions*, LLC, by Meteorological Solutions Inc., Project No. 021008134. February 2010.

Meyer, P.D., Rockhold, M.L., Nichols, W.E., and Gee, G.W., 1996. Hydrologic Evaluation Methodology for Estimating Water Movement Through the Unsaturated Zone at Commercial Low-Level Radioactive Waste Disposal Sites, prepared for U.S. Nuclear Regulatory Commission, NUREG/CR-6346,PNL-10843, 102p. plus appendices.

MFG Inc., 2000. Evaluation of Low-Level Radioactive Waste Containing Chelating Agents, prepared for Envirocare of Utah. December 7, 2000.

MFG, Inc., 2000. Metals Distribution Coefficient Values Relevant to the Envirocare Site, prepared for Envirocare of Utah, September 18, 2000.

Nofziger, D.L., Rajender, K., Nayudu, S.K., and Pei-Yao, S., 1989 (August). CHEMFLO, One-dimensional Water and Chemical Movement in Unsaturated Soils, US EPA model documentation, EPA/600/8-89/076, 106 pp.

Perrier, E.R., and Gibson, A.C., 1980. Hydrologic simulation on Solid Waste Disposal Sites, Technical Resource Document EPA-SW-868, U.S. Environmental Protection Agency, Cincinnati, OH 111 pp.

Porro, I., and P.J. Weirenga, 1993. "Transient and Steady-State Solute Transport Through a Large Unsaturated Soil Column," Ground Water, vol. 31 pp. 193-200.

Rao, P.S.C, Jessup, R.E., and Davidson, J.M., 1987. Mass Flow and Dispersion, in Environmental Chemistry of Herbicides, Vol. 1, R. Grover, editor., CRC Press, p. 21-43.

Richards, L.A. 1931. Capillary Conduction of Liquids in Porous Mediums. *Physics 1*, 318-313.

Richardson, C.W., and Wright, D.A. 1984. WGEN: A Model for Generating Daily Weather Variables. ARS-8, Agricultural Research Service, USDA. 83pp.

Rogers and Associates Engineering Corporation, 1990. Evaluation of the Potential Public Health Impacts Associated With Radioactive waste Disposal at a Site Near Clive, Utah, Rogers and Associates Engineering Corporation, RAE-9004/2-1, June 1990.

Roth, K., Jury, W.A., Fluhler, H., and Attinger, W., 1991. "Transport of Chloride Through an Unsaturated Field Soil," Water Resources Research, vol. 27 pp. 2533-2541.

Schroeder, P.R., and Peyton, R.L., 1995. HELP Modeling Workshop, IGWMC Ground-Water Modeling Short Courses, Colorado School of Mines, Golden, CO.

Schroeder, P.R., Aziz, N.M., Lloyd, C.M., and Zappi, P.A., 1994a. The Hydrologic Evaluation of Landfill Performance (HELP) Model: User's Guide for Version 3, EPA/600/R-94/168A; US EPA Office of Research and Development, Washington, D.C.

Schroeder, P.R., Dozier, T.S., Zappi, P.A., McEnroe, B.M., Sjostrom, J.W., and Peyton, R.L., 1994b. The Hydrologic Evaluation of Landfill Performance (HELP) Model: Engineering Guide for Version 3, EPA/600/R-94/168B; US EPA Office of Research and Development, Washington, D.C.

Sheppard, M.I, and Thibault, D.H., 1990. Default soil solid/liquid partition coefficients, Kds, for four major soil types: a compendium, Health Physics, vol. 59, No. 4 (October), pp. 471-482.

Stephens, D.B., 1996. Vadose Zone Hydrology, CRC Press, Inc., 339 pp.

Utah Department of Environmental Quality (DEQ) Division of Water Quality, 1994. Memorandum from Loren Morton (DWQ) to Dane Finerfrock (DRC) regarding DWQ/USU PATHRAE Contaminant Modeling: Evaluation of Envirocare of Utah's August 30, 1993 Proposed Changes to Embankment Cover Design, February 25, 1994.

Utah Division of Environmental Quality (UDEQ), 2009. Ground Water Quality Discharge Permit Modification, Permit No. UGW450005. 66 pp plus appendices. December 22, 2009.

Whetstone Associates, Inc, 2000a. Envirocare Of Utah Western LARW Cell Infiltration and Transport Modeling, consultants report dated March 2, 2000a. Document Number 4104M.000302.

Whetstone Associates, Inc, 2000b. Soil Distribution Coefficient for Thallium. Technical Memorandum to Tim Orton dated March 29, 2000b. Document Number 4104M.000329

Whetstone Associates, Inc, 2000c. Envirocare of Utah Revised Western LARW Cell Infiltration and Transport Modeling, consultants report dated June 12, 2000c. Document Number 4104M.000612

Whetstone Associates, Inc, 2000d. Envirocare of Utah Revised Western LARW Cell Infiltration and Transport Modeling, consultants report dated July 19, 2000d. Document Number 4104M.000719

Whetstone Associates, Inc, 2000e. Envirocare of Utah Class A, B, & C Cell Infiltration and Transport Modeling, consultants report dated August 1, 2000e. Document Number 4104O.000801

Whetstone Associates, Inc, 2001. "Results of Cf-251 Modeling for the Class A Cell, Using the 898-Year Half Life", technical memorandum to Dan Shrum, Envirocare of Utah from Susan Wyman, Whetstone Associates, dated August 21, 2001, Document Number 4101M.010821, 5 pp

Whetstone Associates, Inc, 2003. "Technical memorandum on 11(e).2 Cell Transport Modeling Using New Zn Kd and Higher Radionuclide Concentrations", technical memorandum to Dan Shrum, Envirocare of Utah from Susan Wyman, Whetstone Associates, dated November 10, 2003, Document Number 4101L.031110, 2 pp.

Whetstone Associates, Inc, 2005. Envirocare of Utah Class A Combined (CAC) Cell Infiltration and Transport Modeling Report, dated November 18, 2005. Document Number 4101W.051118

Whetstone Associates, Inc, 2006b. Envirocare of Utah Class A South Cell Infiltration and Transport Modeling Report, dated December 7, 2007. Document Number 4101L.071207

Whetstone Associates, Inc., 2006a. "Technical Memorandum on Results of Methylene Chloride and Methanol Modeling for the Class A Cell", technical memorandum to Dan Shrum, Envirocare of Utah, from Susan Wyman, Whetstone Associates, January 20, 2006.

Whetstone Associates, Inc., 2007. "Technical Memorandum on Formerly Characteristic Waste Modeling of the Class A and Class A North Cells", technical memorandum to Dan Shrum, Envirocare of Utah, from Susan Wyman, Whetstone Associates, September 25, 2007

Wierenga, P.J., 1995. "Water and Solute Transport and Storage," in Vadose Zone Characterization and Monitoring, edited by L.G. Wilson, L.G. Everett, snd S.J. Cullen, Lewis Publishers, pp. 41-60

Yu, C., C. Loureiro, J.-J. Cheng, L.G. Jones, Y.Y. Wang, Y.P. Chia, and E. Faillace, 1993. Data Collection Handbook To Support Modeling Impacts Of Radioactive Material In Soil, Environmental Assessment and Information Sciences Division, Argonne National Laboratory, Argonne, Illinois, April 1993.

Yu, C., D. LePoire, E. Gnanapragasam, J. Arnish, S. Kamboj, B. M. Biwer, J. J. Cheng, A. Sielen, S. Y. Chen, 2000. Development of Probabilistic RESRAD 6.0 and RESRAD-BUILD 3.0 Computer Codes, Prepared for the Division of Risk Analysis and Applications, Office of Nuclear Regulatory Research, U.S. Nuclear Regulatory Commission, NUREG/CR-6697, December, 2001.